AD NUMBER

**AD822716**

LIMITATION CHANGES

TO:

**Approved for public release; distribution is unlimited.**

FROM:

**Distribution authorized to U.S. Gov't. agencies and their contractors; Critical Technology; OCT 1967. Other requests shall be referred to Air Force Technical Application Center, Washington, DC 20333. This document contains export-controlled technical data.**

AUTHORITY

**usaf ltr, 25 jan 1972**

# LARGE-ARRAY SIGNAL AND NOISE ANALYSIS

## Special Scientific Report No. 12

## ANALYSIS OF LONG-PERIOD NOISE

Prepared by

Frank H. Binder, Program Manager

TEXAS INSTRUMENTS INCORPORATED
Science Services Division
P.O. Box 5621
Dallas, Texas 75222



Contract No. AF 33(657)-16678

Prepared for

AIR FORCE TECHNICAL APPLICATIONS CENTER
Washington, D. C. 20333

Sponsored by

ADVANCED RESEARCH PROJECTS AGENCY
ARPA Order No. 599
AFTAC Project No. VT/6707

18 October 1967

# LARGE-ARRAY SIGNAL AND NOISE ANALYSIS

Special Scientific Report No. 12

## ANALYSIS OF LONG-PERIOD NOISE

Prepared by

Frank H. Binder, Program Manager

TEXAS INSTRUMENTS INCORPORATED
Science Services Division
P.O. Box 5621
Dallas, Texas 75222

Contract No. AF 33(657)-16678

Prepared for

AIR FORCE TECHNICAL APPLICATIONS CENTER
Washington, D. C. 20333

Sponsored by

ADVANCED RESEARCH PROJECTS AGENCY
ARPA Order No. 599
AFTAC Project No. VT/6707

18 October 1967

## TABLE OF CONTENTS



## LIST OF TABLES



## LIST OF ILLUSTRATIONS

LIST OF ILLUSTRATIONS (CONT)

## LIST OF ILLUSTRATIONS (CONT)

LIST OF ILLUSTRATIONS (CONT)

LIST OF ILLUSTRATIONS (CONT)

## LIST OF ILLUSTRATIONS (CONT)

# SECTION I

# INTRODUCTION AND PRINCIPAL CONCLUSIONS

This report presents the results of the analysis of nine long-period noise samples recorded at the Montana LASA between 12 November 1966 and 7 February 1967. This analysis was undertaken to describe the salient characteristics of the long-period noise. Particular attention was given to spectral analysis, coherence among channels, spatial organization, identification of modal content, and identification of noise sources.

Results of the analysis of the long-period noise indicate that

- The noise generally appears to be related to storms and is probably the result of wave activity in the North Atlantic and North Pacific. This storm activity is quite persistent during the winter months but is considerably reduced during other seasons. It would, therefore, be hazardous to extrapolate the conclusions of this study to the long-period noise during other seasons
- The noise is quite time-variable; noise power spectra change in shape and level
- The noise is highly coherent; vertical components can be predicted very well from horizontal or from other vertical instruments
- The coherent-noise peaks above 0.05 cps appear to be predominantly (at least 90 percent) surface-mode energy, which is generally directional
- There is some evidence that a portion of the horizontal energy is Love-wave energy

- The noise below 0.05 cps does not appear to behave as propagating plane waves; however, conclusions about such low-frequency energy must be tentative, for the data samples used in this study were about 80-min long
- Power spectra of similar components are generally space-stationary
- The horizontal components are considerably noisier than the vertical in the range $f < 0.05$ cps and $0.1 < f < 0.2$ cps

Three-component long-period instruments are located at the center of each subarray at the Montana LASA. A map of the subarray locations and their coordinates relative to A0 are shown in Figure I-1. The amplitude response of the instrument-amplifier-filter combination used during the data recording is shown in Figure I-2.

The long-period data are recorded at five samples/sec and, as recorded in the field, fill one magnetic tape in about 80 min. Thus, all samples available to this study were of 80-min or less duration.

Data were resampled by 5 to 1-sec $\Delta t$. This results in a Nyquist folding frequency of 0.5 cps. No antialias filtering was necessary, as the recording system has an effective cutoff below 0.5 cps (Figure I-2).

Overall, data were about 60-percent usable. Some noise samples were entirely discarded as unusable. The major problem was spiking, but there are many instances of dead traces and traces with wild long-period fluctuations.

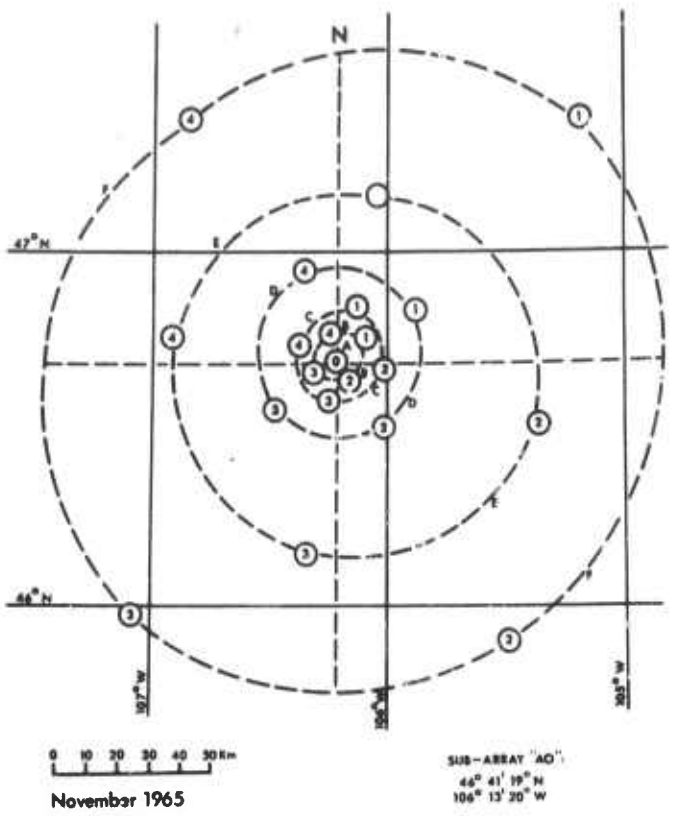


| NAME | AZIMUTH | DELTA-KM | THETA | X | Y |
|---|---|---|---|---|---|
| B1 | 54.902 | 12.312 | 35.098 | 10.07330 | 7.07912 |
| B2 | 141.477 | 7.614 | 308.523 | 4.74223 | -5.95686 |
| B3 | 246.010 | 8.039 | 203.990 | -7.34456 | -3.26849 |
| B4 | 347.011 | 9.063 | 102.989 | -2.03704 | 8.83111 |
| C1 | 23.531 | 18.291 | 66.469 | 7.30259 | 16.77000 |
| C2 | 97.459 | 16.245 | 352.541 | 15.10754 | -2.10883 |
| C3 | 191.498 | 12.981 | 258.502 | -2.58753 | -12.72050 |
| C4 | 294.023 | 12.769 | 155.977 | -11.66298 | 5.19829 |
| D1 | 56.459 | 30.497 | 33.541 | 25.41996 | 16.85062 |
| D2 | 141.708 | 26.250 | 308.292 | 16.26637 | -20.60261 |
| D3 | 232.156 | 25.110 | 217.844 | -19.82894 | -15.40536 |
| D4 | 336.360 | 30.753 | 113.640 | -12.33163 | 28.17227 |
| E1 | 13.507 | 54.221 | 76.493 | 12.66405 | 52.72133 |
| E2 | 106.254 | 68.551 | 343.746 | 65.81109 | -19.18699 |
| E3 | 188.314 | 60.556 | 261.686 | -8.75616 | -59.91960 |
| E4 | 278.849 | 53.706 | 171.151 | -53.06676 | 8.26157 |
| F1 | 45.670 | 109.262 | 44.330 | 78.15803 | 76.35121 |
| F2 | 146.491 | 103.543 | 303.509 | 57.16296 | -86.33393 |
| F3 | 220.066 | 103.487 | 229.934 | -66.61130 | -79.19908 |
| F4 | 325.943 | 97.244 | 124.057 | -54.45840 | 80.56474 |

Figure I-1. Subarray Locations and Their Coordinates Relative to A0

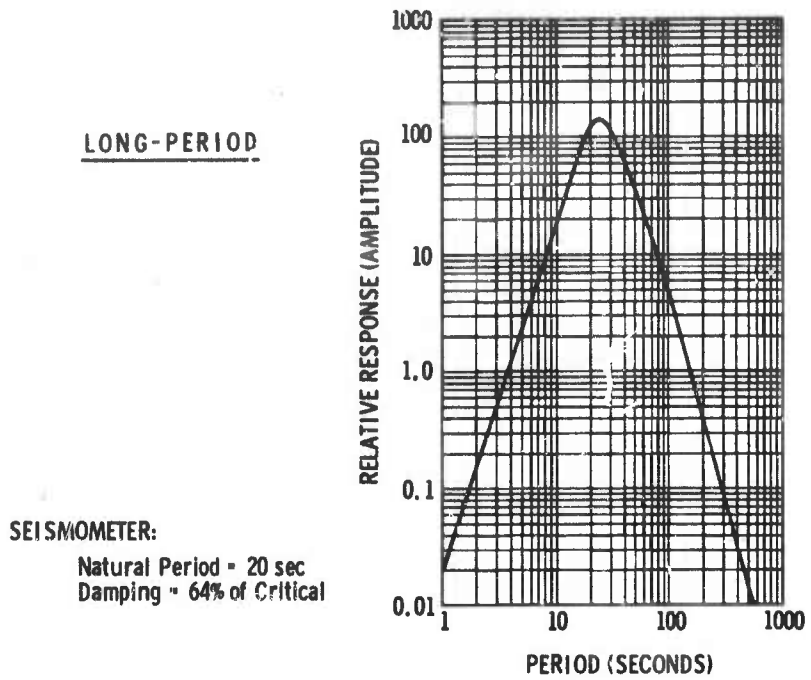


Figure I-2. Amplitude Response of Long-Period Seismometer-Amplifier-Filter Combination

Recording times of the noise samples analyzed in this study are shown in Table I-1.

Table I-1

RECORDING TIMES OF NOISE SAMPLES

| Date | Time |
|---|---|
| 12-13 November 1966 | 22:51:24.4 - 00:11:24.4 |
| 18 November 1966 | 17:19:39.6 - 18:39:31.8 |
| 2 December 1966 | 21:37:00.5 - 22:49:50.9 |
| 3 December 1966 | 04:17:00.5 - 05:36:59.9 |
| 3 December 1966 | 05:37:00.5 - 06:56:59.9 |
| 13 December 1966 | 13:02:01.6 - 14:22:01.0 |
| 21 December 1966 | 04:22:57.7 - 05:40:57.1 |
| 28 December 1966 | 03:02:01.7 - 04:22:01.1 |
| 7 February 1967 | 20:34:02.4 - 21:54:01.8 |

Noise-analysis techniques used included wiggle-trace playbacks, power spectra, determination of multichannel coherence from multiple coherences, and wavenumber spectra. Details of the implementation of these techniques and comments pertinent to their use follow.

The main purpose of the wiggly-trace playbacks was for quality control. Playbacks were presented only for some noise samples, and these are not always played back with similar amplification.

All power spectra were high-resolution, maximum entropy spectra, calculated from prediction-error filters using a technique invented by John Burg of Texas Instrument Incorporated. Mr. Burg will present details of the technique at the Fall Conference of the Society of Exploration Geophysicists.

The scales, in units of $(\mu m)^2$/cps at 0.04 cps, come from the one available long-period calibration are shown in Table I-2.

These calibration data were averaged and the average taken as the gain ratio (digital units) / (μm ground motion). This factor was applied to all noise samples except the 28 December samples which had an unknown scalar multiplication during initial processing. Therefore, the absolute scales must be considered only an approximate figure.

In relating the power spectrum of one sensor to another, the calibration data have been ignored. No multiplication correction has been applied to any of the spectra for three reasons. First, the power spectral densities are, in general, very similar in the region of the most coherent-noise energy (0.06 cps). Secondly, the 25-sec period sinusoidal calibration is at a considerably lower frequency than the range of greatest interest to the noise studies. Finally, the single calibration is separated in time by a considerable period from most of the noise recordings.

Table I-2

MAGNIFICATION LEVELS FOR LASA
LONG-PERIOD INSTRUMENTS
(6 March 1967)

| Location | LPZ (cts/μ) | LPN (cts/μ) | LPE (cts/μ) |
|---|---|---|---|
| A0 | 394.9 | 422.3 | 404.5 |
| B1 | 378.4 | 379.5 | 393.1 |
| B2 | 387.6 | 399.3 | 393.6 |
| B3 | 359.3 | 357.8 | 360.0 |
| B4 | 426.7 | 432.7 | 438.9 |
| C1 | 390.1 | 370.7 | 383.9 |
| C2 | 382.9 | 382.6 | 356.2 |
| C3 | 422.5 | 376.8 | 432.6 |
| C4 | 407.4 | 393.1 | 417.2 |
| D1 | 369.2 | 409.2 | 413.2 |
| D2 | 374.9 | 391.0 | 369.5 |
| D3 | 374.2 | 408.6 | 366.8 |
| D4 | 371.5 | 382.8 | 392.7 |
| E1 | 176.5 | 332.5 | 406.5 |
| E2 | 401.3 | 422.6 | 421.6 |
| E3 | 374.1 | 434.9 | 462.7 |
| E4 | 501.6 | 422.4 | 393.5 |
| F1 | 358.0 | 373.3 | 372.9 |
| F2 | 392.8 | 388.9 | 393.4 |
| F3 | 413.2 | 429.3 | 421.9 |
| F4 | 399.7 | 403.4 | 468.8 |

Thus, in comparing power spectra at different times and/or locations, one must keep in mind that no correction for differing seismometer responses has been included.

Multichannel coherences were obtained by calculating a multiple coherence. The vertical scale is actually 1 - (coherence)$^2$ — as the statisticians define coherence — and can be interpreted as the percent of the total power in the primary trace which is not predictable from a linear combination of the other traces. These results are presented as a function of frequency.

The estimate is biased and the bias increases as the number of channels increases. Also the absolute bias is a function of the true coherence; that is, if prediction error is estimated at 1 percent, the data are very probably about 99-percent predictable. However, a prediction error of 90-percent, with from 5 to 15 channels used in prediction, indicates that the data are essentially random at those frequencies. A more detailed discussion of the multiple coherence is given in another report.[1]

The actual calculations were done from a crosspower matrix obtained by taking the direct transform of 4096 time points (68.3 min), setting $\Phi_{ij}(f) = F_i^*(f)\, F_j(f)$, and smoothing over about 80 adjacent frequencies. With $\Delta f = 1/n\Delta t$, this results in a smoothing interval of 0.02 cps. Such a smoothing interval considerably reduces the coherence between certain of the E- and F-ring sensors (the ones in line with the direction of propagation) and A0.[1] However, this smoothing is necessary to give the estimates adequate stability. The effect is considerably reduced when the whole E or F ring is included in the coherence. Some sensors are always so located, with respect to the direction of propagation, that there is comparatively little moveout relative to A0.

In general, poor traces were detected by observing playbacks and were eliminated before processing. However, it was sometimes difficult to tell which traces were poor enough to destroy correlation. Therefore, several traces were processed in the determination of multiple coherences which were essentially uncorrelated with other traces due to spikes, etc. The result was traces that did not appreciably reduce prediction error.

Wavenumber spectra were calculated by standard technique of expanding the array in correlation space, weighting the locations by the cross-powers (or autopower), and taking a 2-dimensional Fourier transform. This results in a spectral window which is convolved with the true spectrum to give the wavenumber spectral estimates displayed in this report.

Crosspower matrices were calculated again by taking the direct transform of 4096 time points and setting $\Phi_{ij}(f) = F_i^*(f) F_j(f)$. Smoothing was done over about 40 frequencies ($\Delta f = 1/n\Delta t$, resulting in a smoothing interval of 0.01 cps.

Except for the 28 December 1966 noise sample, wavenumber spectra were calculated for one horizontal component only. The 28 December noise sample was processed first, and the similarity of the wavenumber spectra formed from the three different components suggested that spectra for all three components probably would contribute little additional information.

Azimuthal power-distribution plots were obtained by integrating the power spectra over sectors with a 20° central angle and bounded by velocity circles of 5 km/sec and 2 km/sec. This was done for all samples except for the 28 December 1966 sample, which was integrated over 15° sectors bounded by the velocity circle V = 2 km/sec and the origin ($V = \infty$). The 2- to 5-km/sec range was chosen to include most of the spreading of surface-mode noise power ($V \approx 3$ to 3.5 km/sec) due to the spectral window.

Integrals of the power over the sectors are divided by the zero spatial lag and plotted on polar coordinate paper on a logarithmic scale, increasing outward. These wavenumber spectra are the 2-dimensional Fourier transforms of sampled spatial autocorrelation functions which are not, in general, possible autocorrelations. Thus, the spectrum so derived is not positive everywhere. Sectors which gave a negative total power have been left blank.

Surface weather maps for the nearest 6-hr period are presented for each noise sample to estimate wave activity. This can only be done in a gross manner from the weather maps. Inquiries are being made to see if charts of wave activity, which are made each 12 hr by the Navy, can be obtained. A more detailed report of the correlation between wave activity and long-period noise will be forthcoming.

## SECTION II
## DATA PRESENTATIONS

The data are presented chronologically with short comments about the salient features of each noise sample.

For a pilot study, the 12 November and 28 December 1966 noise samples were processed first and, thus, were studied more intensively. For the remainder of the noise samples, the processing was essentially standardized. An overall discussion of the long-period noise characteristics is presented in Section III.

Figure II-1 shows a 550-sec section of the 12 November noise sample. The noise appears to arrive in strong bursts. This is most evident for the vertical sensors but can also be seen on the east-west sensors.

Figure II-2 shows the power spectra from subarrays A0, F1, and F2. Salient features of the 12 November power spectra are

- Spectra of like components are quite consistent spatially above approximately 0.05 cps
- Above 0.05 cps, the spectra are characterized by a peak near 0.06 cps and a broad peak from 0.12 to 0.22 cps
- The horizontal components show 6- to 10-db higher power density than vertical components in the 0.12- to 0.22-cps range
- There is no seismic energy above 0.25 cps

Figure II-3 shows the multiple coherences among vertical traces for the 12 November noise sample. The noise is quite predictable from the D ring (30 km from A0) only at the 0.06-cps power-density peak. Coherence falls off sharply below 0.05 cps and above 0.22 cps.

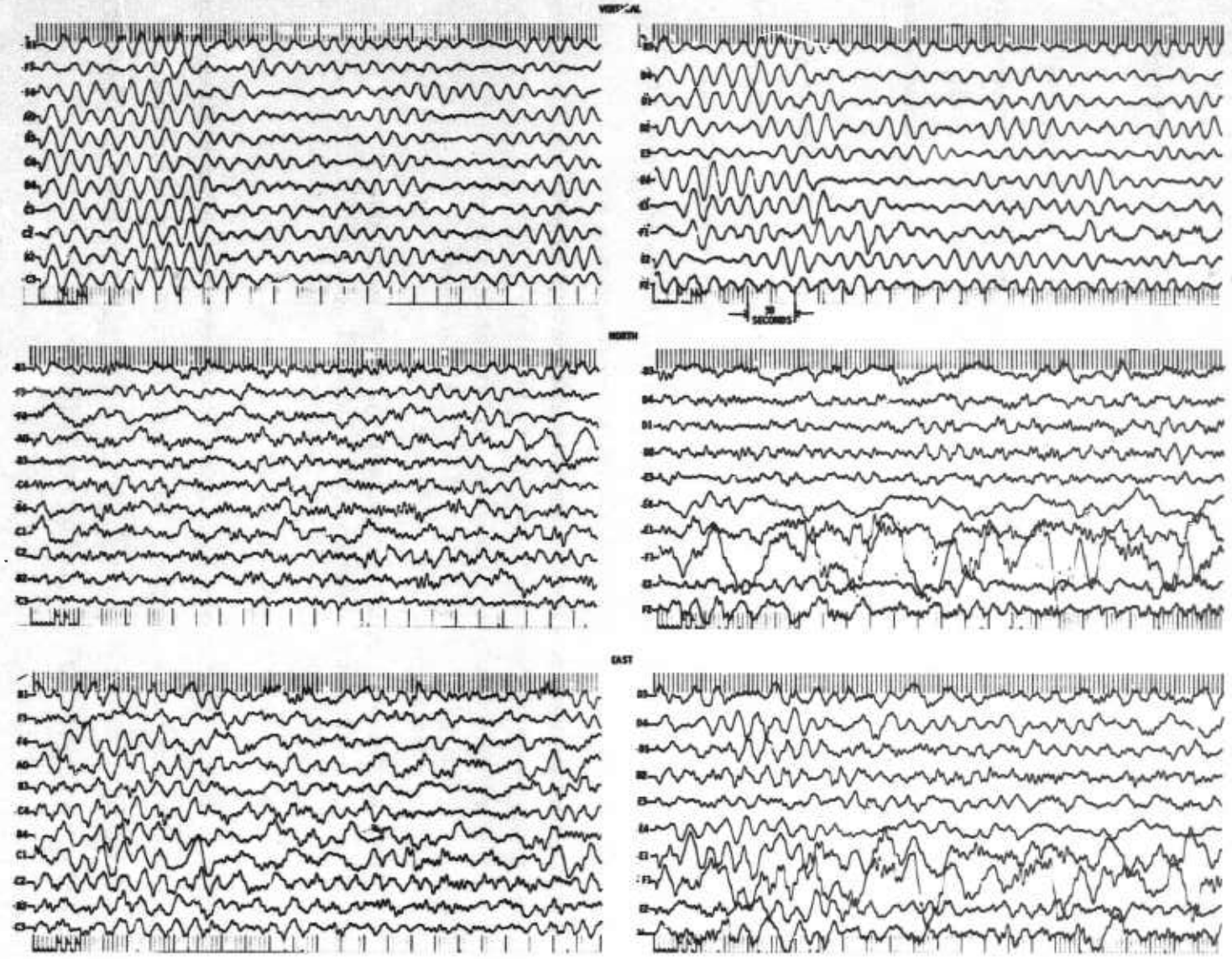


Figure II-1. Portion of 12 November 1966 Noise Sample

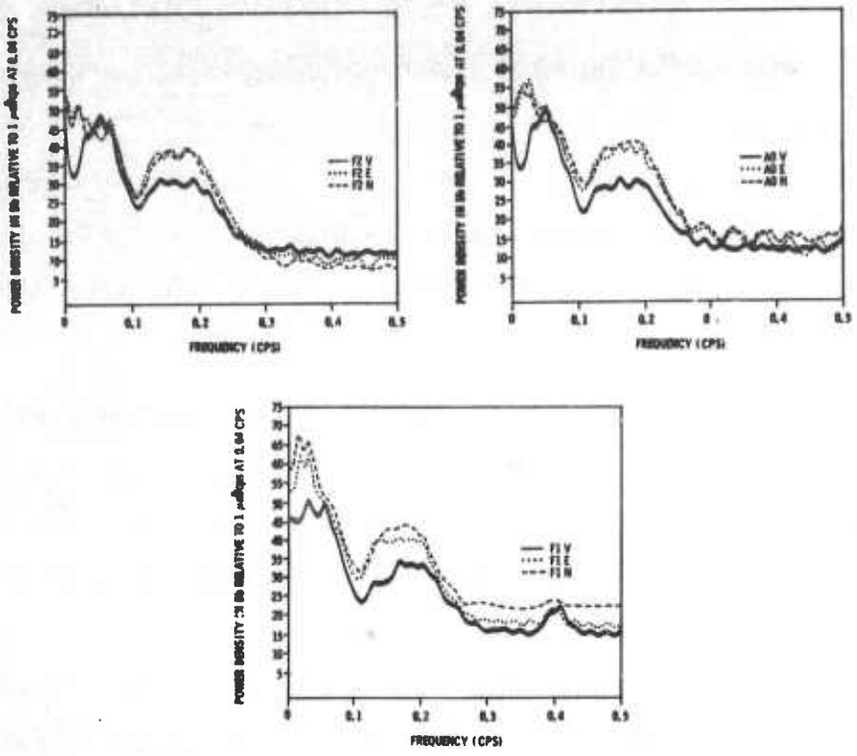


Figure II-2. Power Spectra of 12 November 1966 Noise

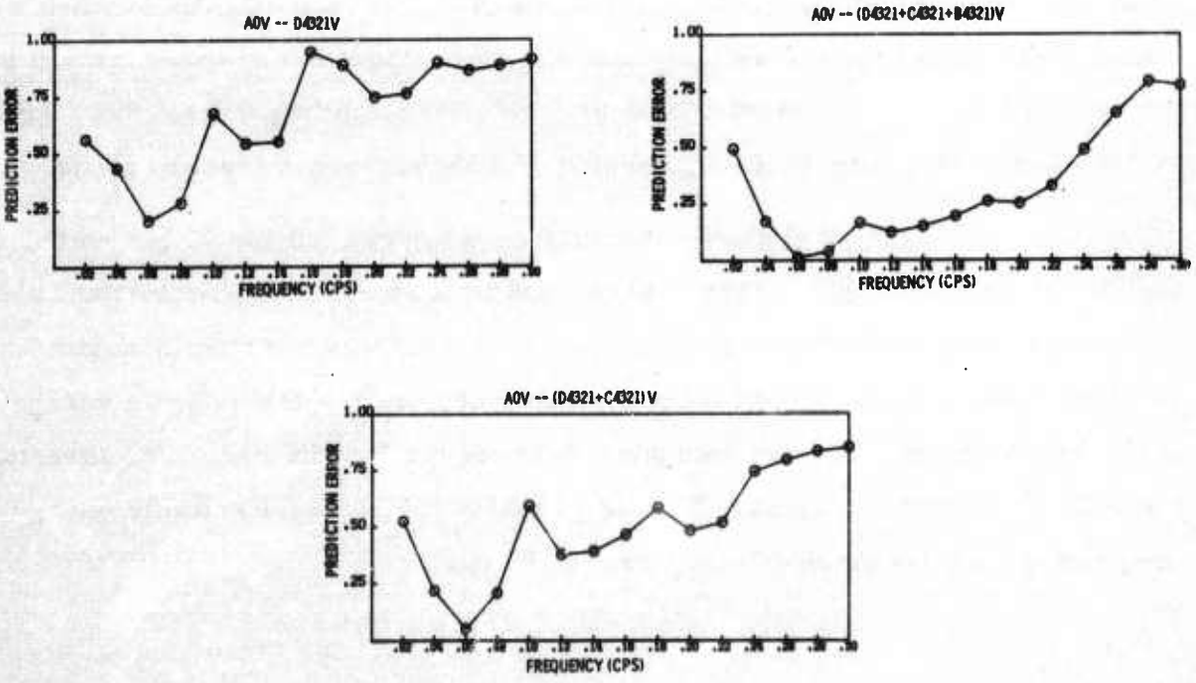


Figure II-3. Multiple Coherences Between Vertical Components for 12 November 1966 Noise Sample

Figure II-4 shows the multiple coherences of the A0 vertical sensor with various combinations of horizontal sensors. The 0.06-cps peak is highly predictable from nearby north-south, east-west horizontal components but not from horizontal components located only at A0. This suggests a dominant Rayleigh-mode source which has considerable azimuthal distribution.[2]

Figure II-5 through II-8 show the wavenumber spectra and azimuthal power distribution for the vertical and north-south components at 0.06, 0.08, 0.14, and 0.16 cps. The wavenumber spectra suggest that energy near the 0.07-cps peak is dominated by a fairly narrow azimuthal source to the northeast within apparent horizontal velocity of about 3.5 km/sec. There is also a possible source to the west, but it is considerably weaker. In general, the vertical and north-south components give similar results; however, the horizontal components tend to give a somewhat more "smeared out" spectrum. The 0.12- to 0.22-cps peak is apparently dominated by the same broad azimuthal source coming from the northeast and a source slightly south-of-west. Near 0.15 cps, the velocity appears to be about 3 km/sec. Spectra of the vertical components show a peak at a velocity slightly greater than 4 km/sec at 0.16 cps. This may be an expression of a higher-order trapped mode.

Figure II-9 shows the surface weather map for 13 November 1966 at 0000 hr with the LASA array represented as a star. The North Atlantic near Greenland and Scandinavia was stormy, and a front was passing through Newfoundland. These occurrences probably account for the seismic energy from the northeast. A front was passing along the Pacific coast in a direction about S15° W from the LASA. This is probably the cause of seismic energy originating slightly south-of-west near 0.15 cps.

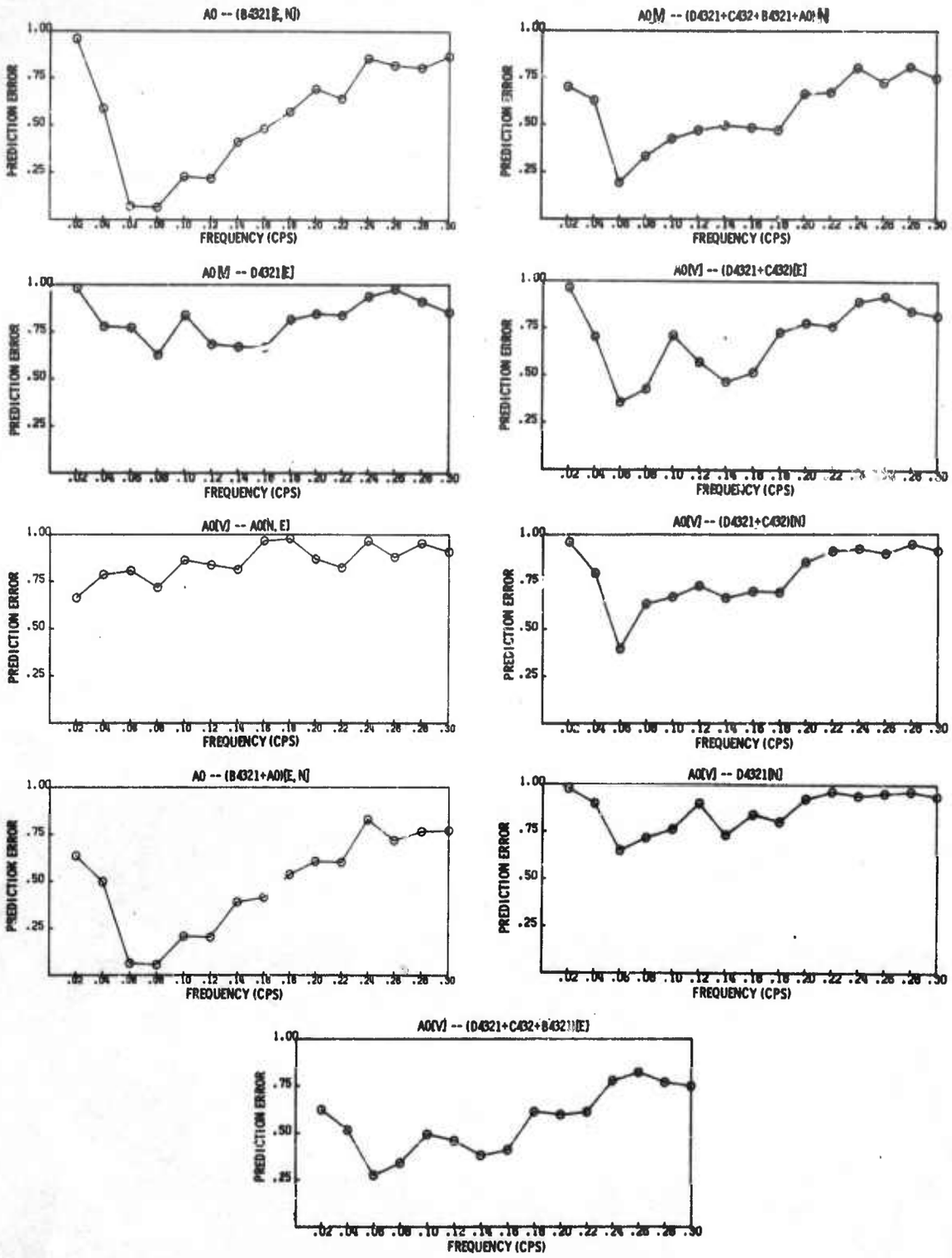


Figure II-4. Multiple Coherences Between A0 Vertical and Combinations of Horizontal Sensors

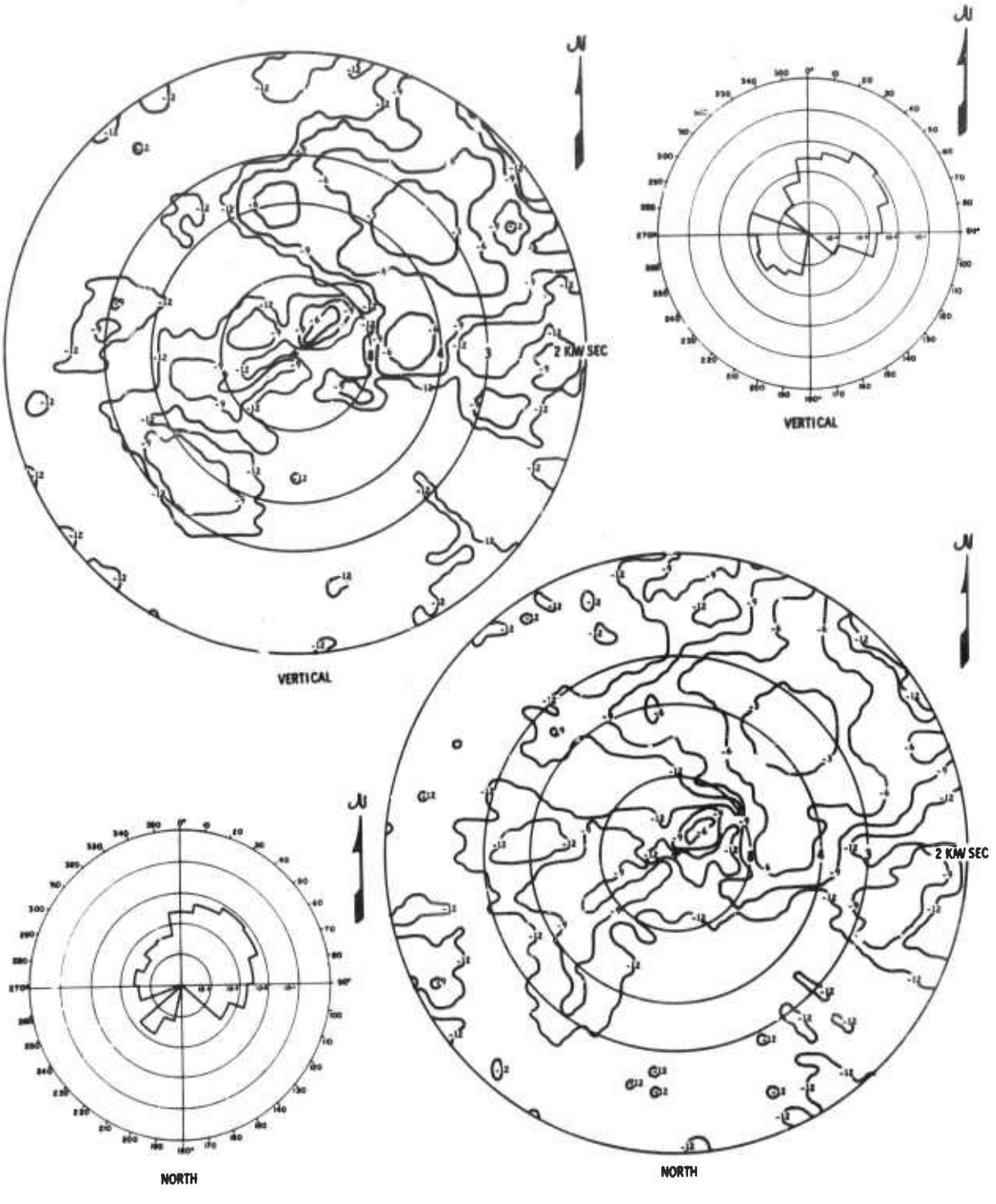


Figure II-5. Wavenumber Spectra and Azimuthal Power Distribution at 0.06 cps, 12 November 1966

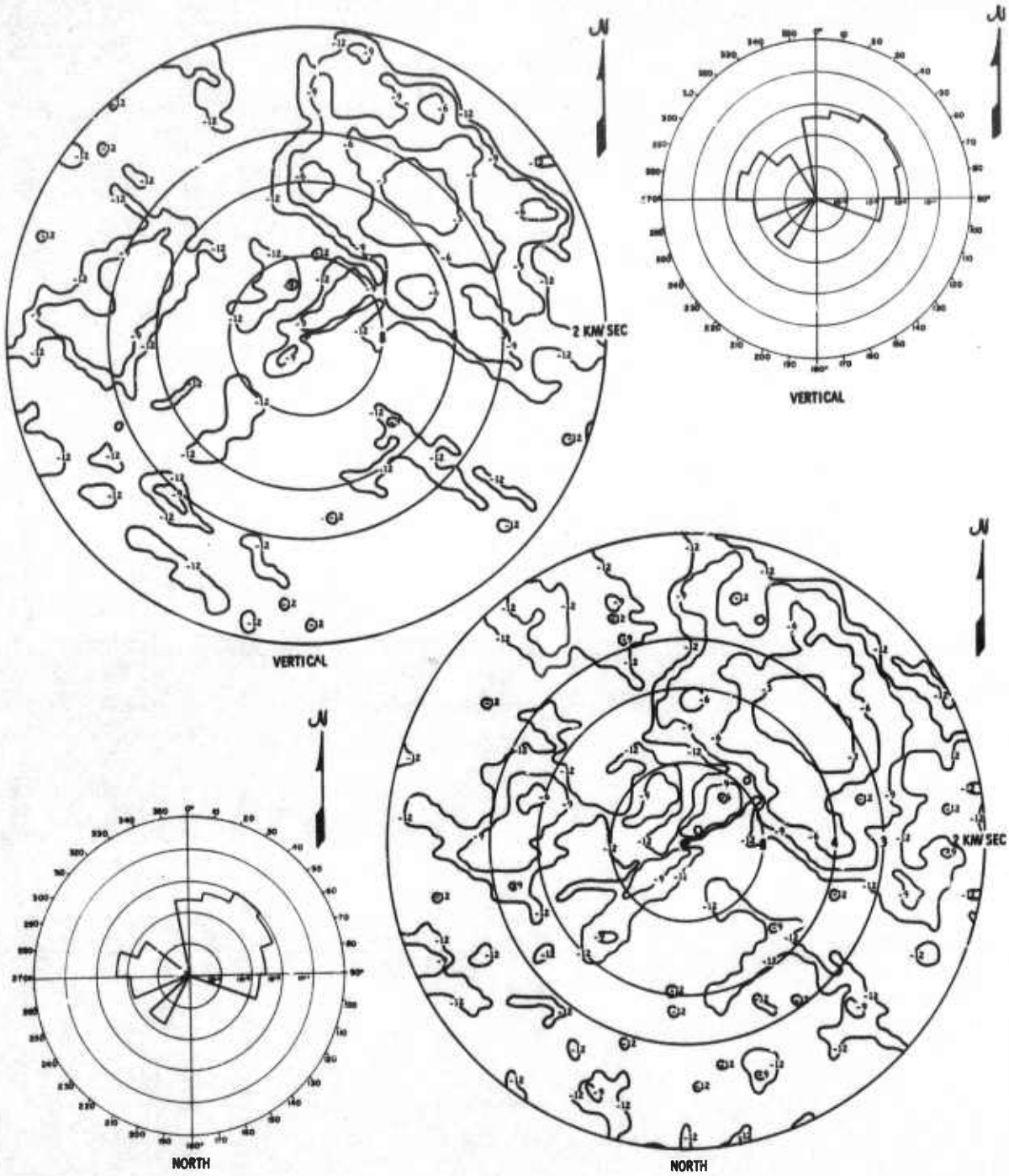


Figure II-6. Wavenumber Spectra and Azimuthal Power Distribution at 0.08 cps, 12 November 1966

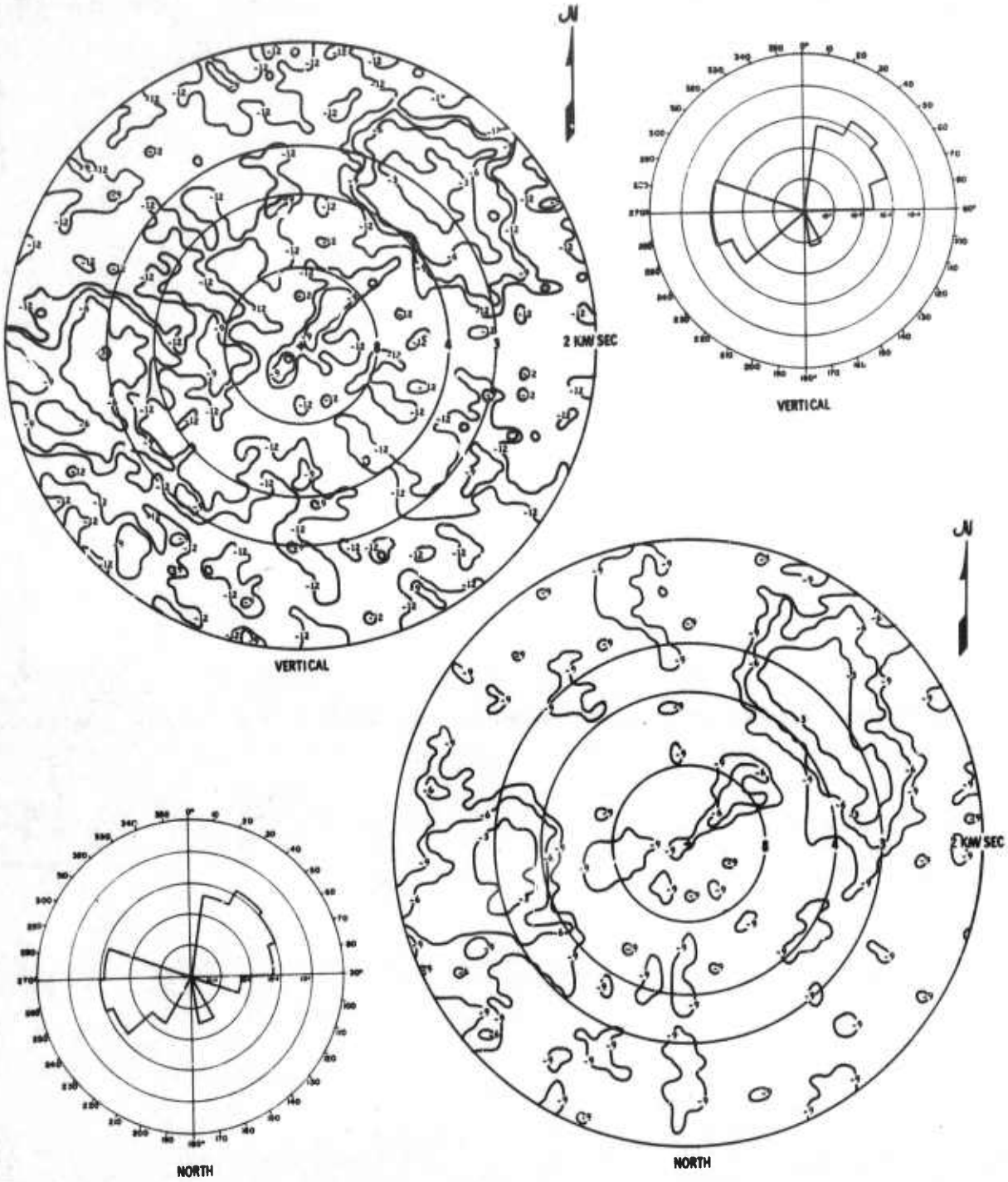


Figure II-7. Wavenumber Spectra and Azimuthal Power Distribution at 0.14 cps, 12 November 1966

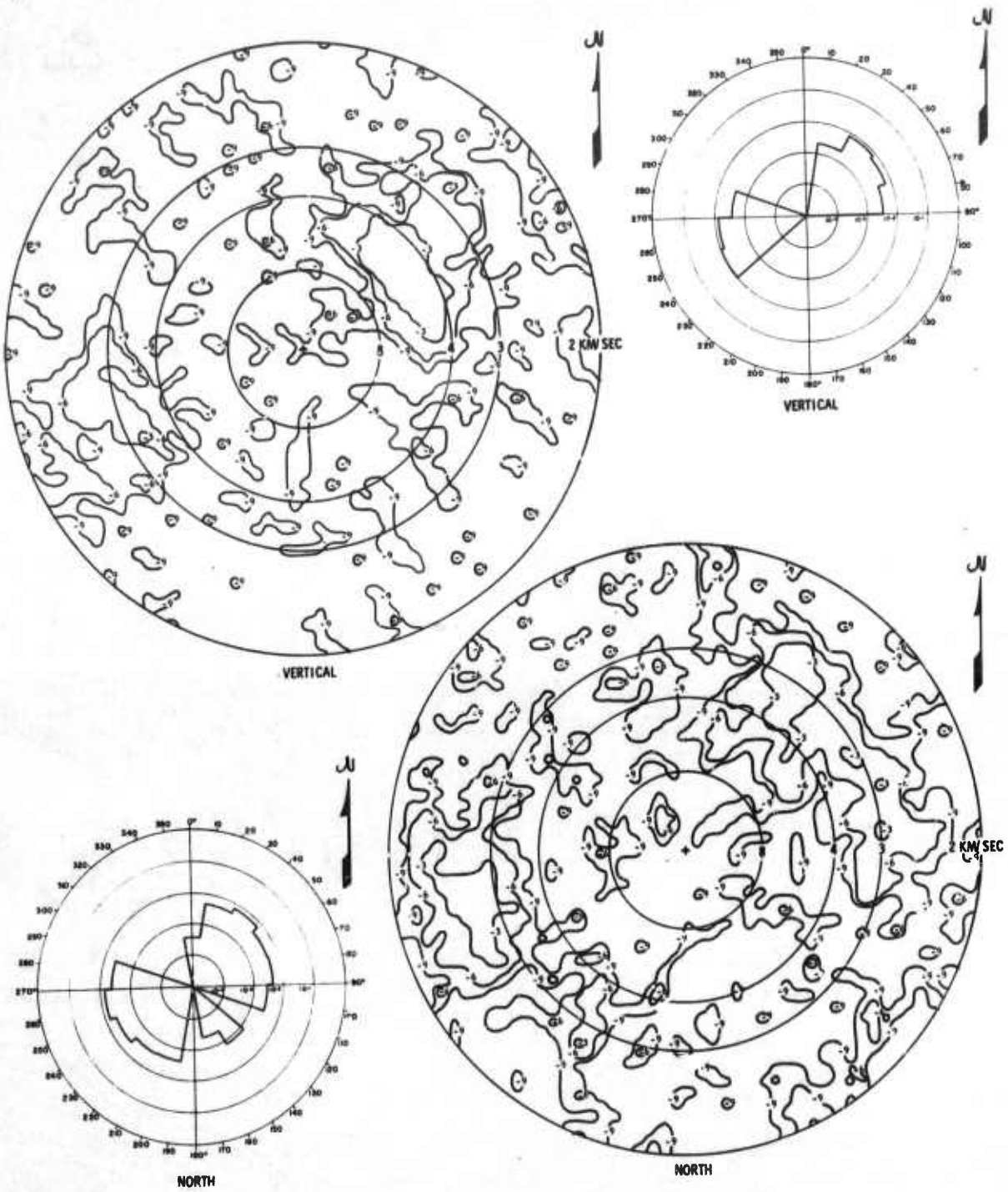


Figure II-8. Wavenumber Spectra and Azimuthal Power Distribution at 0.16 cps, 12 November 1966

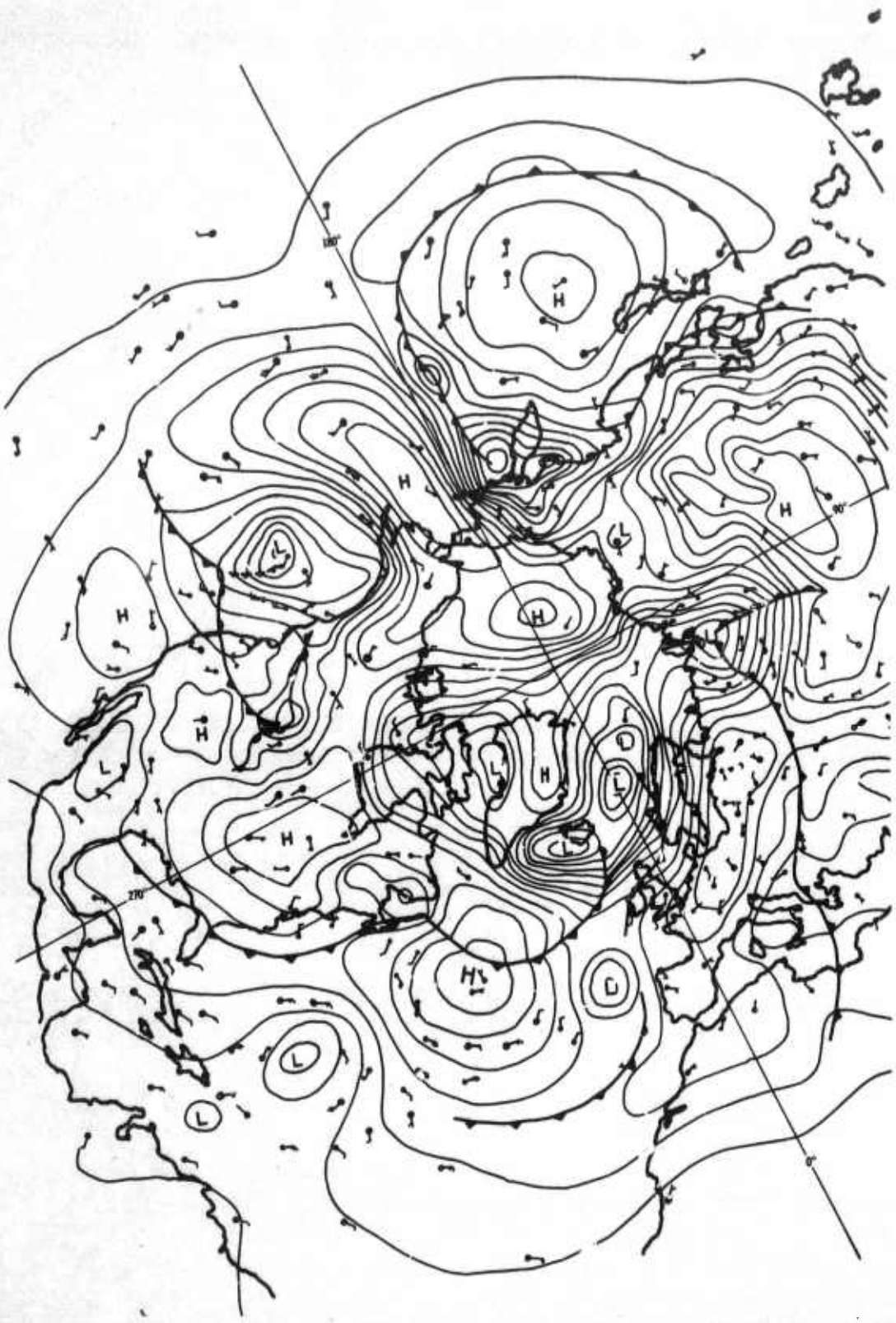

Figure II-9. Surface Weather Map for 13 November 1966 at 0000 Hr

Figure II-10 shows power spectra from A0, F2, F3, and F4 for the 18 November noise sample. These power spectra have the following salient characteristics:

- A peak near 0.05 cps for the spectra of the vertical seismometers
- A broad peak in the 0.12- to 0.22-cps range
- General spatial similarity of spectra of like components (horizontal and vertical) above 0.05 cps
- Spectra of horizontal components 5 to 10 db noisier than those of vertical components in 0.12- to 0.22-cps range
- No appreciable seismic energy above 0.25 cps

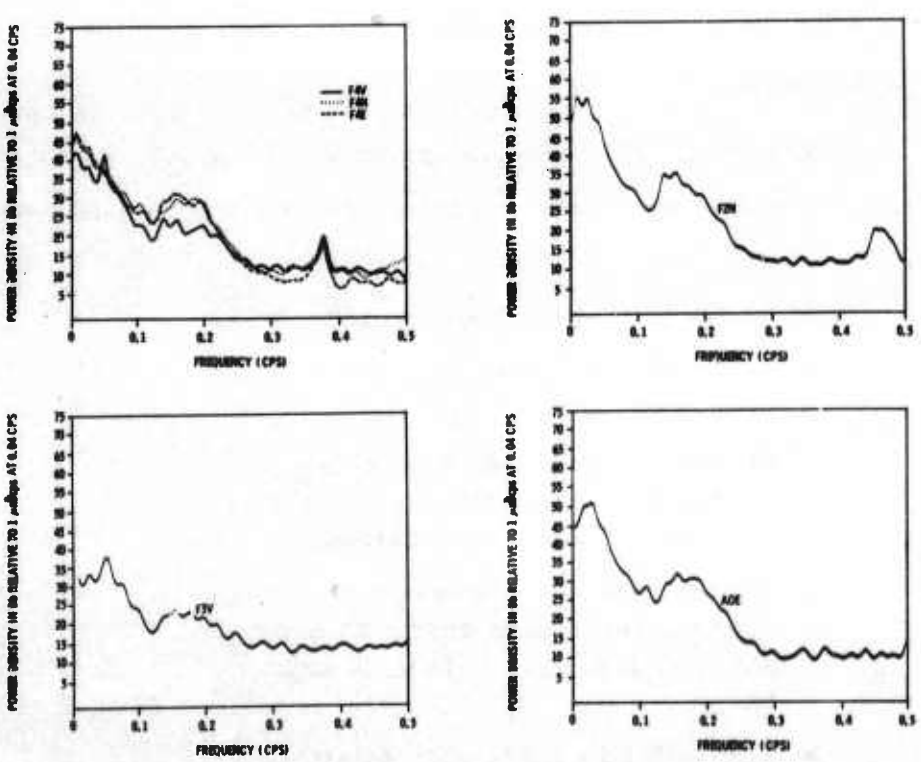

Figure II-10. Power Spectra of 18 November 1966 Noise

Figures II-11 and II-12 show the wavenumber spectra and aximuthal power distribution plots for the vertical and east-west components at 0.05 and 0.14 cps, respectively. Spectra from the two different components show power-density peaks from the northeast and southwest with velocity of about 3.5 km/sec. The vertical component spectra indicate peaks of about equal intensity from N65-70°E and about S40°W. The east-west component spectra show a broad peak from the east and a weaker peak from the southwest. At 0.14 cps, the vertical and east-west spectra show a broad azimuthal peak to the east-northest and a peak to the southwest. The dominant peak from the east-northeast has a velocity of about 3 km/sec.

Figure II-13 shows the weather map for 18 November 1966 at 1800 hr. A front extends through the Great Lakes and the Nova Scotia coastline that probably generates the seismic energy from the east-northeast. There is a front off the California coast which may be generating the seismic energy from the southwest.

Figure II-14 shows power spectra from A0, E2, E3, F1, and F2 for the 2 December 1966 noise sample. Salient features of these spectra are

- There is a sharp peak near 0.05 cps
- A broad peak exists in the 0.12- to 0.20-cps range
- Similar components (horizontal and vertical) have similar spectra above 0.05 cps at different locations
- The horizontal components are 5- to 10-db noisier than vertical components in the 0.12- to 0.20-cps range
- There is no appreciable seismic energy above the 0.27-cps range

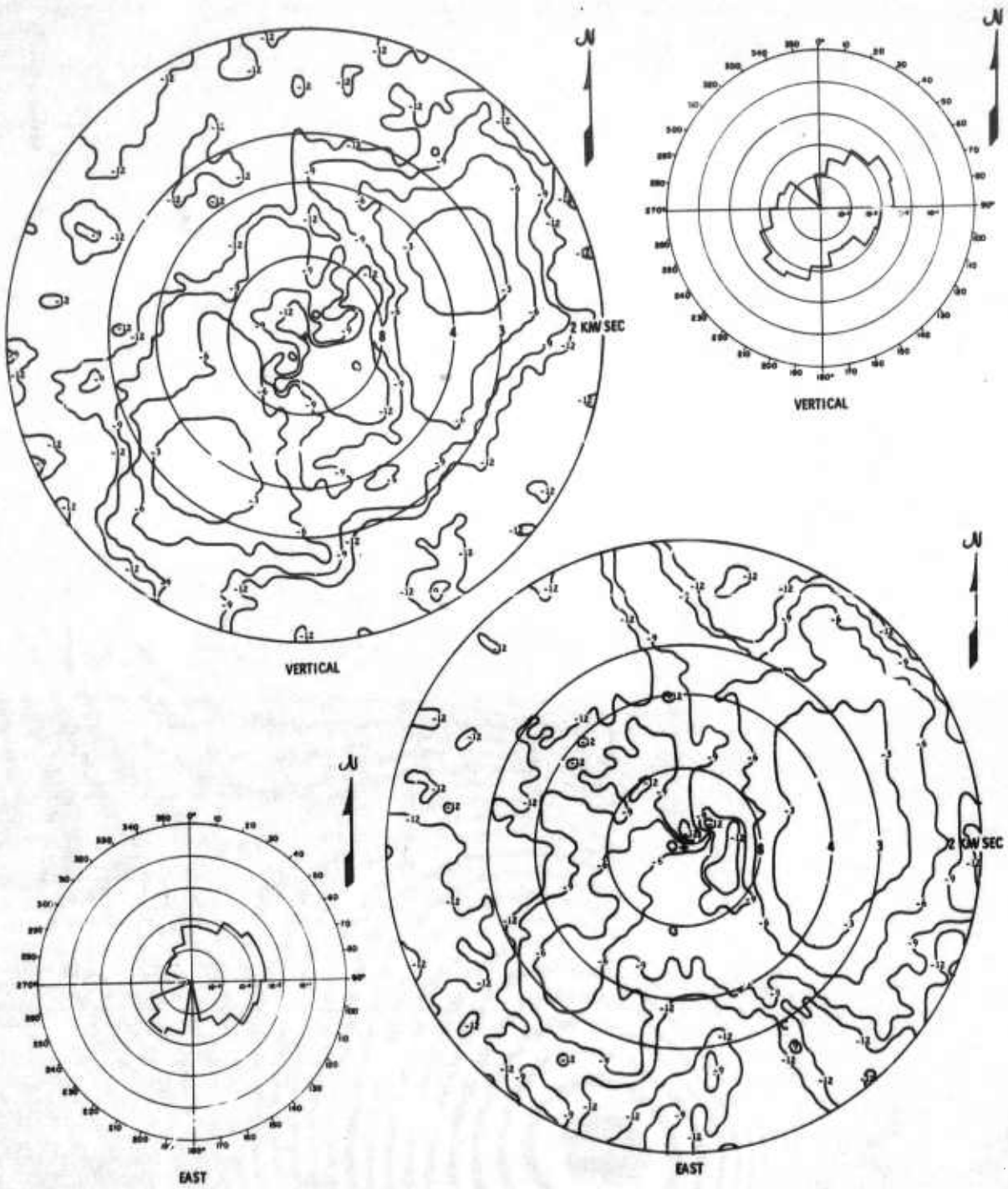


Figure II-11. Wavenumber Spectra and Azimuthal Power Distribution at 0.05 cps, 18 November 1966

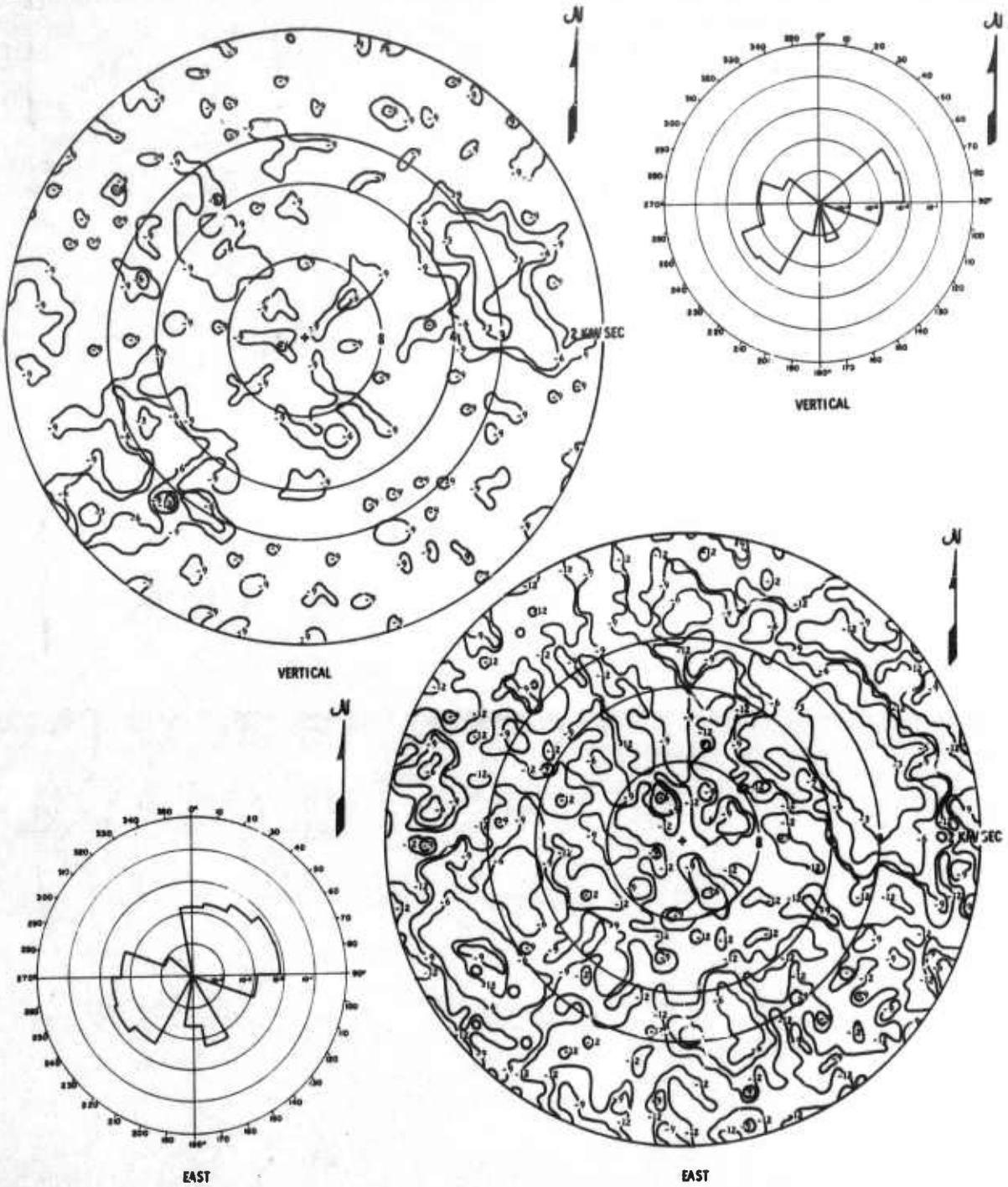


Figure II-12. Wavenumber Spectra and Azimuthal Power Distribution at 0.14 cps, 18 November 1966


Figure II-13. Surface Weather Map for 18 November 1966 at 1800 Hr

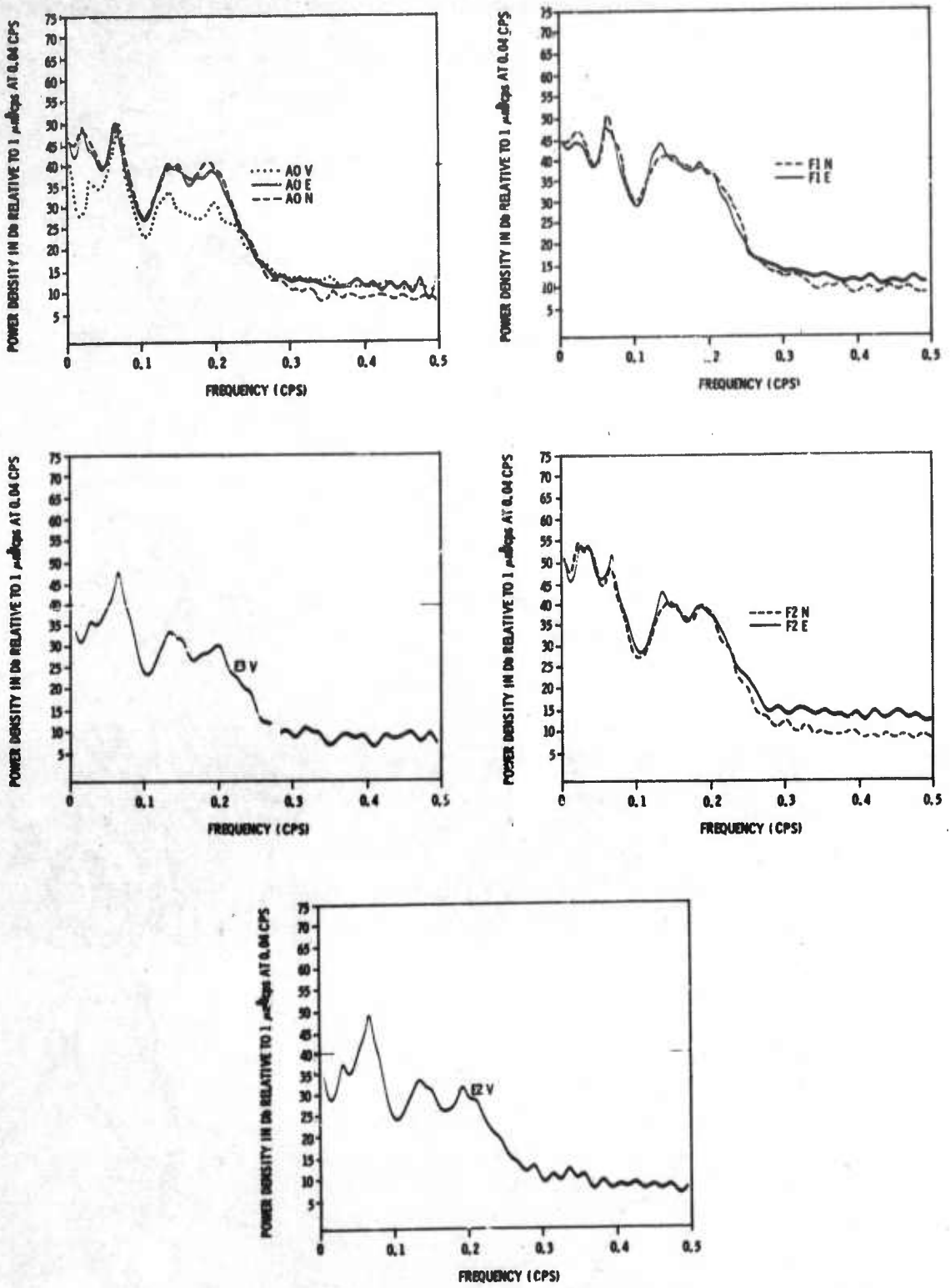


Figure II-14. Power Spectra of 2 December 1966 Noise

Figures II-15 and II-16 show the multiple coherences between vertical and north-south components, respectively. The A0 vertical component is quite predictable near 0.06 cps, even from sensors more than 50 km away from A0 (E and F rings). The A0 north-south component is only slightly less predictable than the vertical component. Coherence falls off sharply below 0.05 cps on both components and above 0.22 cps for the north-south component.

Figure II-17 shows the predictability of the A0 vertical component from various combinations of horizontal components. The 0.06-cps peak is very predictable from nearby horizontal components and is quite predictable (75 percent) from horizontal components at A0. The A0 vertical component is moderately predictable up to 0.15 cps from nearby horizontal components.

Figures II-18, II-19, and II-20 show the wavenumber spectra and azimuthal power distribution of the vertical and east-west components at 0.06, 0.08, and 0.14 cps, respectively. At 0.06 and 0.08 cps, the spectra of both components are dominated by a source centered between N40-45°E with an associated velocity of about 3.3 km/sec. In addition, there is a weaker peak from the west with similar velocity at 0.08 cps. At 0.14 cps, the dominant source for both components is still from the northeast; however, the peak appears to have shifted somewhat to the north. The weaker peak to the west is still evident on the vertical component spectrum and has an apparent velocity of about 3 km/sec.

The 2 December noise sample was recorded from 21:37:00.5 to 22:49:50.9 hrs. Two 3 December noise samples were studied. These were recorded from 04:17:00.5 to 05:36:59.9 and from 05:37:00.5 to 06:56:59.9 hr. Thus, there were two back-to-back 80-min samples, separated by about 6 hr from the previous 2 December noise sample. These noise samples can be used to estimate the short-term time stability of the noise field. The two 3 December noise samples will be referred to as Dec 3A and Dec 3B, respectively.

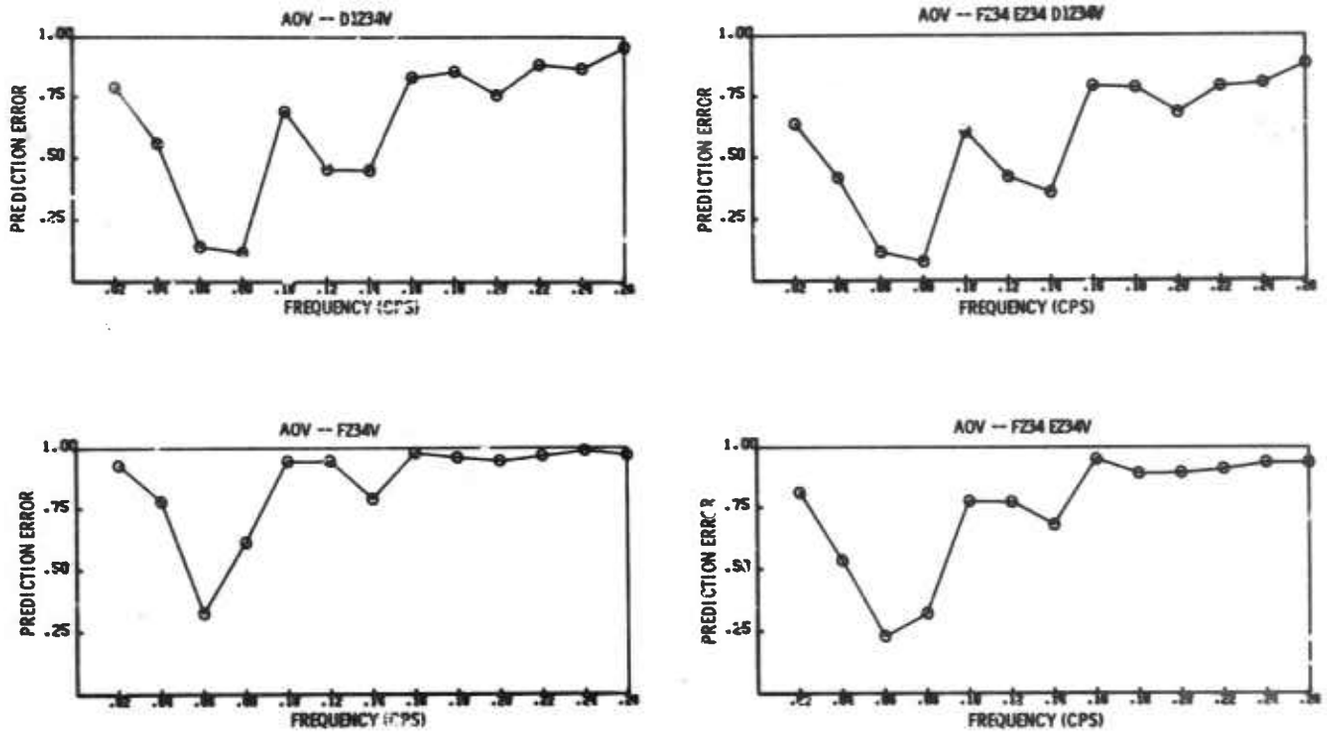


Figure II-15. Multiple Coherences Between Vertical Components, 2 December 1966

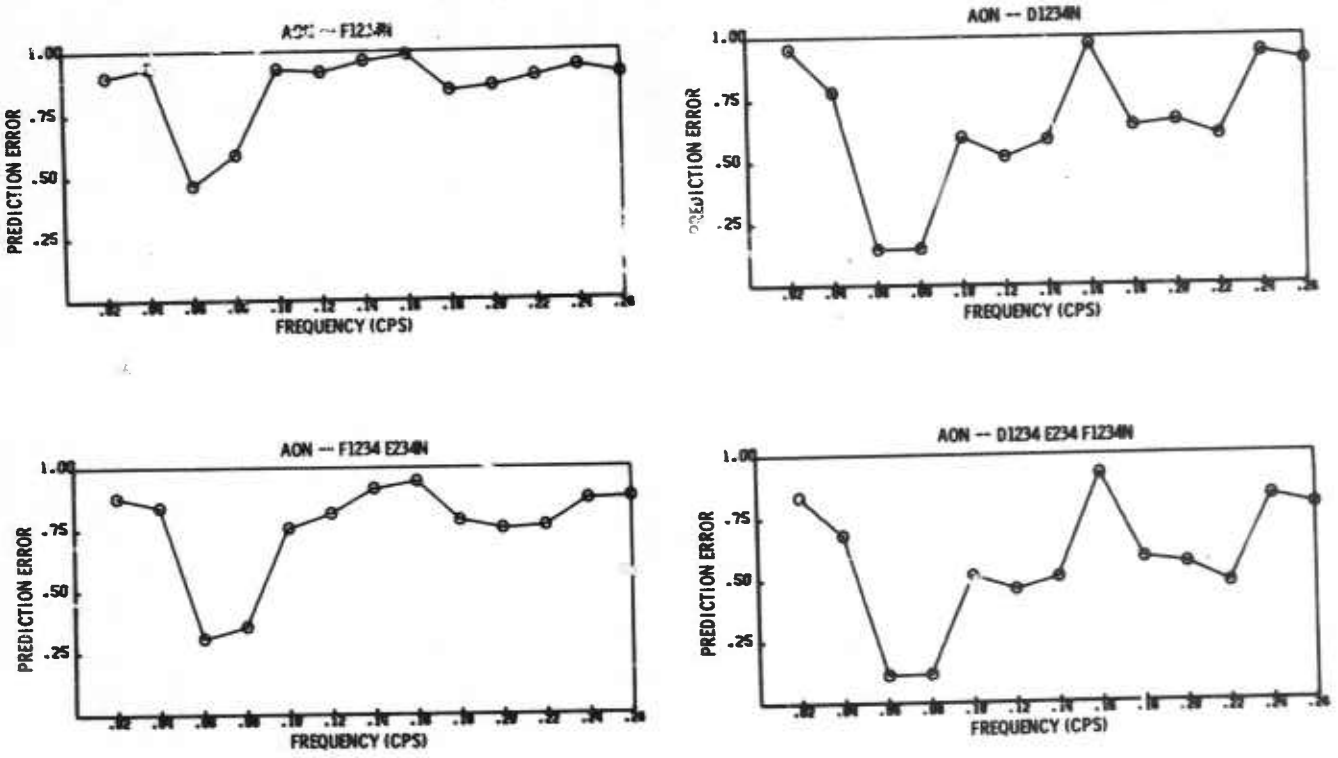


Figure II-16. Multiple Coherences Between Horizontal Components, 2 December 1966

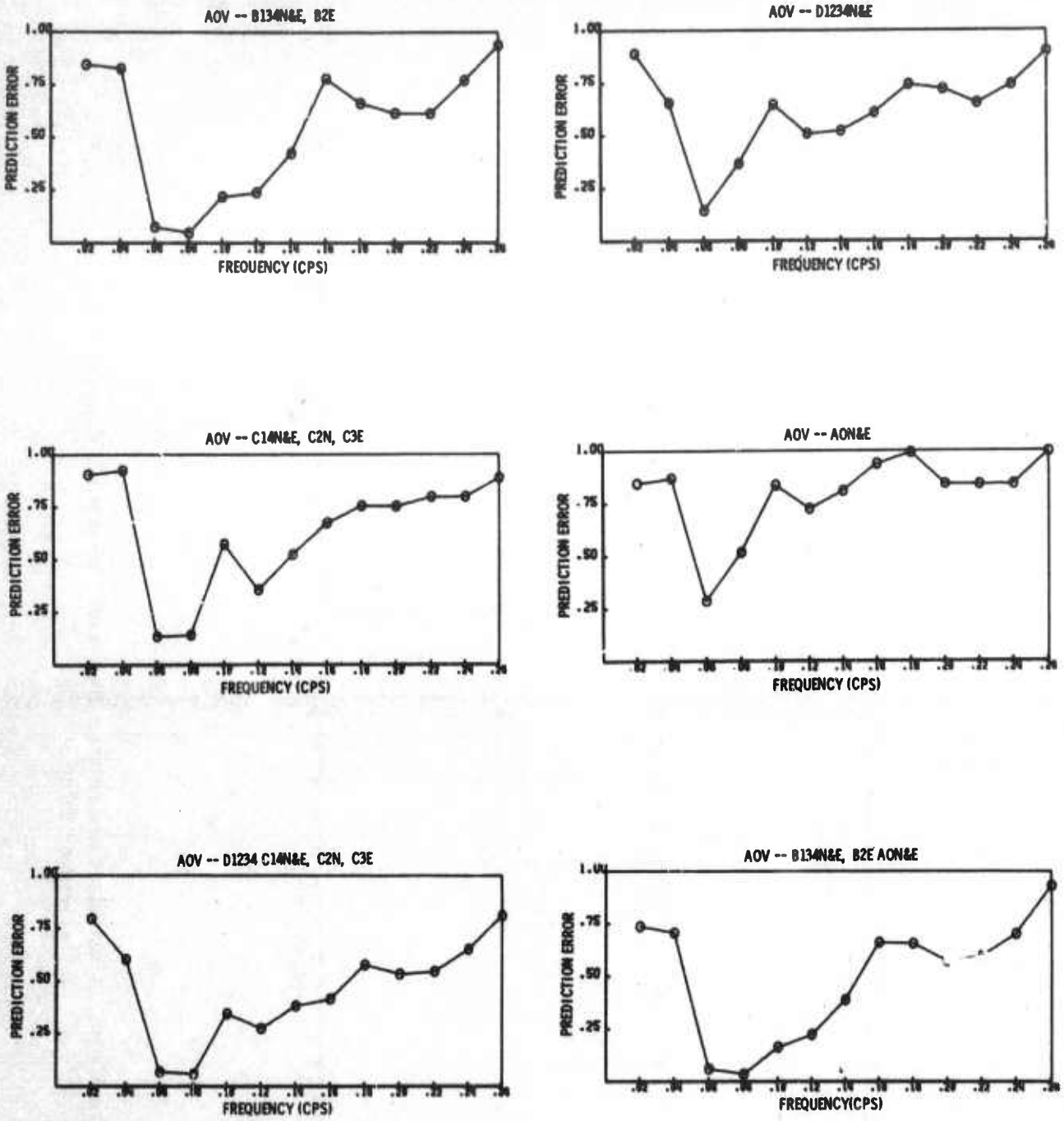


Figure II-17. Predictability of the A0 Vertical Component from Combinations of Horizontal Components, 2 December 1966

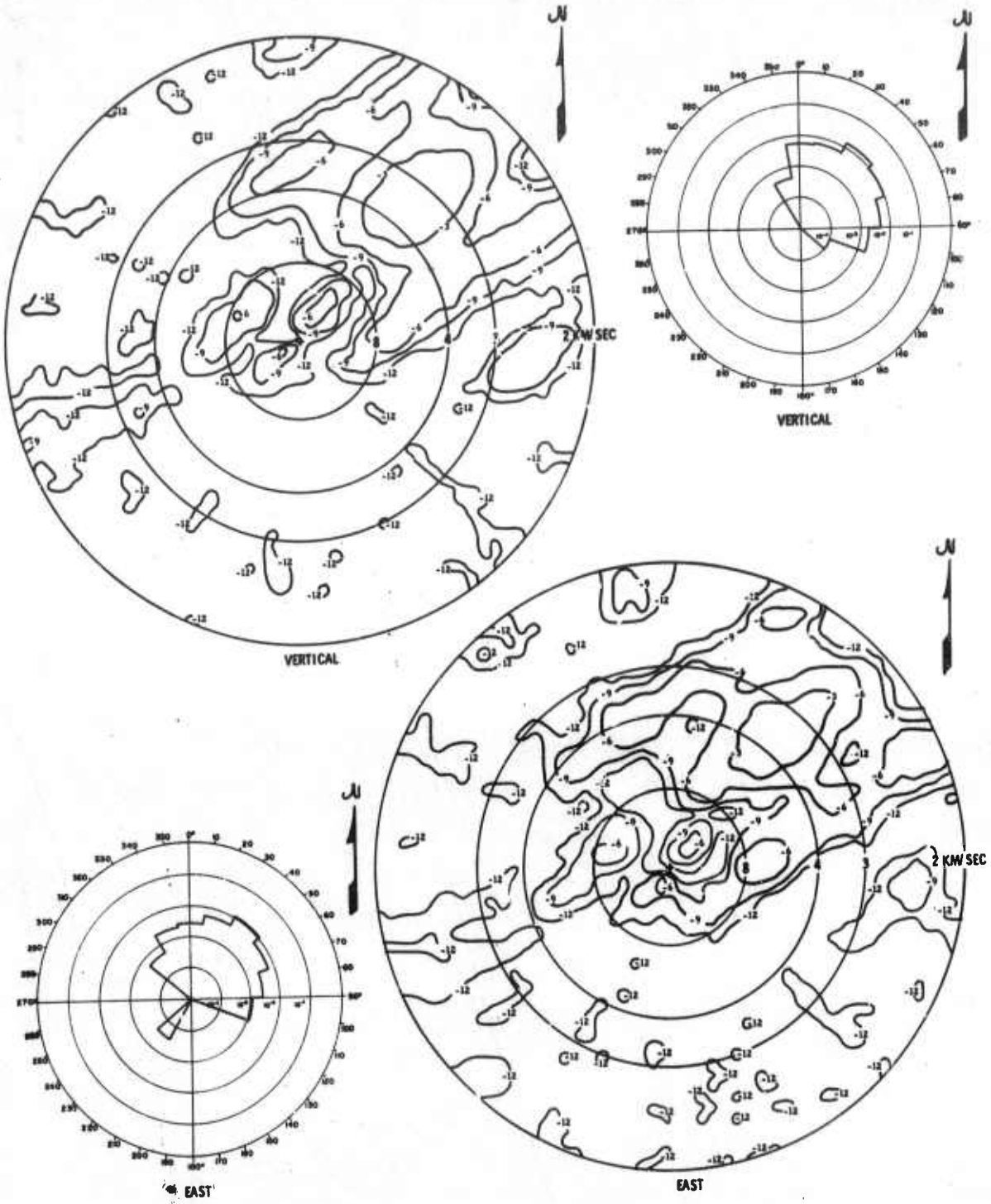


Figure II-18. Wavenumber Spectra and Azimuthal Power Distribution at 0.06 cps, 2 December 1966

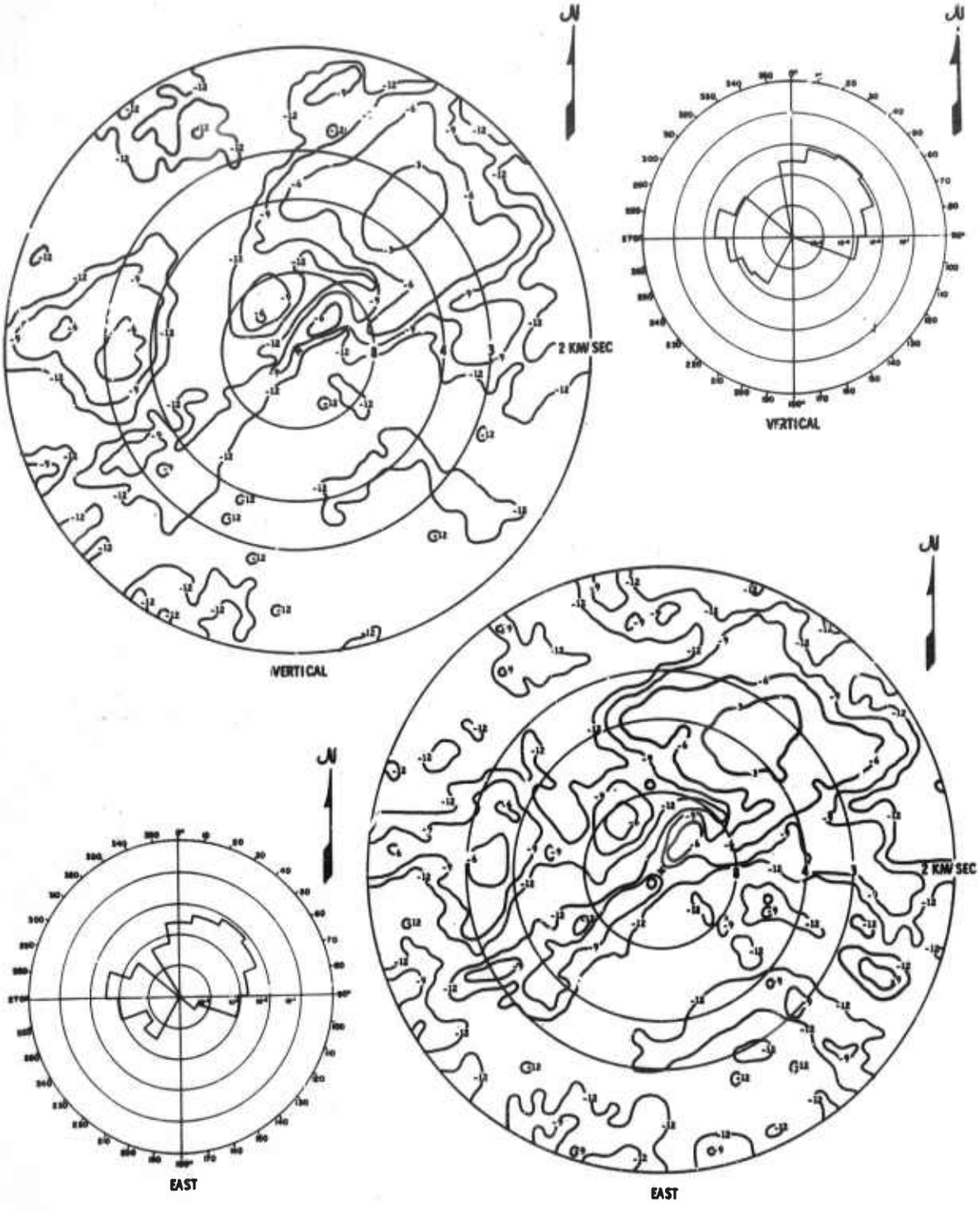


Figure II-19. Wavenumber Spectra and Azimuthal Power Distribution at 0.08 cps, 2 December 1966

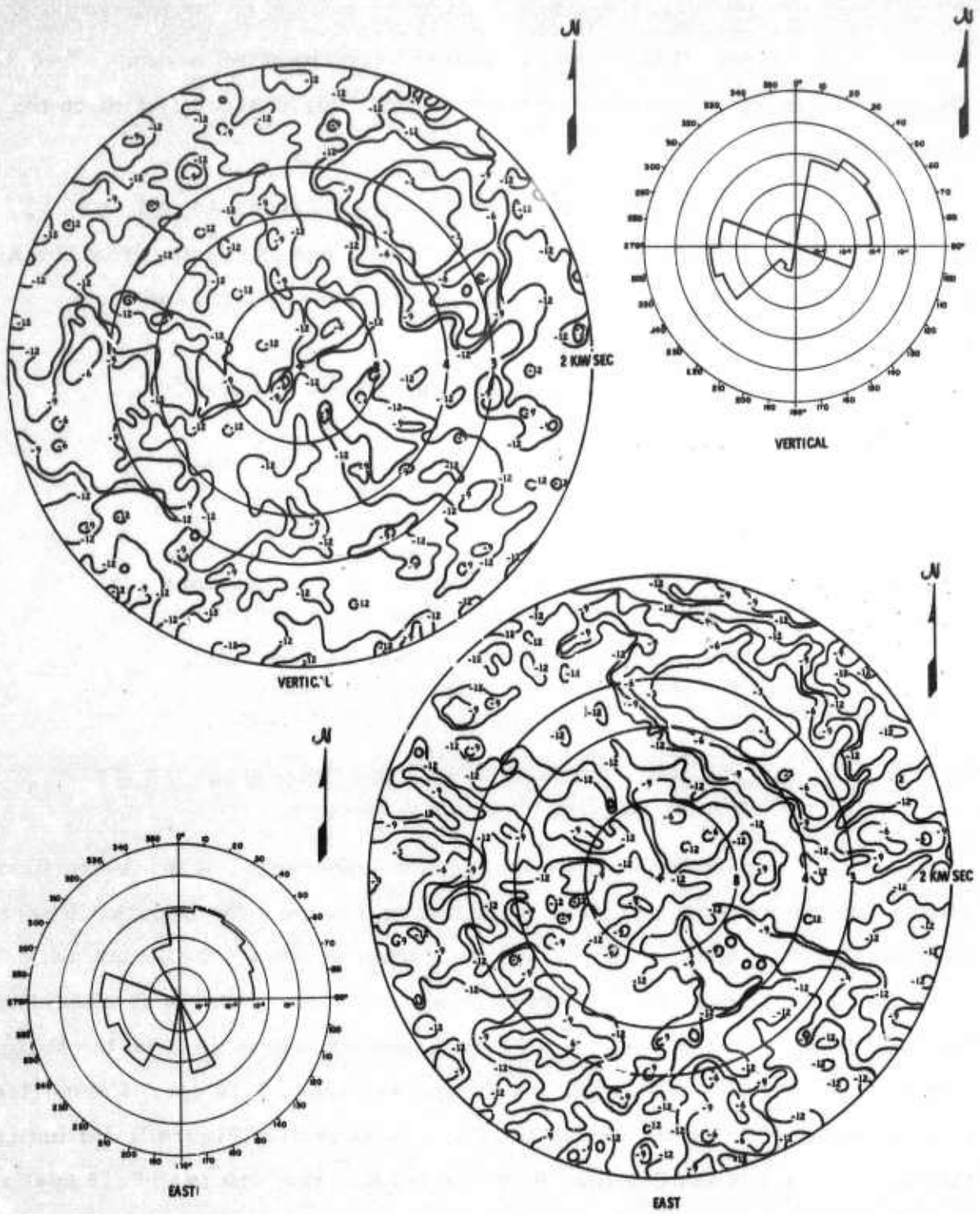


Figure II-20. Wavenumber Spectra and Azimuthal Power Distribution at 0.14 cps, 2 December 1966

Figure II-21 shows a 600-sec segment of noise sample Dec 3A. The seismic energy appears to arrive in bursts; this is most evident on the vertical traces.

Figure II-22 shows power spectra from the A0, F1, F2, F3, and F4 locations for Dec 3A. Figure II-23 shows power spectra from the A0, F1, and F4 locations for Dec 3B. Considering these spectra and the 2 December spectra (Figure II-12):

- Spectra for Dec 3A and Dec 3B are essentially identical
- Spectra for both 2 December and 3 December noise samples are quite similar from about 0.05 to 0.15 cps; there is a decided change in the 0.15- to 0.25-cps band; the 3 December sample has considerably less power than does the 2 December spectra from 0.15 to 0.25 cps
- The like-component (vertical and horizontal) spectra are quite similar at different locations above 0.05 cps for Dec 3A and Dec 3B
- There is no appreciable seismic energy in Dec 3A and Dec 3B above 0.25 cps

Figure II-24 shows the multiple coherences of the A0 vertical component with various combinations of vertical outputs for Dec 3A. Power near the 0.06-cps peak is very predictable from sensors over 30-km away from A0 (D ring) and is strongly predictable even from sensors as distant as 100 km (Fring). The peak near 0.13 cps is quite predictable from the D ring. Coherence drops off sharply below 0.05 cps and above 0.16 cps. Comparison of these multiple coherences with the 2 December noise (Figure II-14) indicates that the results are similar near 0.06 cps but that the peak near 0.13 cps is significantly more predictable for Dec 3A.

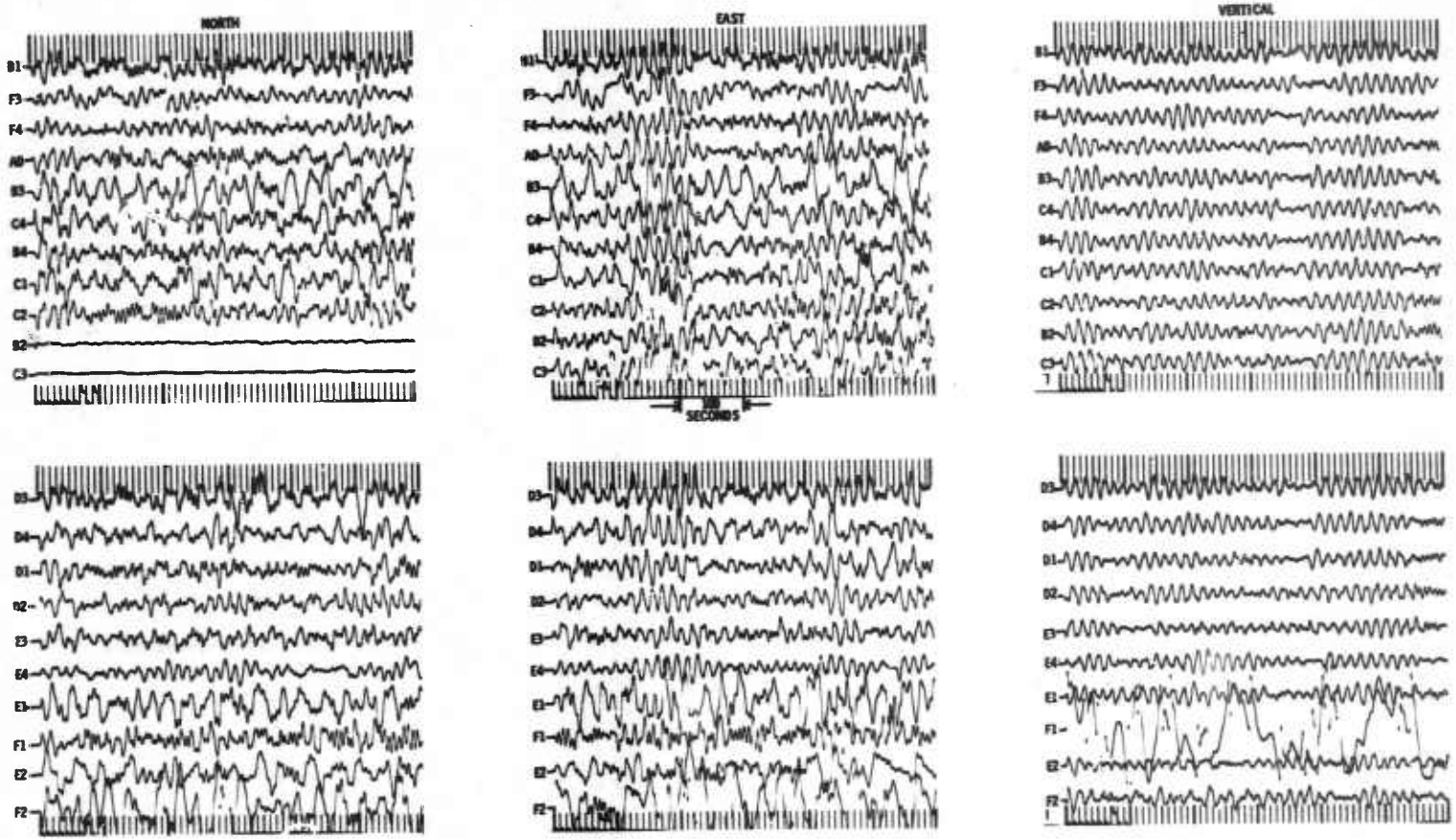


Figure II-21. Portion of 3 December 1966 Noise Sample

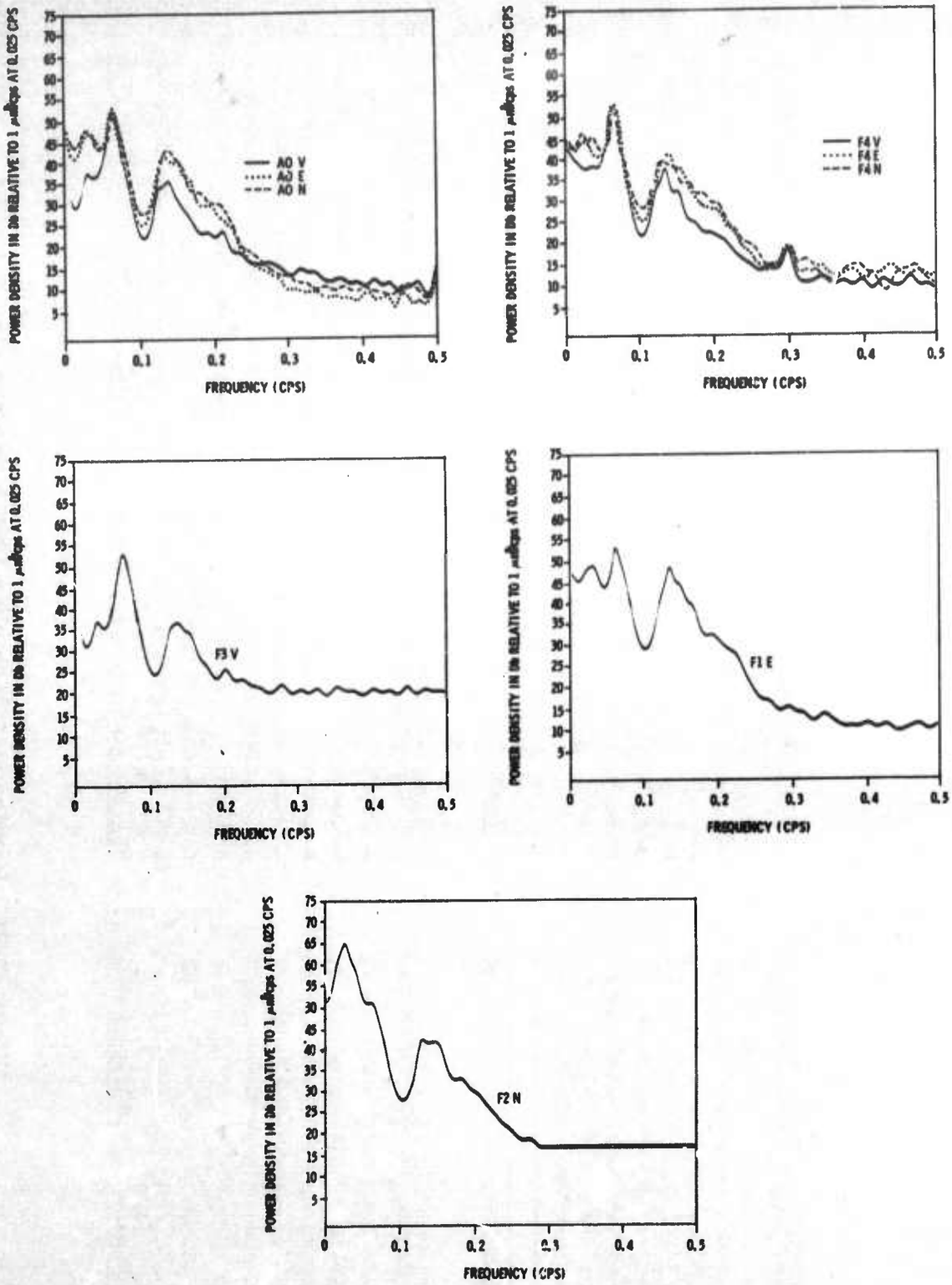


Figure II-22. Power Spectra of Dec 3A Noise

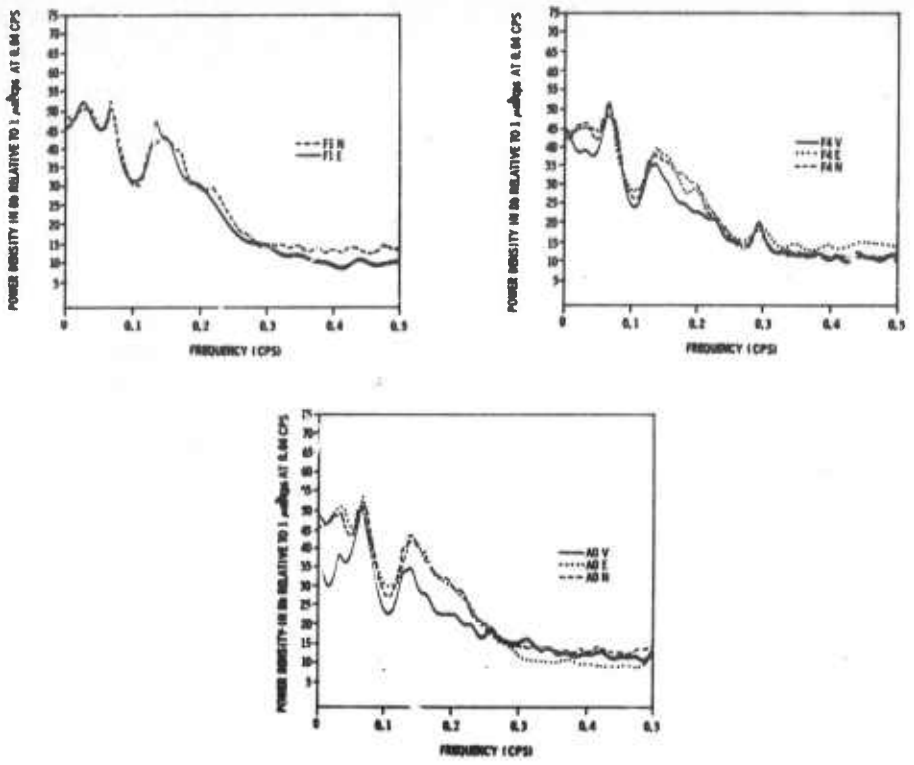

Figure II-23. Power Spectra of Dec 3B Noise

Figure II-25 shows the multiple coherences of the A0 north-south component with various combinations of north-south components for Dec 3A. The north-south component is also quite coherent across the entire array near 0.06 cps but is slightly less coherent than the vertical component. The north-south component is definitely less coherent than the vertical for the peak near 0.13 cps. Coherence drops off sharply below 0.05 cps and above 0.15 cps. Comparing these coherences with those for the 2 December noise sample (Figure II-15) indicates that both the 0.06-cps peak and the 0.13-cps peak are less predictable using the 2 December noise sample.

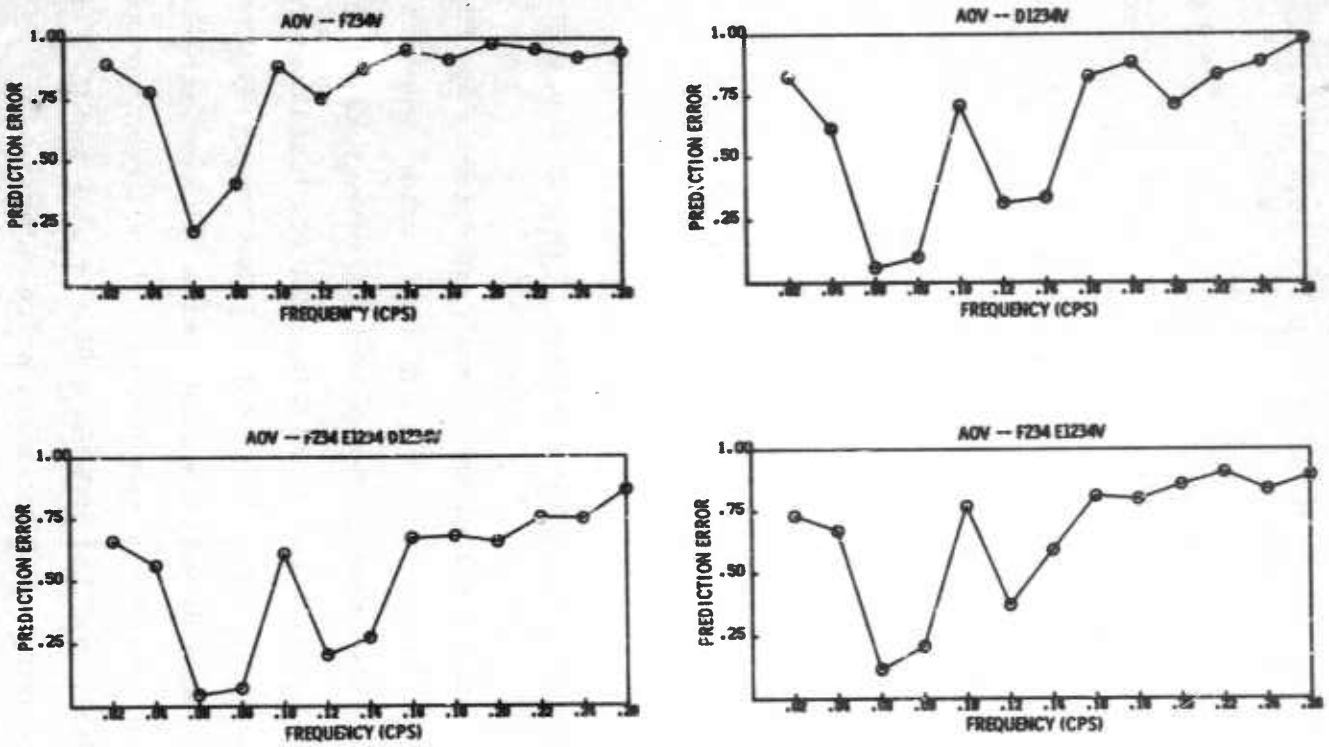


Figure II-24. Multiple Coherences Between the A0 Vertical Component and Combinations of Vertical Components, 3 December 1966

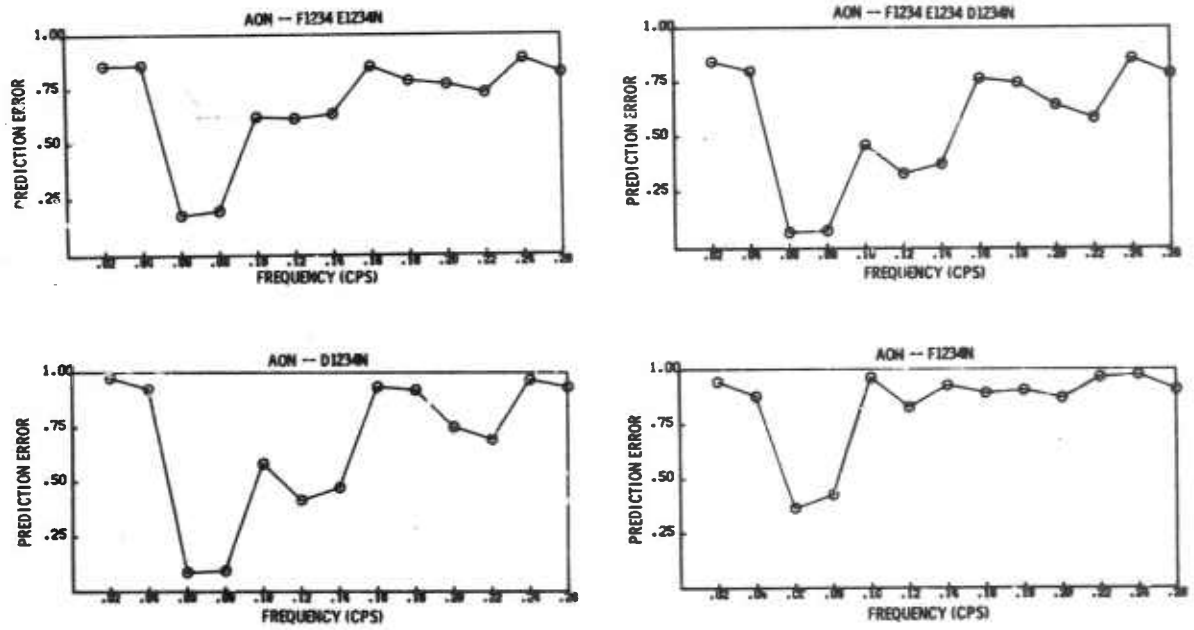


Figure II-25. Multiple Coherences Between the A0 North-South Component and Combinations of North-South Components, 3 December 1966

Figure II-26 shows the multiple coherences between A0 vertical and various combinations of horizontal sensors for Dec 3A. The peak near 0.06 cps is extremely predictable from the nearby horizontals and also from horizontals 30-km distant (D ring). Comparison of these coherences with those obtained from the 2 December noise sample (Figure II-16) indicates that the 0.06-cps peak is slightly more predictable for both 3 December noise samples, and the 0.13-cps peak is definitely more predictable for the 3 December noise samples. This is particularly evident when A0 vertical is predicted from A0 north-south and east-west coherences.

Figure II-27 shows the wavenumber spectra and azimuthal power distribution for the vertical and east-west components for Dec 3A at 0.06 cps. Wavenumber spectra and azimuthal power distribution for the vertical and north-south components for Dec 3B at 0.07 cps are shown in Figure II-28. Figure II-29 shows the wavenumber spectra and azimuthal power distribution for the vertical and east-west components for Dec 3A at 0.08 cps. All these spectra are very similar. They are entirely dominated by a source from N40°E which has a velocity of about 3.5 km/sec. Comparison of these spectra with those of similar frequencies for the 2 December noise sample (Figures II-18 and II-19) indicates that the dominant noise source was the same for the two samples which were taken 6 hr apart.

Figure II-30 shows the wavenumber spectra and azimuthal power distribution for the vertical and east-west components for Dec 3A at 0.14 cps. Wavenumber spectra and azimuthal power distribution for the vertical and north-south components are shown in Figure II-31 for Dec 3B at 0.14 cps.

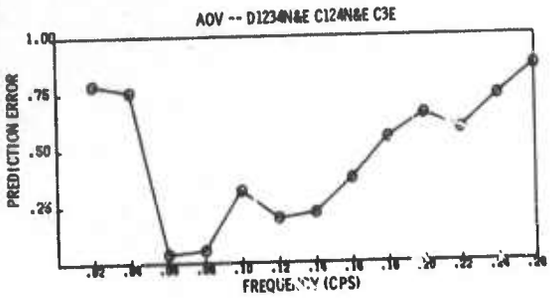


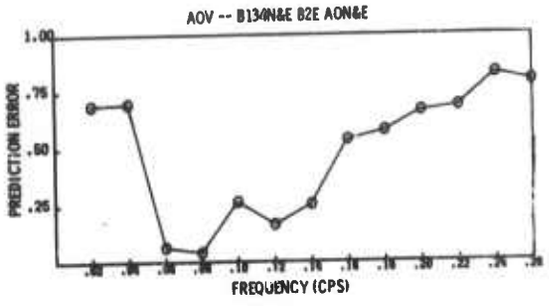


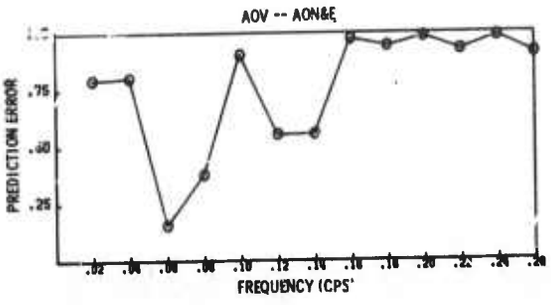


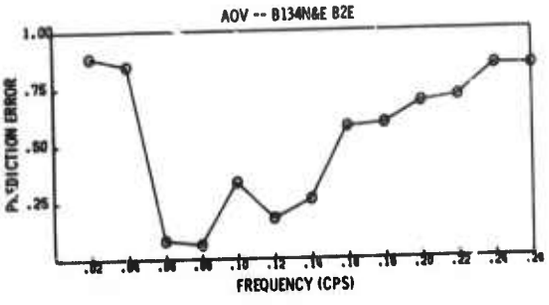


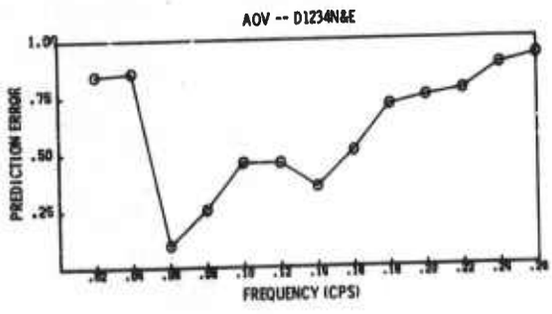


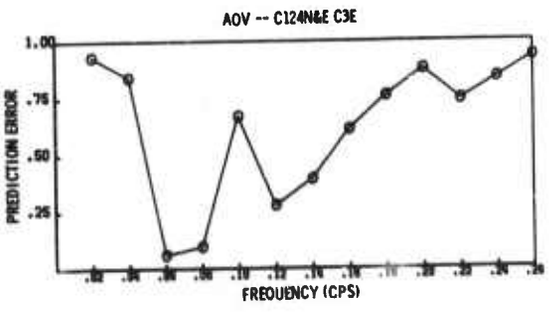


Figure II-26. Multiple Coherences Between the A0 Vertical Component and Combinations of Horizontal Sensors, 3A December 1966

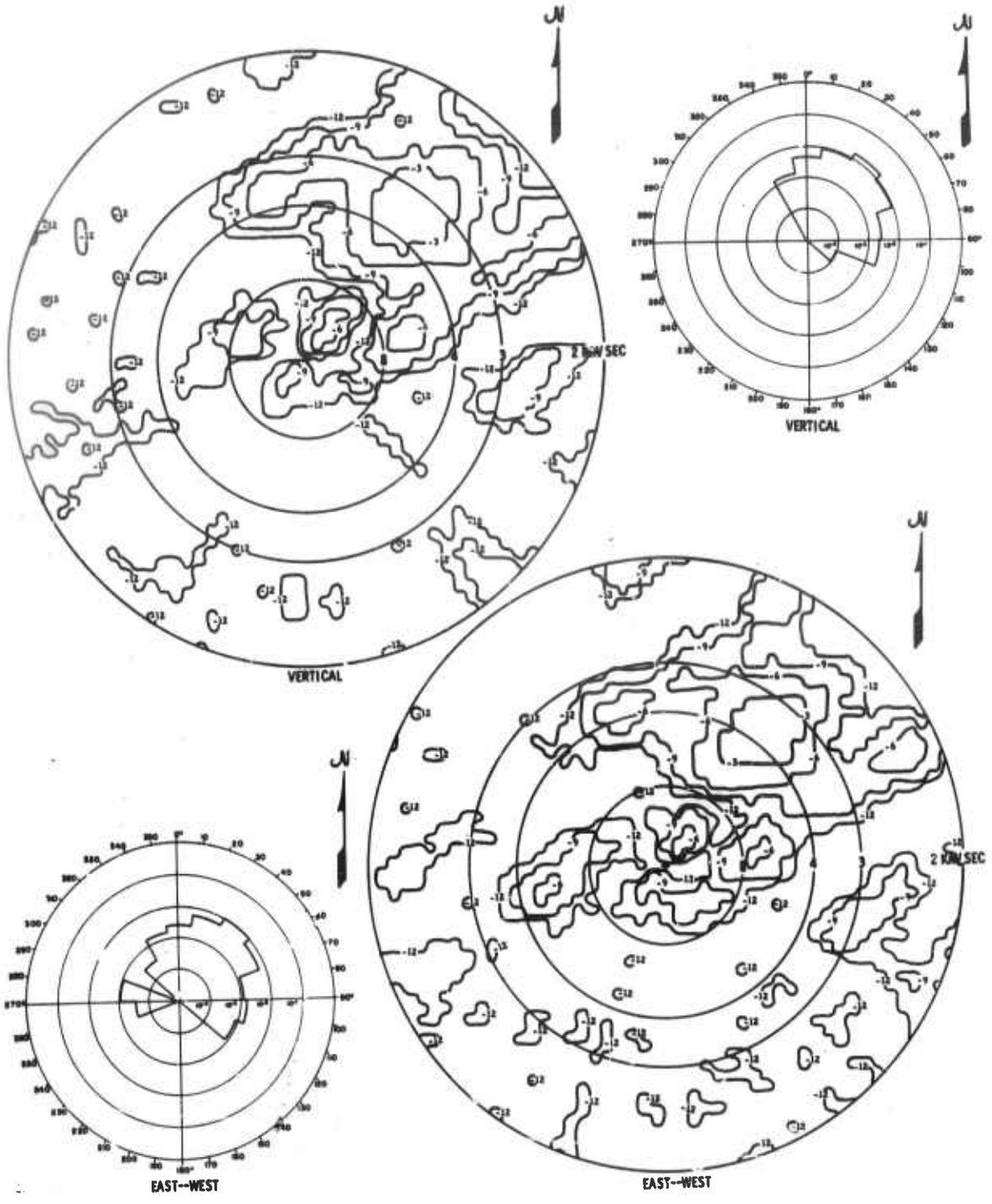


Figure II-27. Wavenumber Spectra and Azimuthal Power Distribution at 0.06 cps, 3A December 1966

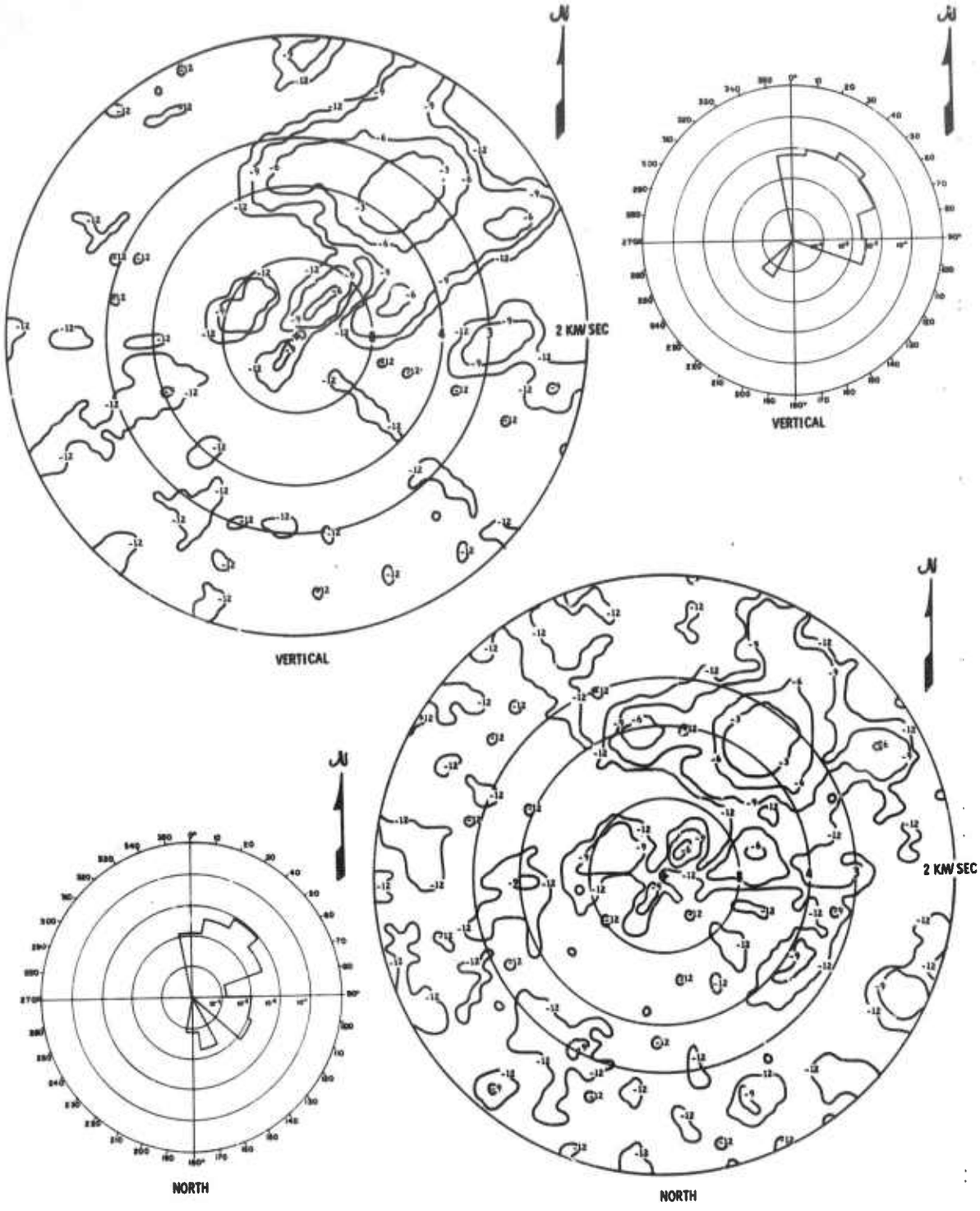


Figure II-28. Wavenumber Spectra and Azimuthal Power Distribution at 0.07 cps, 3B December 1966

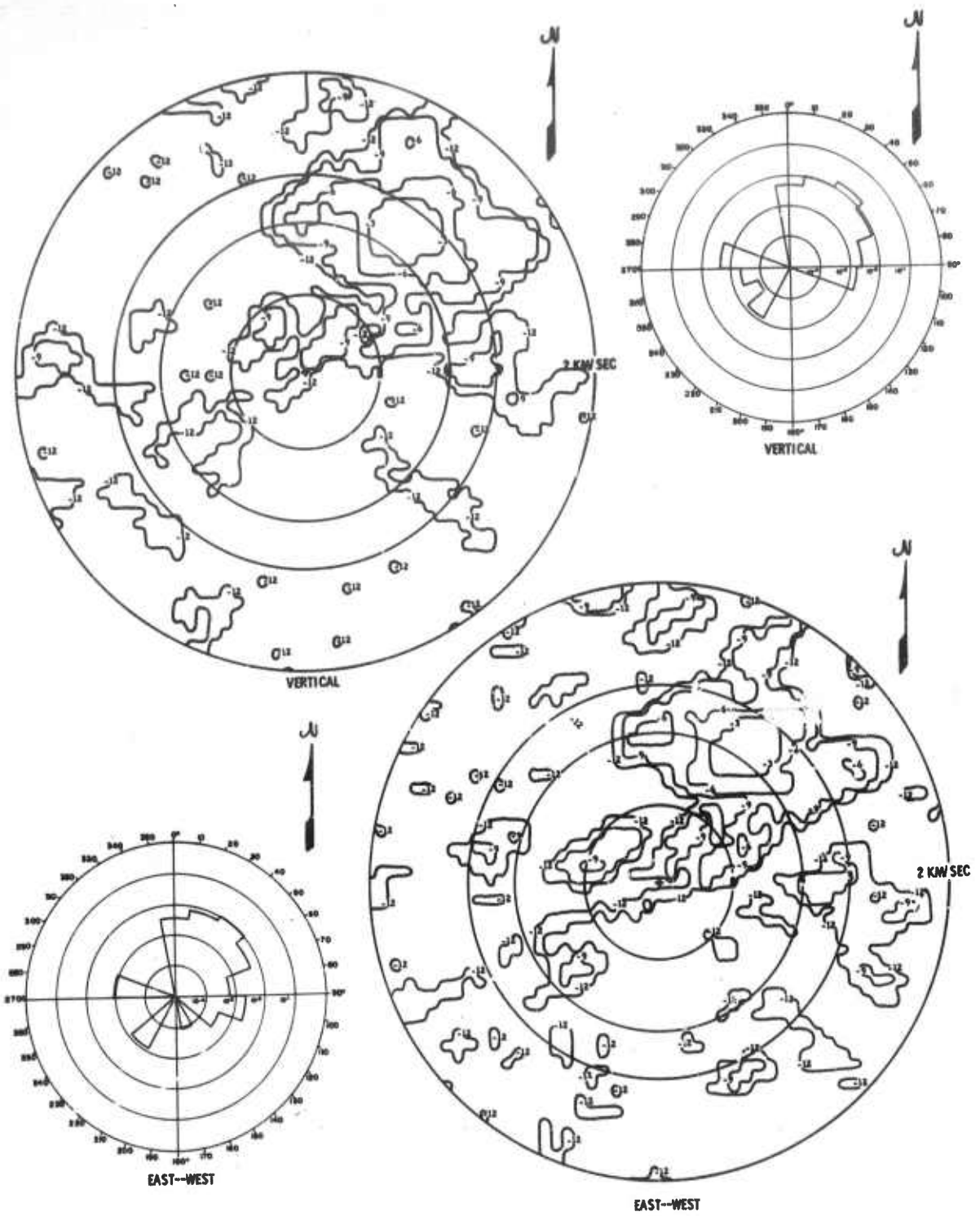


Figure II-29. Wavenumber Spectra and Azimuthal Power Distribution at 0.08 cps, 3A December 1966

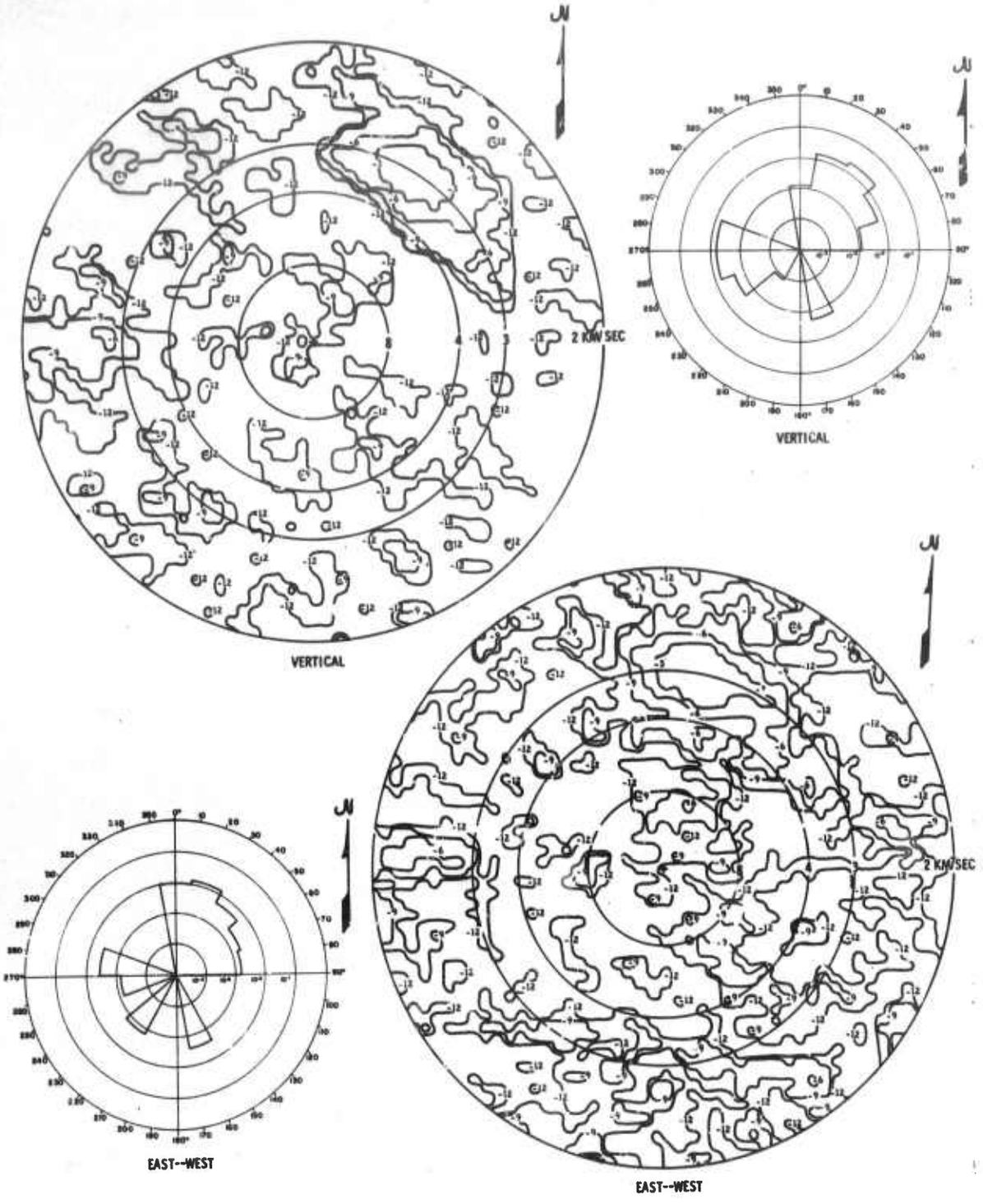


Figure II-30. Wavenumber Spectra and Azimuthal Power Distribution at 0.14 cps for Dec 3A Noise Sample

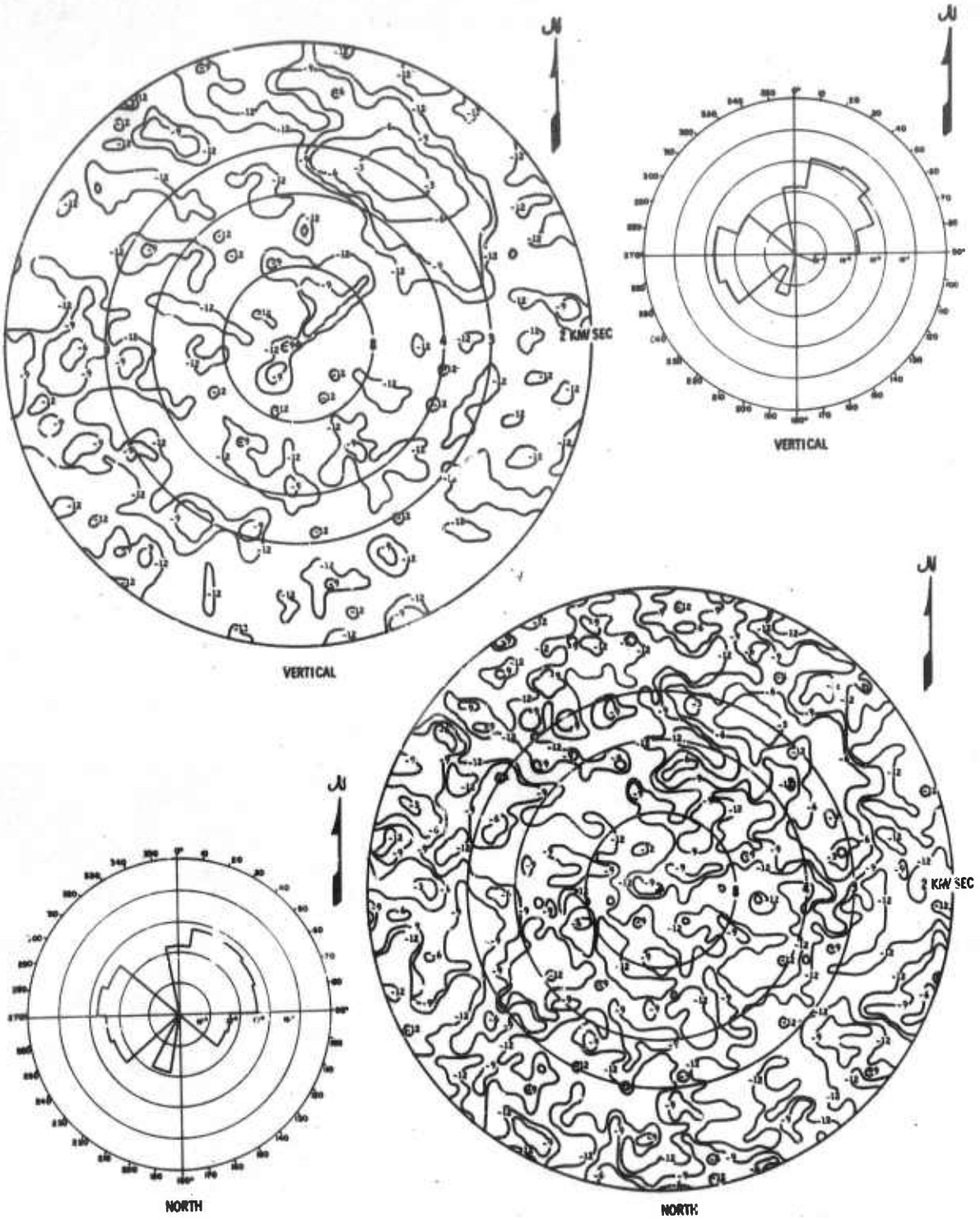


Figure II-31. Wavenumber Spectra and Azimuthal Power Distribution at 0.14 cps for Dec 3B Noise Sample

The vertical components are very similar and quite simple. They are dominated by a source from about N35°E with a velocity of 3 km/sec and have a secondary peak from the west at a slightly lower velocity.

The horizontal components are generally similar but have a much higher background of random peaks. The dominate peak from the northeast is smeared out in azimuth. Comparison of these 0.14-cps spectra with those at the same frequency for the 2 December noise samples (Figure II-20) indicates that the spectra are generally quite similar for the two noise samples which were taken 6 hr apart.

Figure II-32 shows the surface weather map on 3 December taken at 0000 hr. There is a large storm front between Baffin Island and Greenland which may cause the peak from the northeast. There is also a strong low-pressure center off the coast of Washington. Circulation around this low may cause the wave activity along the west coast, accounting for the secondary source to the west.

Figure II-33 shows a 600-sec segment of the 13 December noise sample. This noise sample appears quite uniform (no energy bursts). Power spectra from the A0, F2, and F3 locations are shown in Figure II-34. Examination of these spectra indicates

- The spectra are characterized by a general frequency fall-off and a null at 0.1 cps, rather than their being dominated by peaks
- The horizontal and vertical components have fairly similar spectra above approximately 0.04 cps
- The horizontal components are 3- to 10-db noisier in the 0.1- to 0.2-cps range
- There is no appreciable seismic energy above 0.27 cps

Figure II-32. Surface Weather Map for 3 December 1966 at 0000 Hr

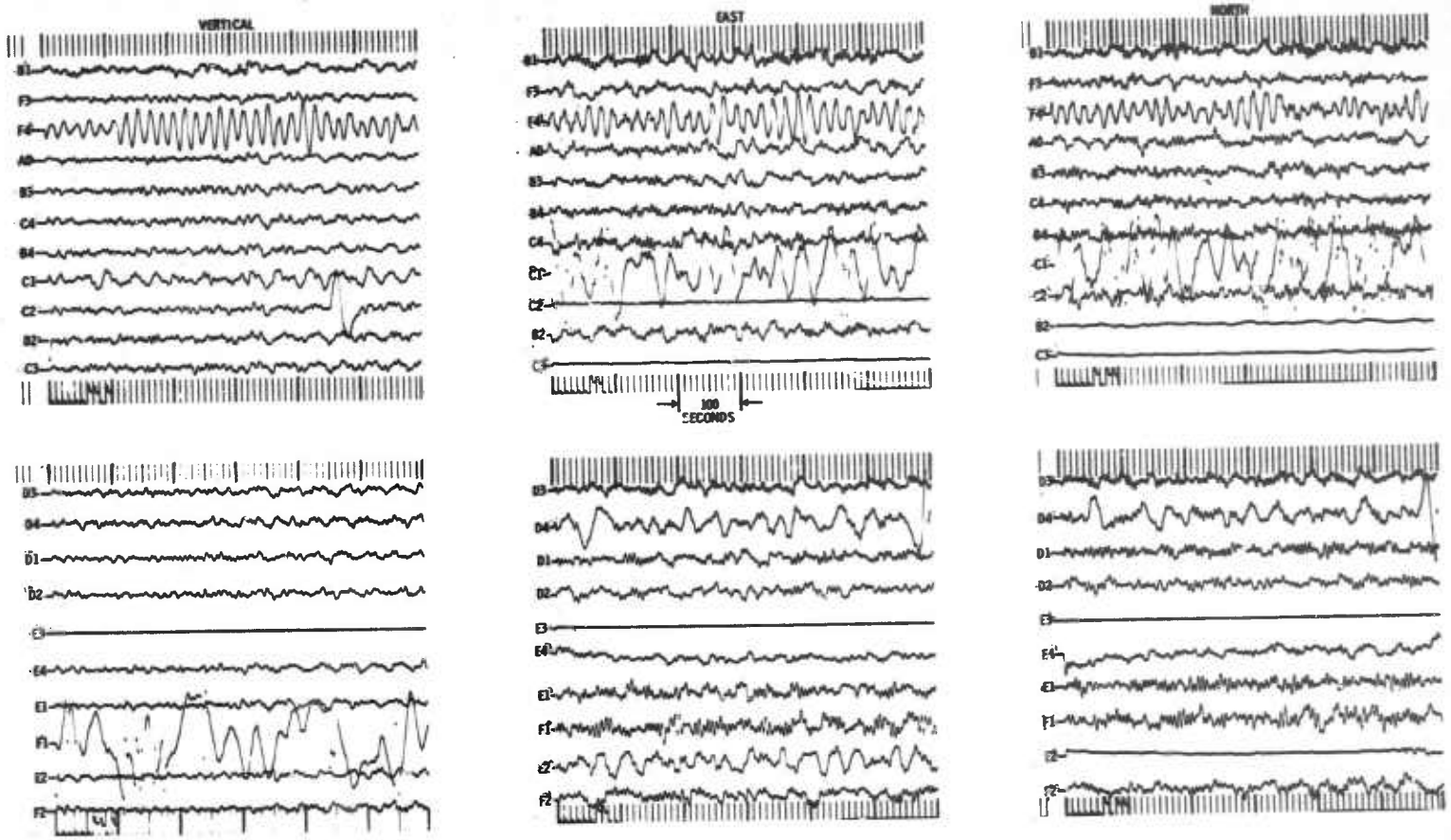


Figure II-33. Portion of 13 December 1966 Noise Sample

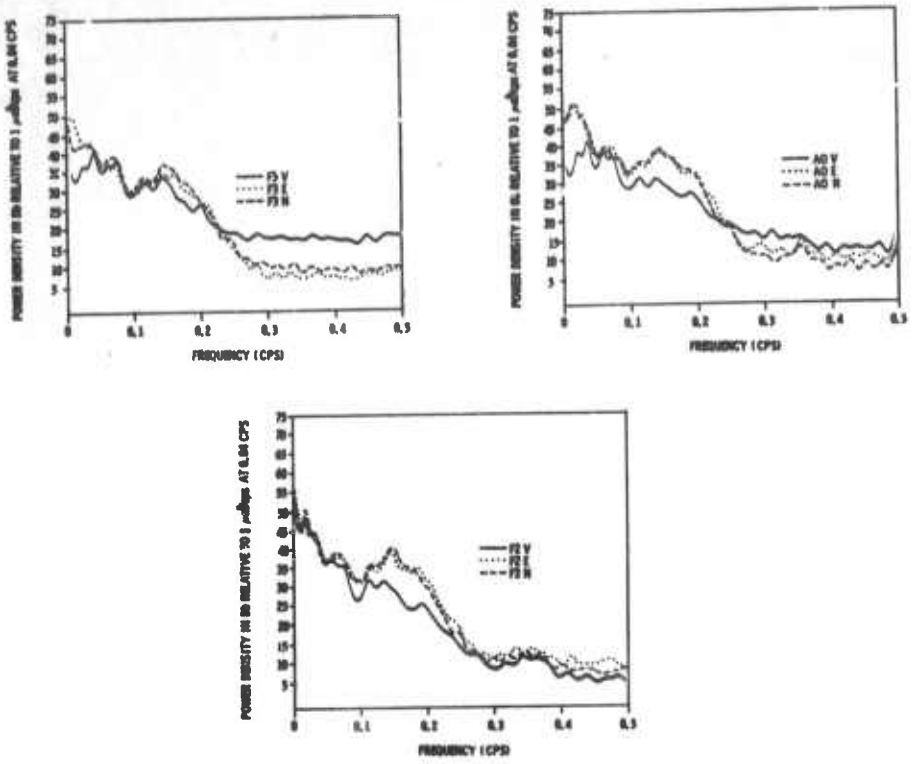

Figure II-34. Power Spectra of 13 December 1966 Noise

Figure II-35 shows the multiple coherences between A0 vertical and various combinations of vertical components. Coherence is quite poor below 0.05 at a distance of 100 km (F ring) and nil above this frequency. Coherence is good at a distance of 30-km (D ring) in the 0.04- to 0.09-cps range. No dominating coherence peaks occur in this noise sample.

Figure II-36 shows the multiple coherences between A0 north-south and various combinations of north-south components. The north-south components show essentially nc coherence at a distance of 50-km (E ring) and good coherence only at a peak near 0.08 cps at a distance of 30-km (D ring).

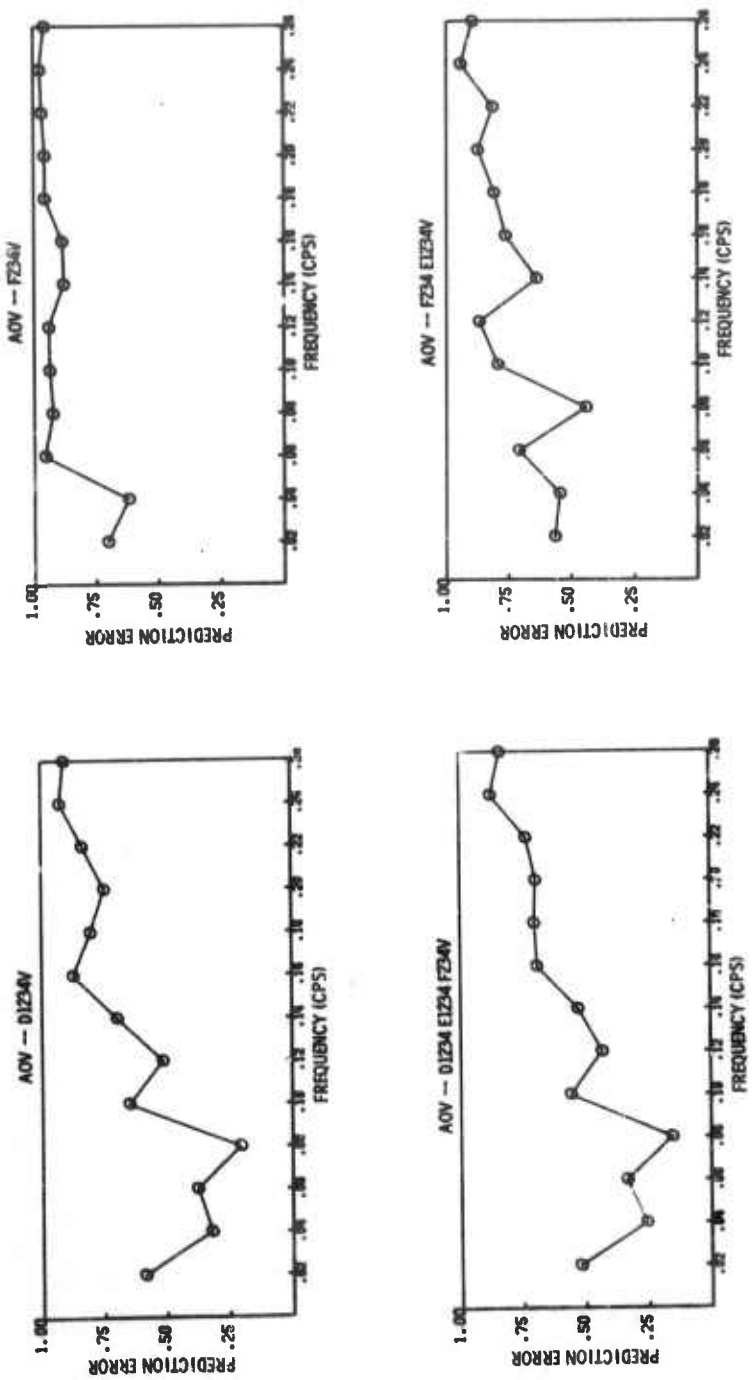


Figure II-35. Multiple Coherences Between the A0 Vertical Component and Combinations of Vertical Components, 13 December 1966

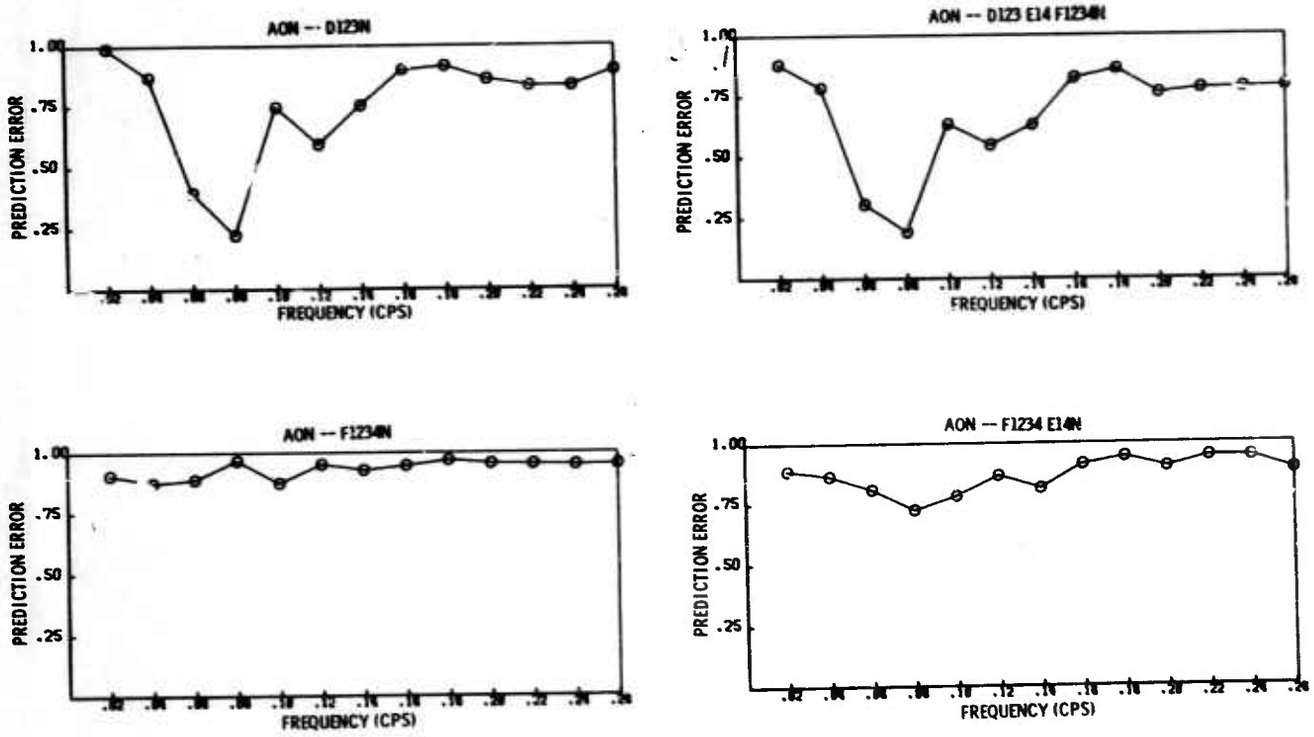


Figure II-36. Multiple Coherences Between A0 North-South and Combinations of North-South Components, 13 December 1966

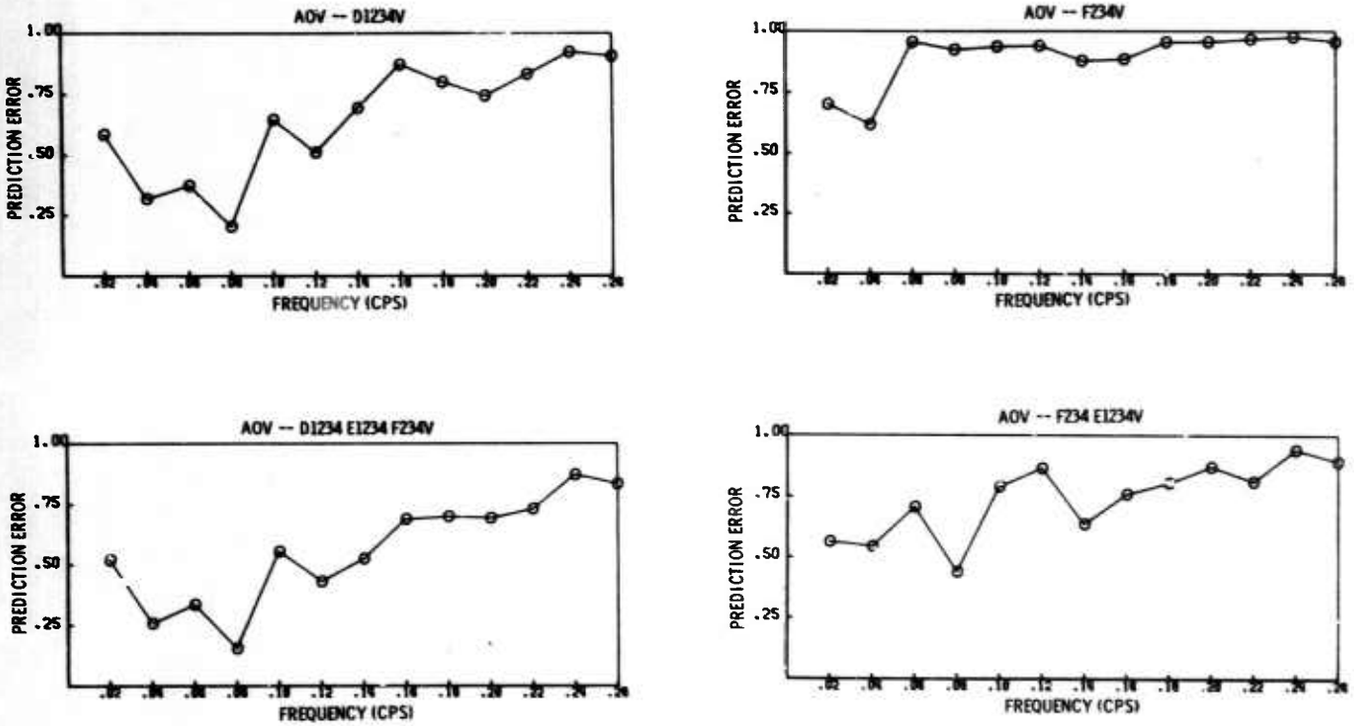


Figure II-35. Multiple Coherences Between the A0 Vertical Component and Combinations of Vertical Components, 13 December 1966

Figure II-37 shows the multiple coherences between A0 vertical and various combinations of horizontal components. The A0 vertical component is strongly predictable from nearby horizontal components between 0.05 and 0.12 cps. The low-frequency coherence (below 0.05 cps) falls off sharply. Single-point coherence A0 vertical to A0 north-south and east-west) is quite low except near 0.12 cps. It should be pointed out that a rather high number of questionable traces occurred in the E and F rings for this noise sample, which could make the coherences involving these traces unusually low.

Figures II-38 and II-39 show the wavenumber spectra and azimuthal power distributions for the vertical and east-west components at 0.06 and 0.08 cps, respectively. At these frequencies, both components show a peak of broad azimuthal distribution from the west and a somewhat lesser peak of considerable azimuthal distribution from the northeast. The velocities are about 3.5 km/sec.

Wavenumber spectra and the azimuthal power distributions for the vertical and east-west components at 0.14 cps are shown in Figure II-40. The vertical component shows a peak from N33°E with a velocity of approximately 2.9 km/sec and a peak with a roughly similar velocity distributed in azimuth from N55°W to S60° W.

The east-west component spectrum shows a split peak from the northeast which is distributed over a fairly large azimuth. The peak is split into velocities of about 3.0 km/sec and 3.9 km/sec, possibly indicating a higher-order surface mode. There is also a strong peak from a generally westerly direction with a velocity of about 3.0 km/sec.

Figure II-41 shows the surface weather map on 13 December at 1200 hr. The North Atlantic was quite stormy near the southern tip of Greenland, which may account for the spectral peak from the northeast.

A 600-sec segment of the 21 December noise sample is shown in Figure II-42. This noise sample appears to be moderately uniform.

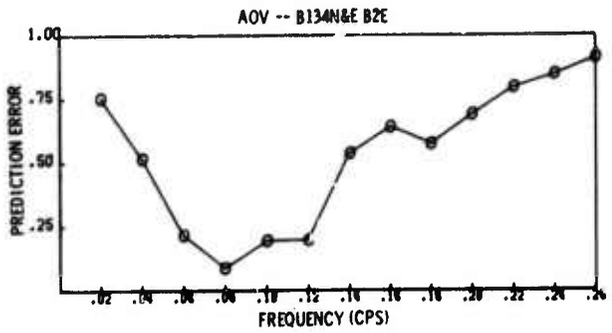


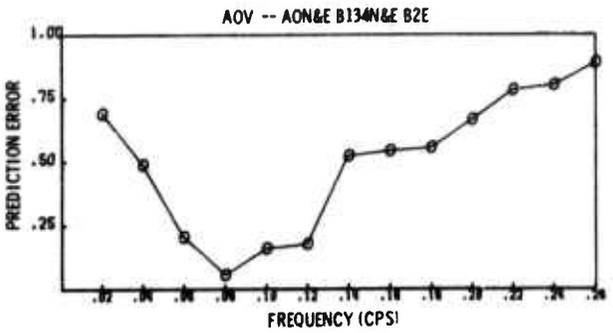


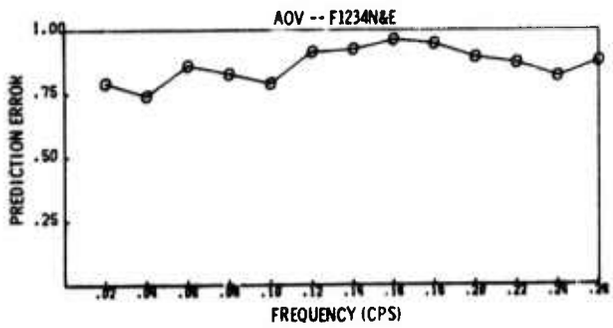


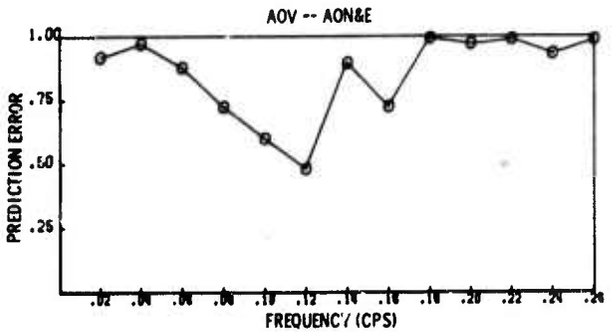


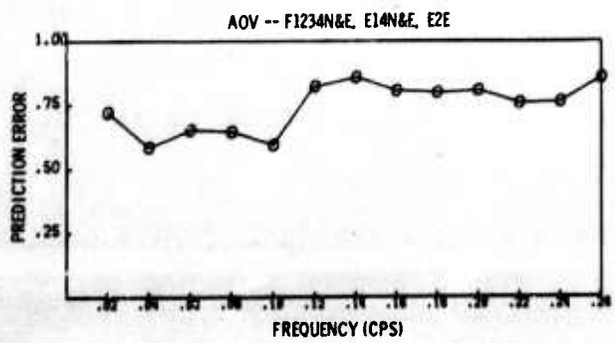


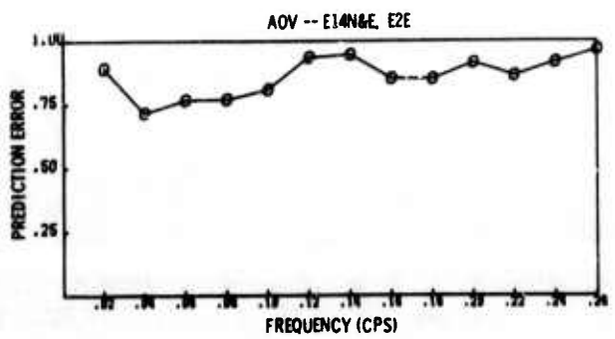


Figure II-37. Multiple Coherences Between A0 Vertical and Combinations of Horizontal Components, 13 December 1966

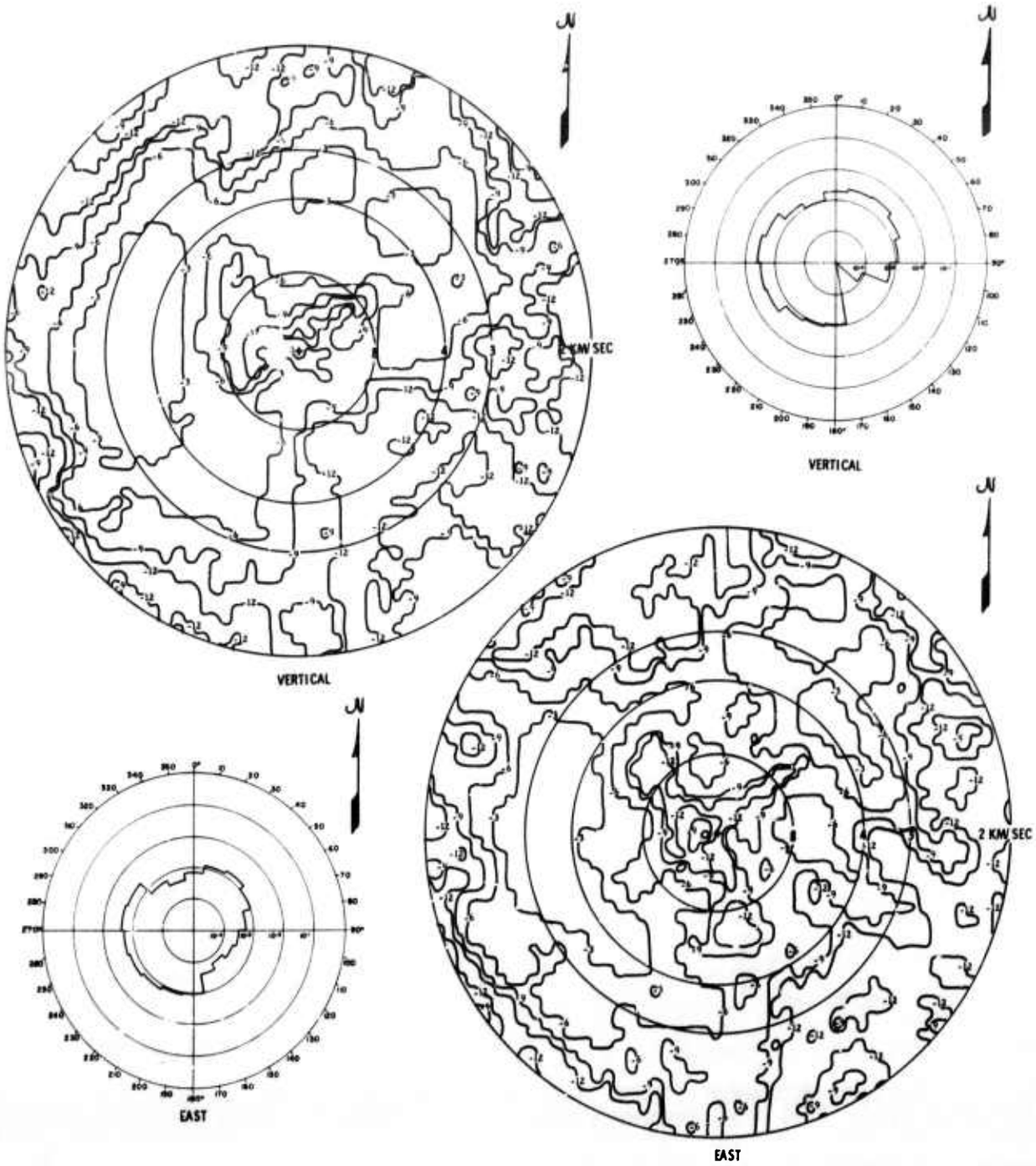


Figure II-38. Wavenumber Spectra and Azimuthal Power Distirbution at 0.06 cps, 13 December 1966

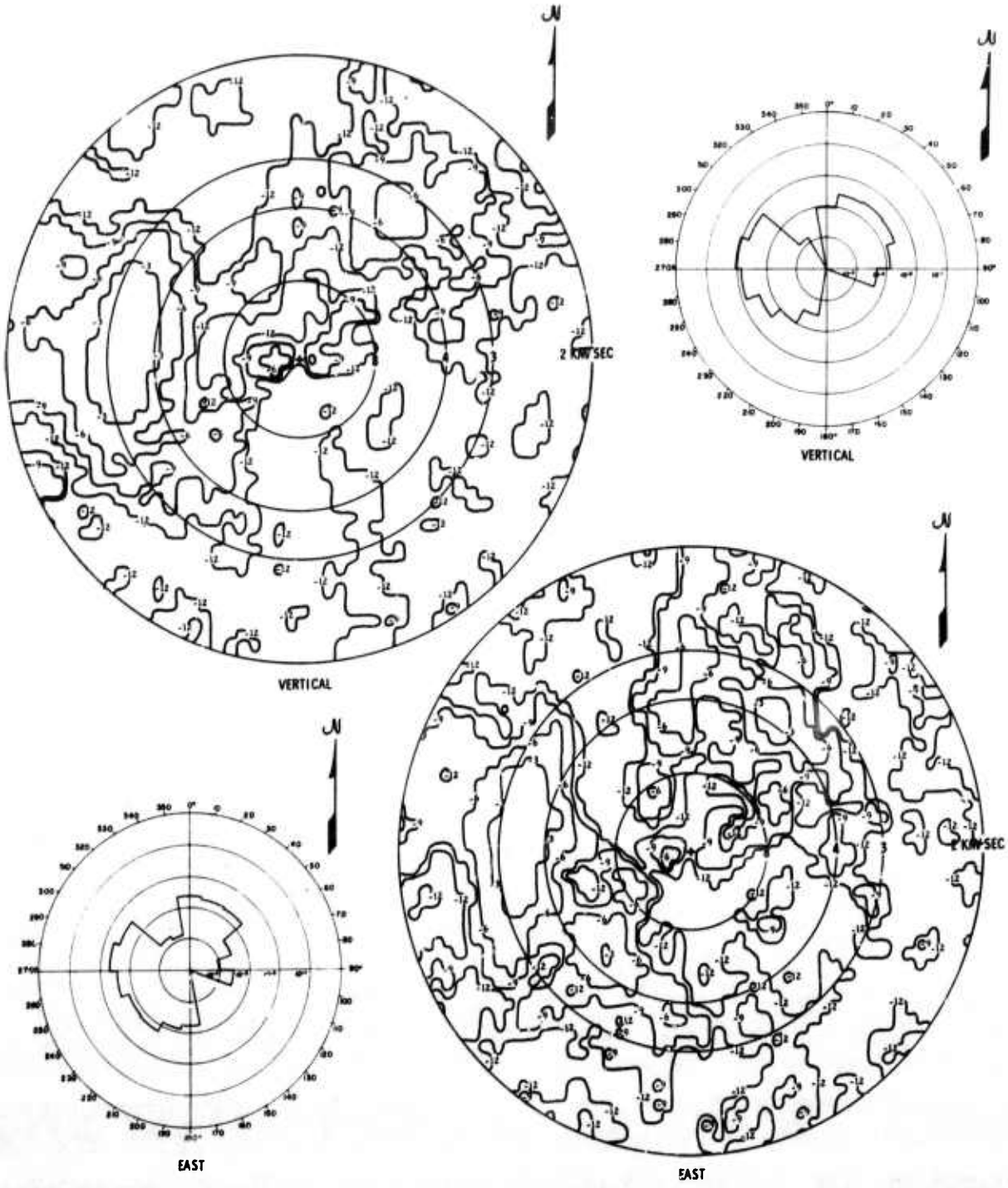


Figure II-39. Wavenumber Spectra and Azimuthal Power Distribution at 0.08 cps, 13 December 1966

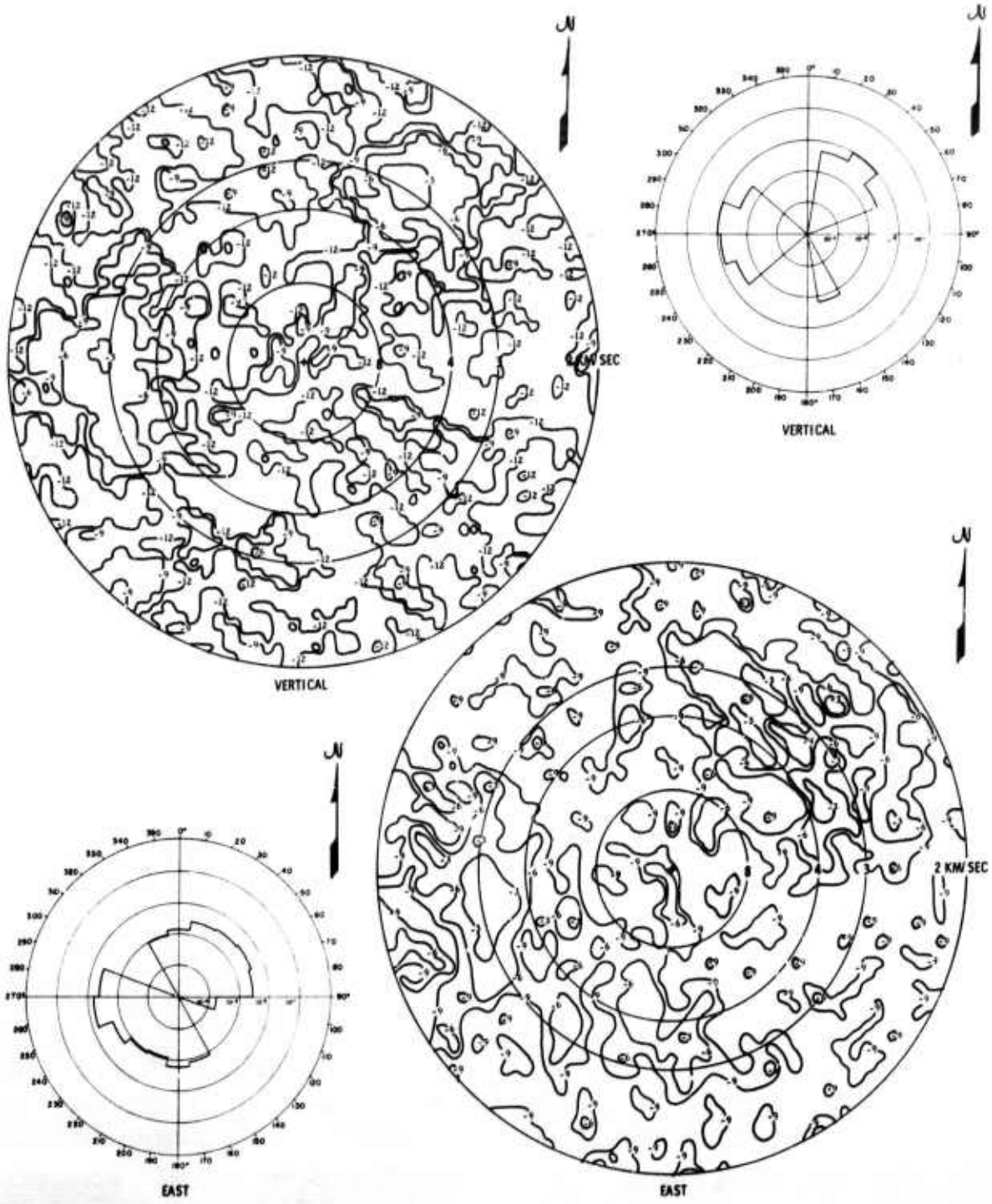


Figure II-40. Wavenumber Spectra and Azimuthal Power Distribution at 0.14 cps, 13 December 1966

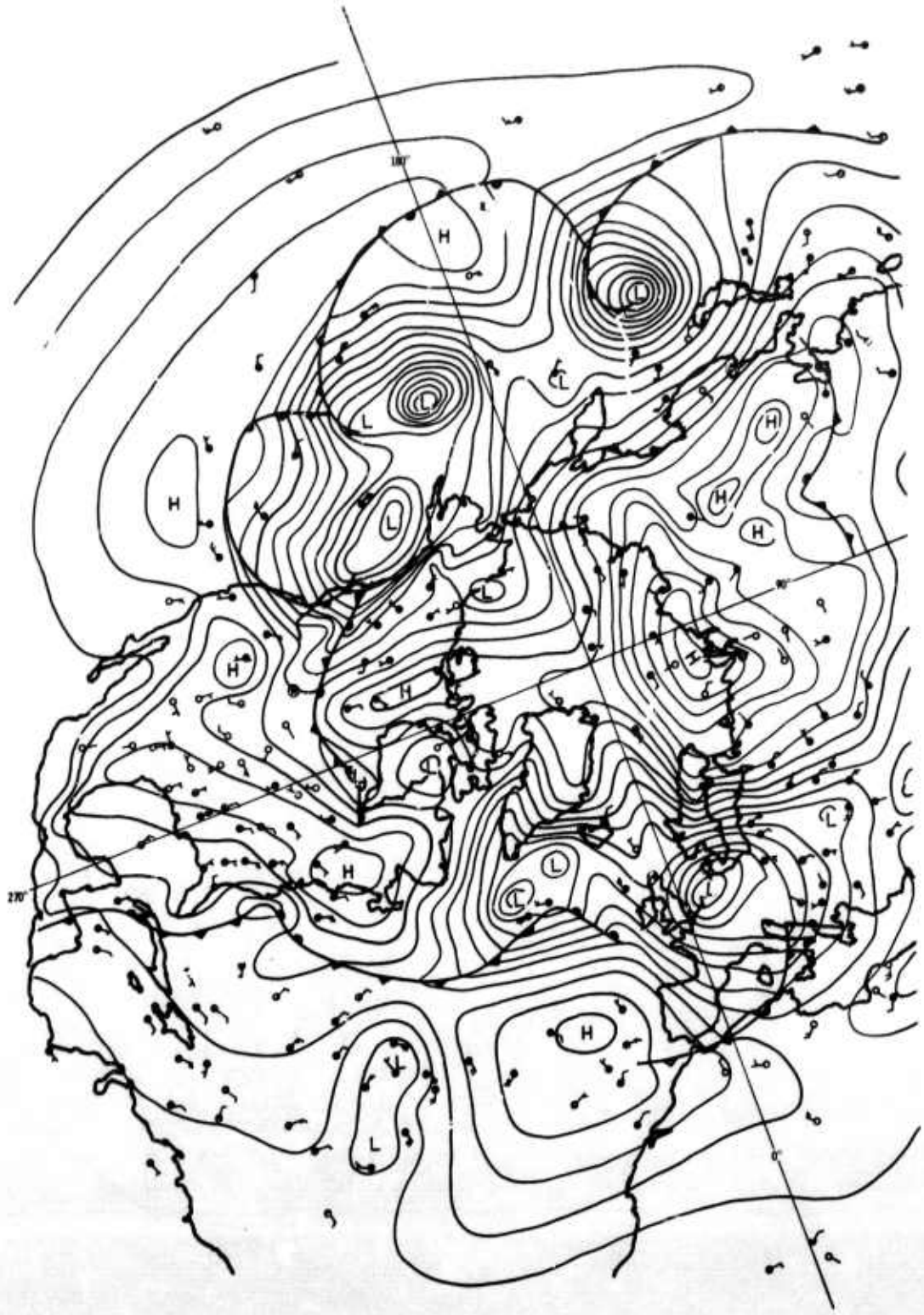


Figure II-41. Surface Weather Map for 13 December 1966 at 1200 Hr

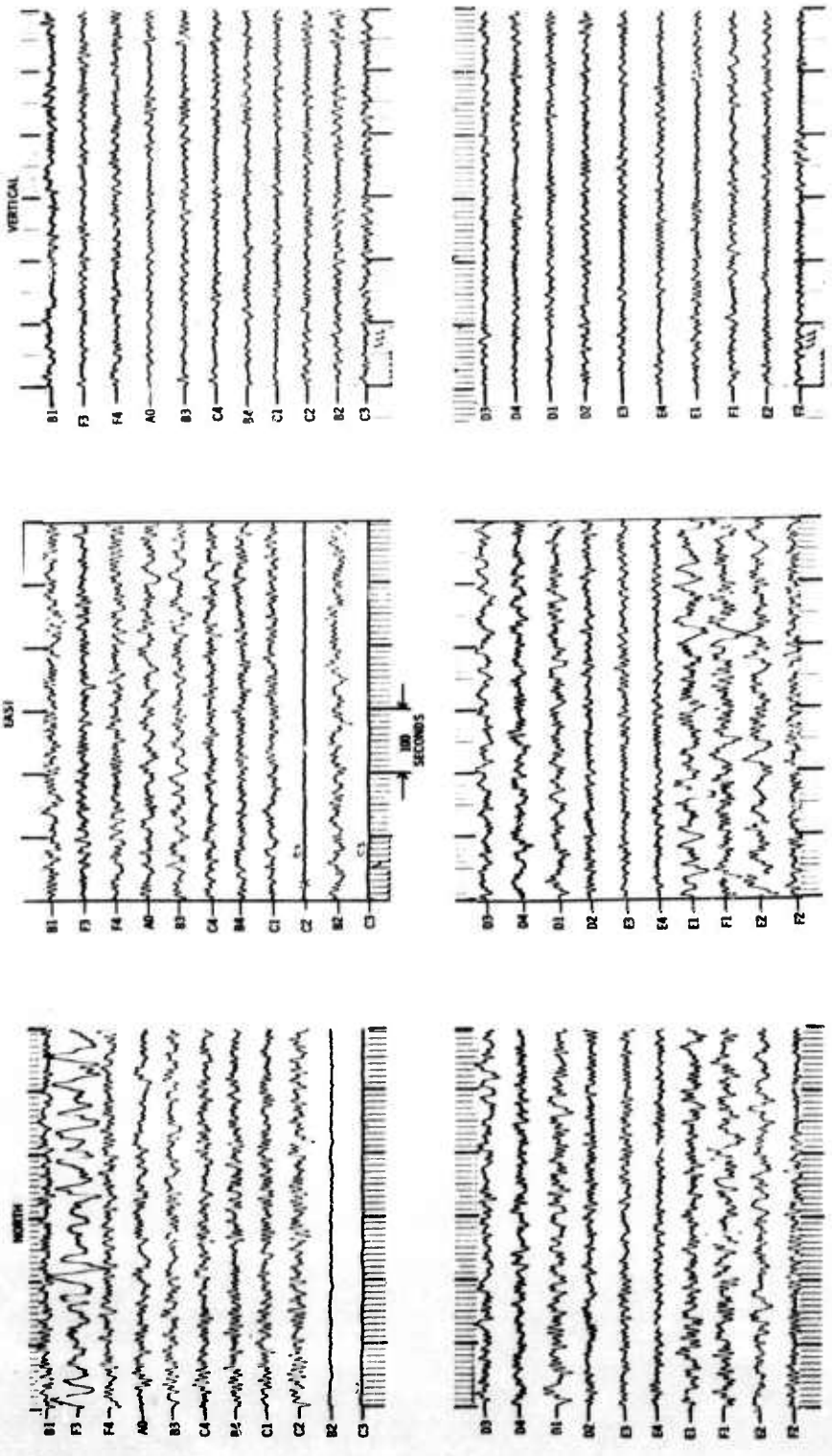


Figure II-42. Portion of 21 December 1966 Noise Sample

Figure II-43 shows power spectra from the A0, F3, and F4 locations. Examination of these spectra indicates that the spectra (all components) show two distinct peaks of about equal magnitude, one in the 0.04- to 0.08-cps range and the other between 0.11 and 0.14 cps. Like components (horizontal and vertical) have similar spectra above 0.04 cps at all locations. Horizontal components are 0- to 5-db noisier than vertical components in the 0.12- to 0.22-cps range. There is no appreciable seismic energy above 0.27 cps.

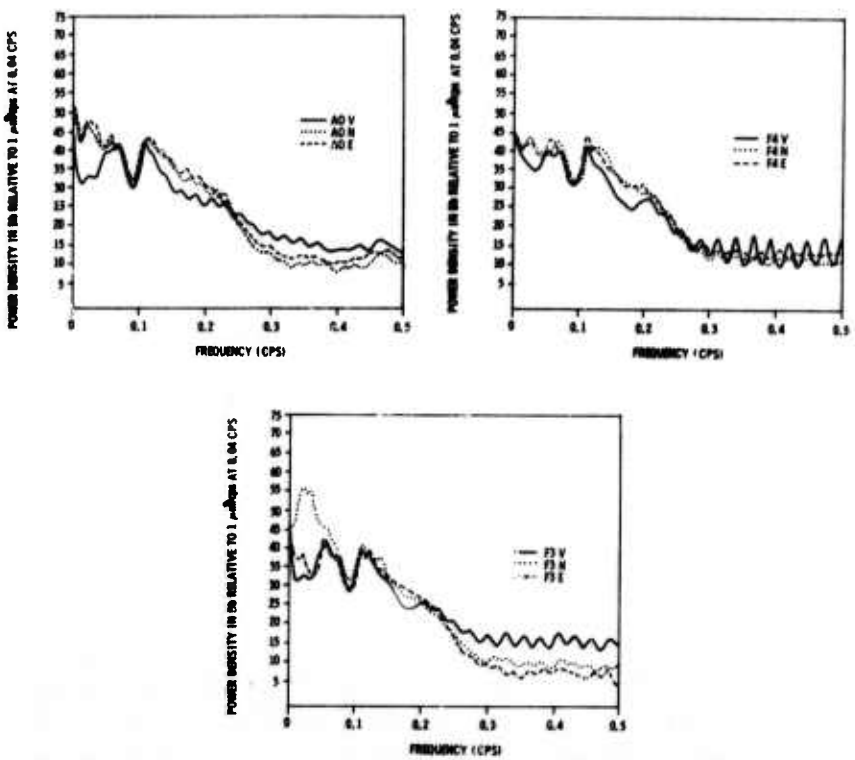


Figure II-43. Power Spectra of 21 December 1966 Noise

Figure II-44 shows the multiple coherences between A0 vertical and various combinations of vertical components for the 21 December noise sample. Multiple coherences between A0 north-south and various other combinations of north-south components for the 21 December noise sample are shown in Figure II-45. Figure II-46 shows the multiple coherences between A0 vertical and various combinations of horizontal components for the 21 December noise sample. Examination of these coherences indicates that

- There is essentially no coherence at distances of 100 km (F ring) for either the vertical or horizontal components
- Near 0.07 cps, both the vertical and north-south components are quite predictable (80 percent) from 30-km away (D ring)
- Near 0.12 cps, the vertical component is significantly more predictable than the north-south component from a distance of 30 km
- The low-frequency ($f < 0.05$ cps) coherence falls off sharply
- The A0 vertical component is very predictable in the range 0.06 to 0.14 cps from nearby horizontal components
- The A0 vertical component is also quite predictable from horizontal components 30-km away (D ring)
- There is little point coherence (A0 vertical from A0 north-south and east-west) except near 0.12 cps

Figure II-47 shows the wavenumber spectra and azimuthal power distribution for the vertical and east-west components at 0.06 cps for the 21 December noise sample. Both spectra are dominated by a peak from the southwest which has considerable azimuthal distribution and velocity of approximately 3.5 km/sec. Also, the east-west component spectrum has weaker peaks from N30°E and N75°E, while the vertical component spectrum has an additional peak at N30°E.

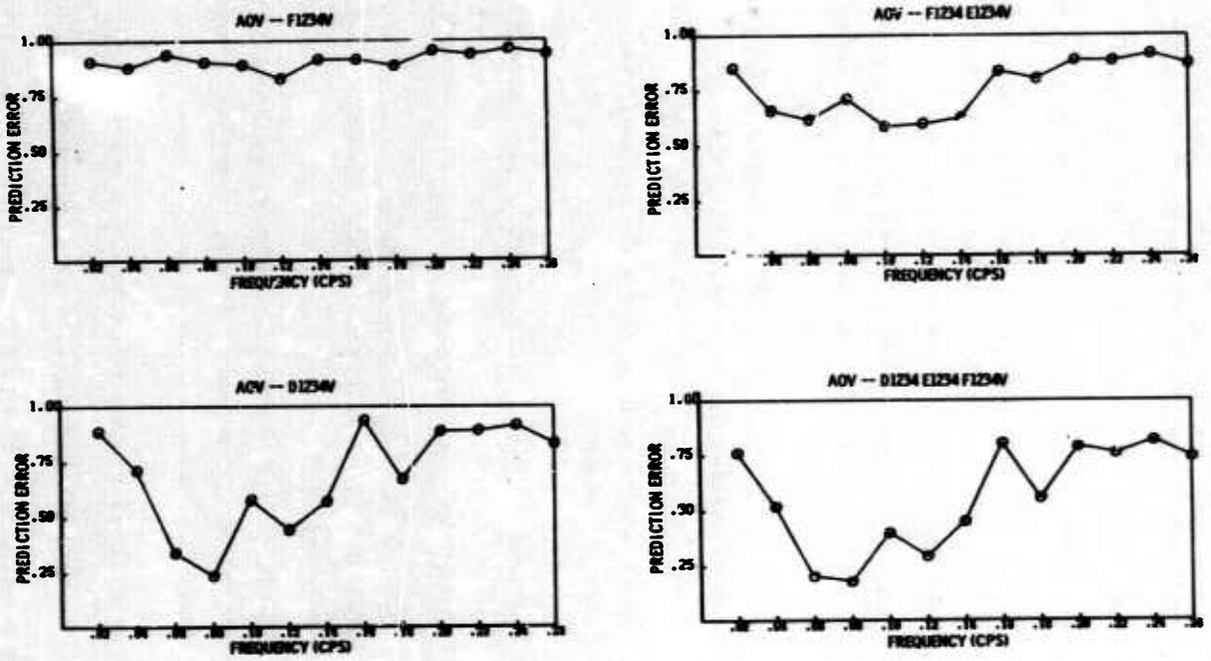


Figure II-44. Multiple Coherences Between A0 Vertical and Combinations of Vertical Components, 21 December 1966

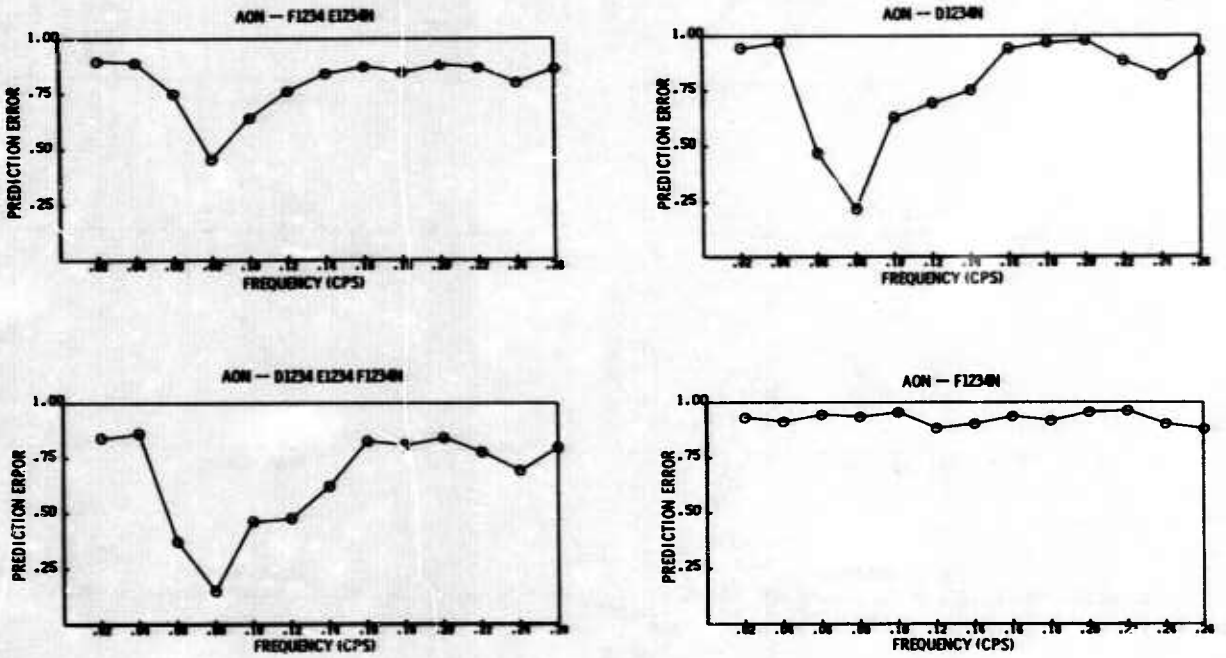


Figure II-45. Multiple Coherences Between A0 North-South and Combinations of North-South Components, 21 December 1966

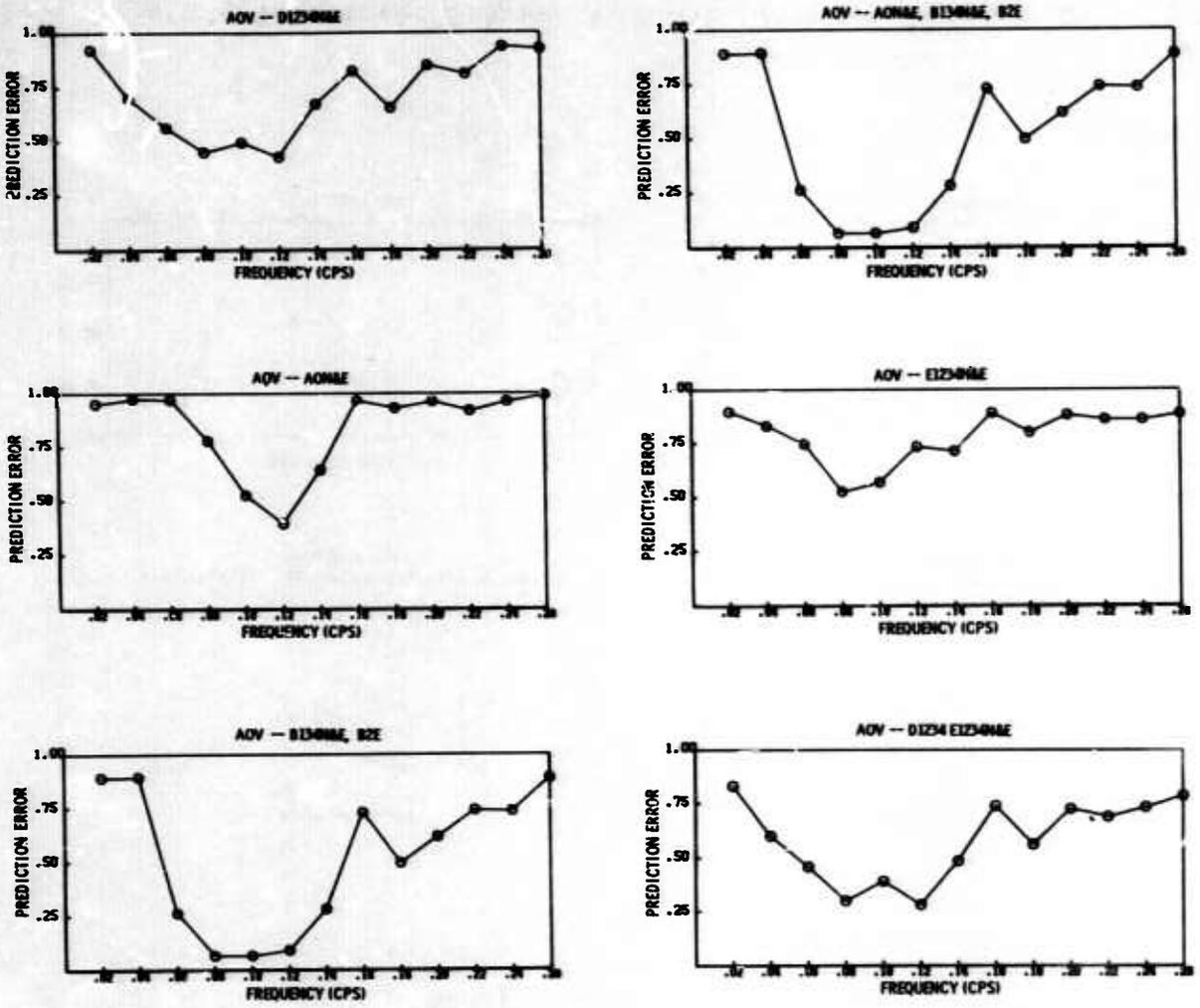


Figure II-46. Multiple Coherences Between A0 Vertical and Combinations of Horizontal Components, 21 December 1966

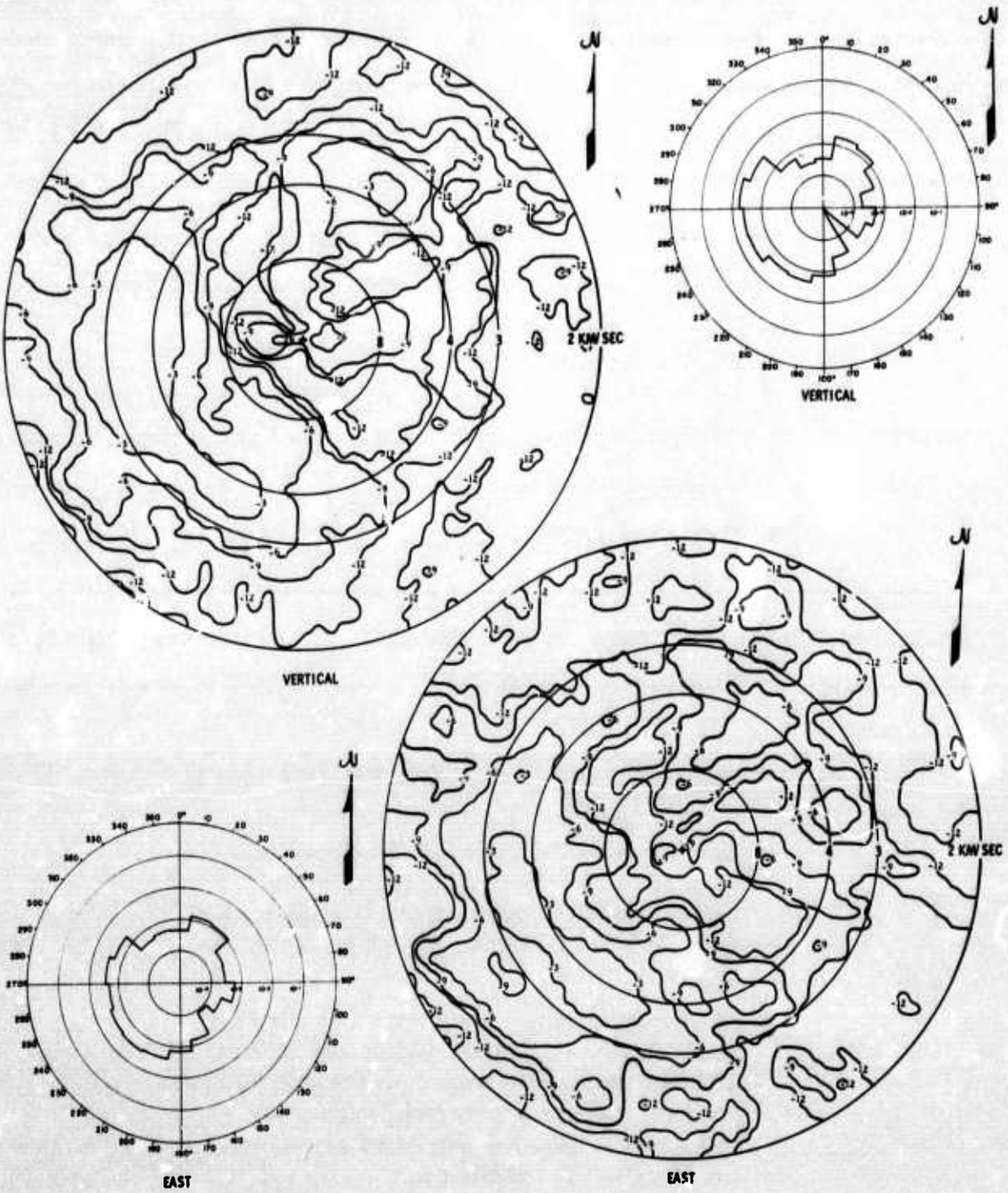


Figure II-47. Wavenumber Spectra and Azimuthal Power Distribution at 0.06 cps, 21 December 1966

Wavenumber spectra and azimuthal power distribution for the vertical and east-west components at 0.12 cps for the 21 December noise sample are shown in Figure II-48. Both components are dominated by power coming from the southwest (as was also true at 0.06 cps). The secondary peaks from the northeast are no longer present.

Figure II-49 shows the surface weather map on 21 December 1966 at 0600 hr. A front was crossing the California coast, which probably generated the seismic energy from the southwest.

A 600-sec segment of the 28 December noise sample is shown in Figure II-50. The seismic energy appears to have some bursts of activity, at least in the vertical component.

Figure II-51 shows the power spectra from all good traces for the 28 December noise sample. It should be noted that the scale factor is uncertain (compared to other days) in this data and the spectra, therefore, are in units of relative power density only. Examination of these spectra indicates

- The spectra are dominated by strong peaks near 0.07 and 0.13 cps
- The horizontal and vertical components have similar power density near 0.07 cps, but the vertical components are generally down about 5 db in the region of the 0.13-cps peak
- Like components (horizontal and vertical) generally have similar power spectra at all locations above approximately 0.05 cps; however, there are certain subarrays (E4 and F3) which seem to be somewhat lower at the 0.13-cps peak
- There is essentially no seismic energy above 0.25 cps

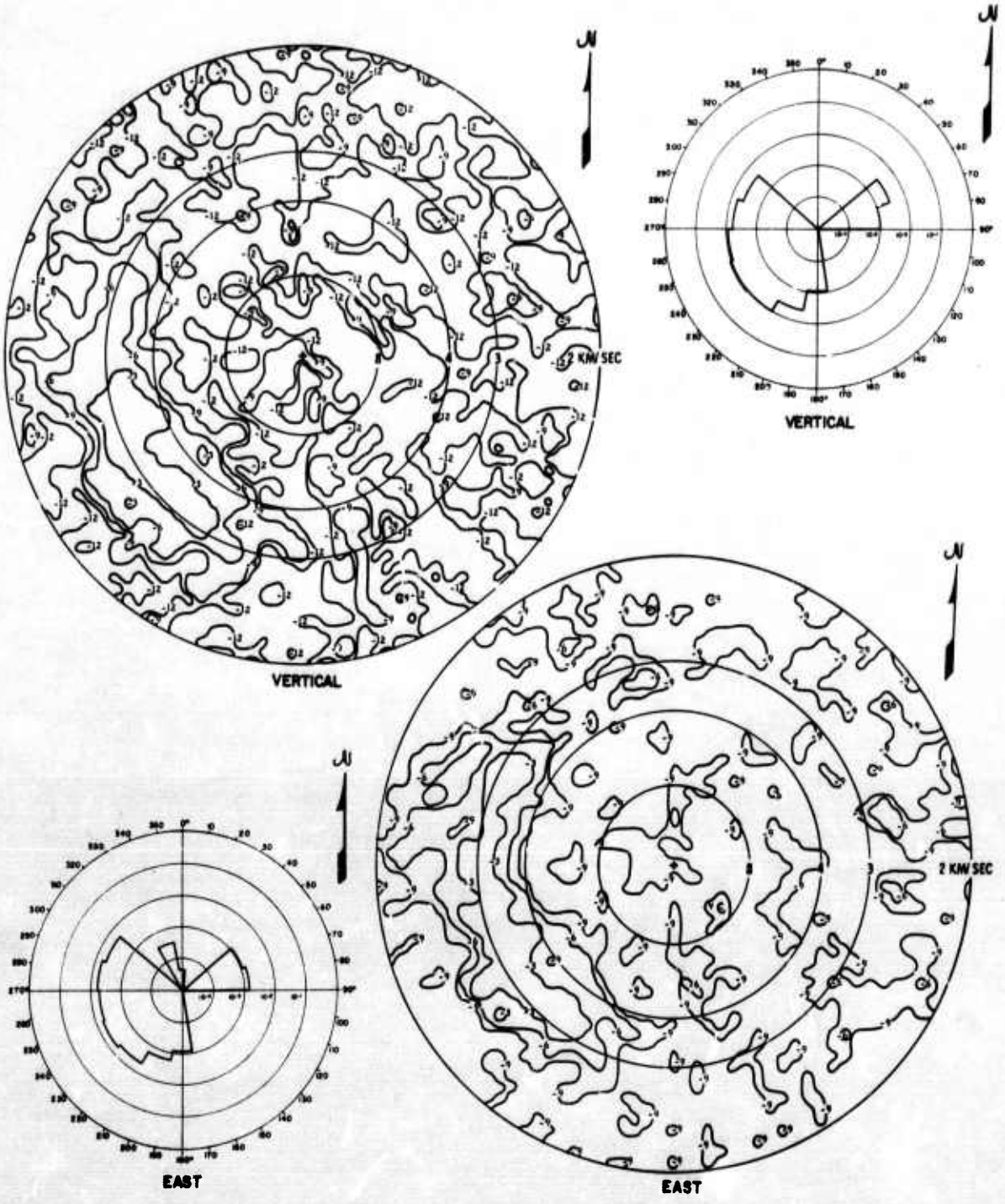


Figure II-48. Wavenumber Spectra and Azimuthal Power Distribution at 0.12 cps, 21 December 1966

Figure II-49. Surface Weather Map for 21 December 1966 at 0600 Hr

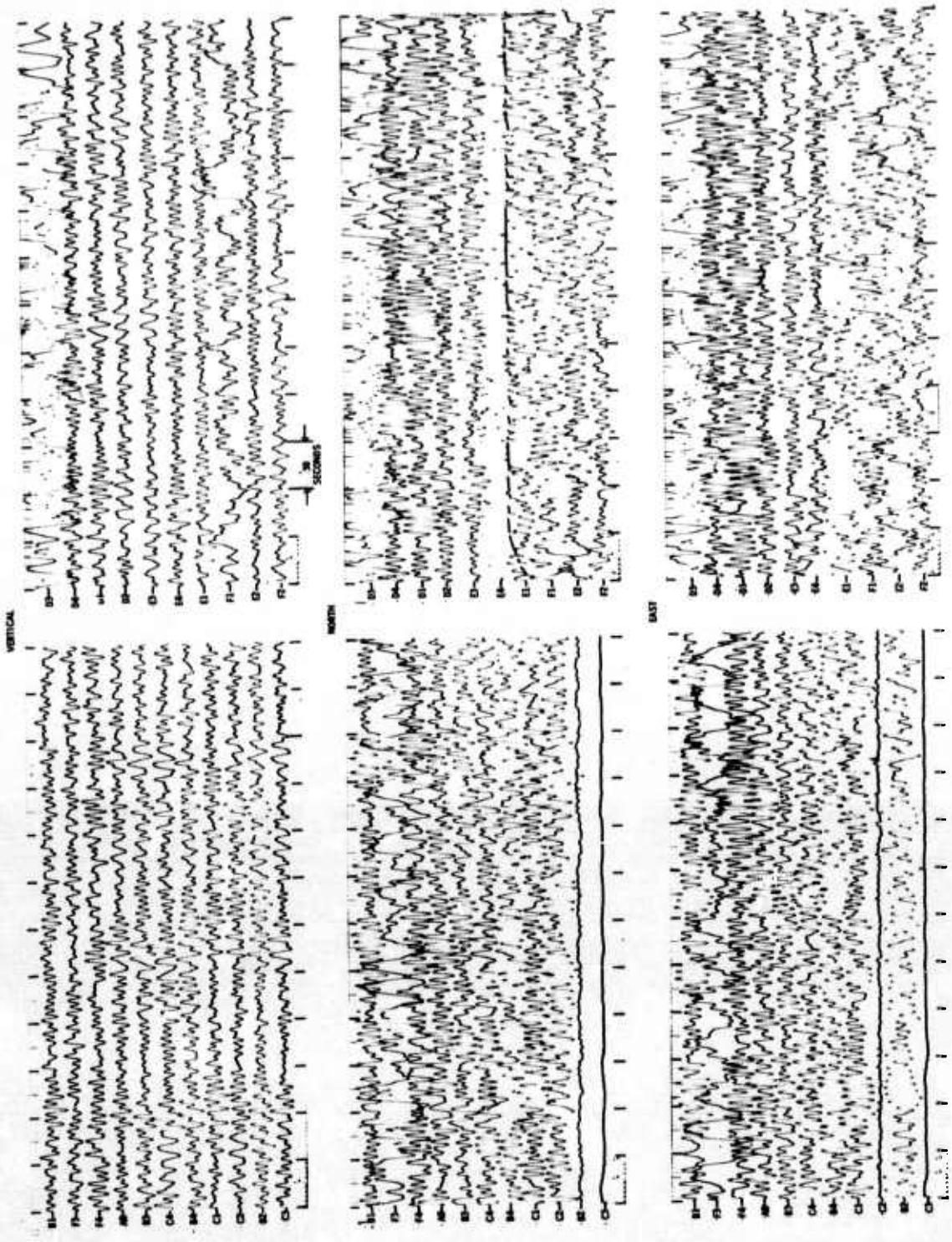


Figure II-50. Portion of 28 December 1966 Noise Sample

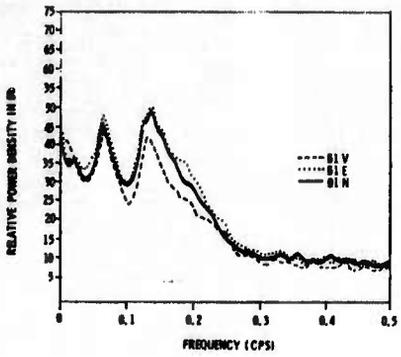
B1 V
B1 E
B1 N
FREQUENCY (CPS)

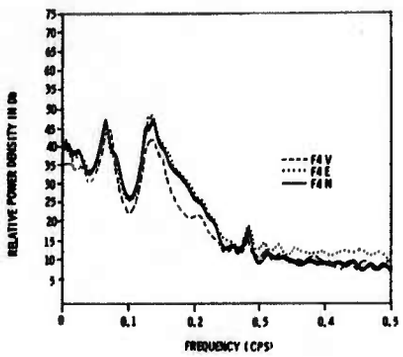
F4 V
F4 E
F4 N
FREQUENCY (CPS)

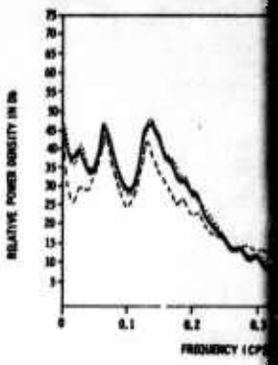

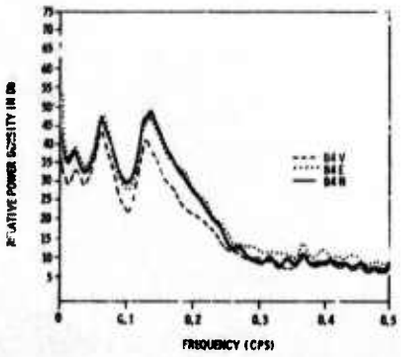
B4 V
B4 E
B4 N
FREQUENCY (CPS)

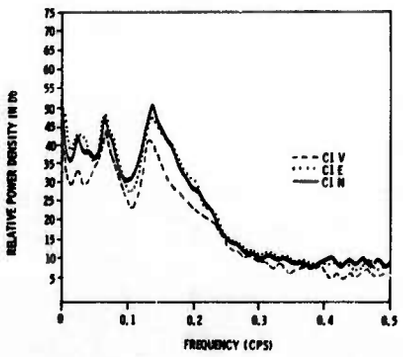
C1 V
C1 E
C1 N
FREQUENCY (CPS)

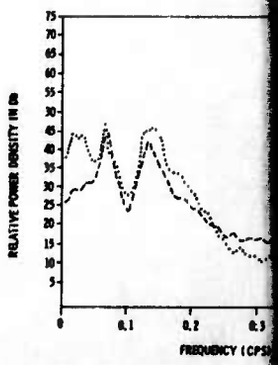

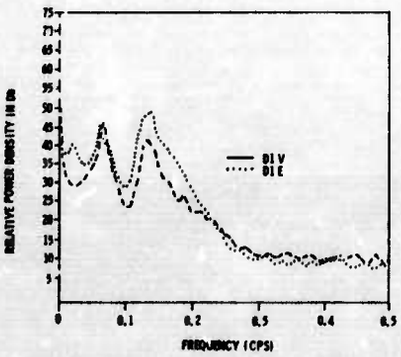
B1 V
B1 E
FREQUENCY (CPS)

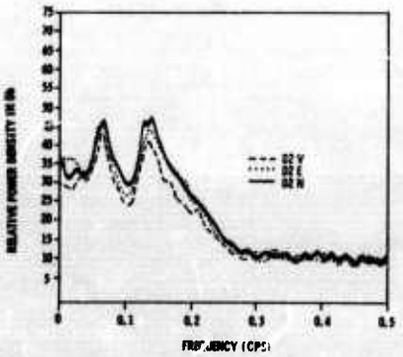
B2 V
B2 E
B2 N

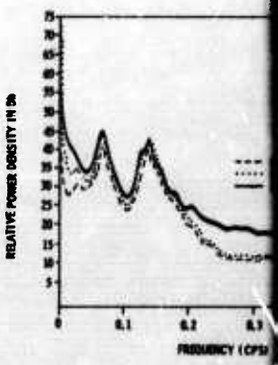

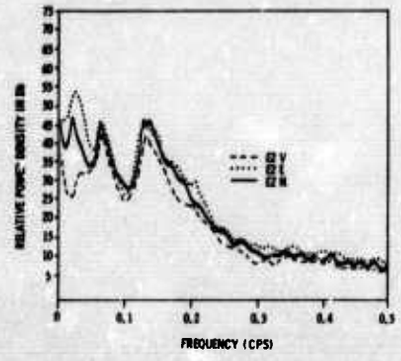
FREQUENCY (CPS)

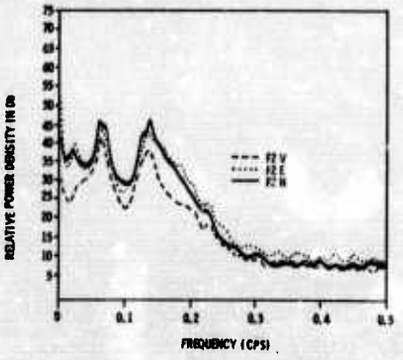
FREQUENCY (CPS)

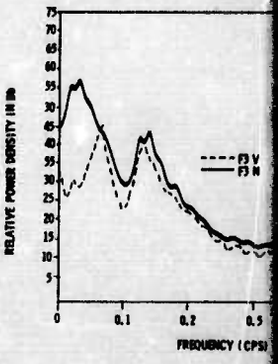
F3 V
F3 N
FREQUENCY (CPS)

Fi

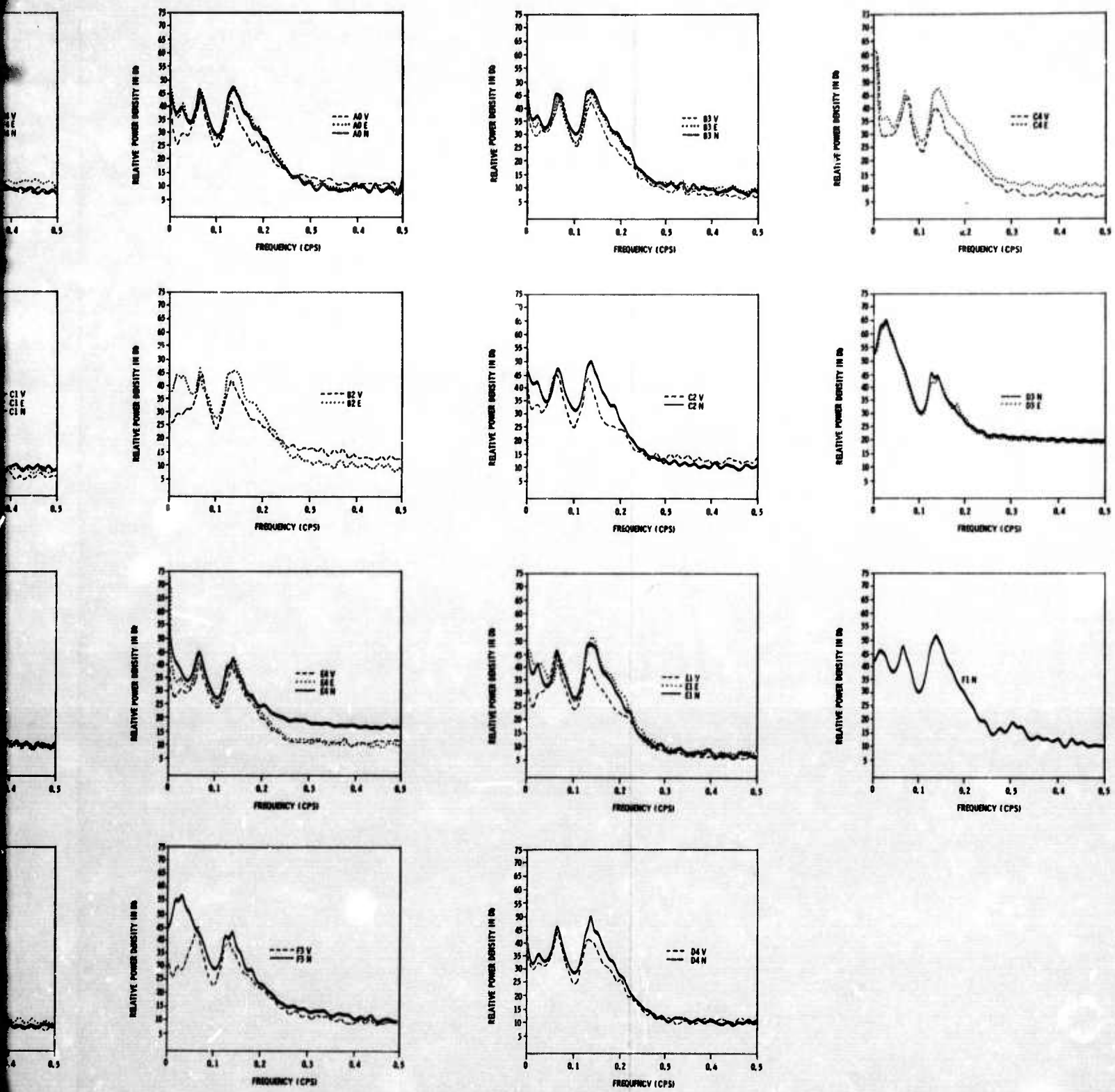


Figure II-51. Power Spectra of 28 December 1966 Noise

Figure II-52 shows the coherences between A0 vertical and various combinations of other vertical components. For distances of 100 km (F ring), the vertical component is moderately predictable (45 percent) near 0.07 cps and 25-percent predictable near 0.13 cps. The two power peaks are about 75 percent predictable using sensors spaced 50-km apart (E and F rings).

Coherences between A0 north-south and east-west and various combinations of horizontal sensors are shown in Figure II-53. Examination of these coherences indicate

- The east-west component is more predictable than the north-south component. This is most evident when the prediction of A0 north-south from D4, D2, and D1 north-south is compared to the prediction of A0 east-west from D4, D2, and D1 east-west
- The north-south component is about 70-percent predictable near 0.07 cps and 50-percent predictable near 0.13 cps from sensors over 50 km apart (E and F rings). This predictability is significantly less than the vertical-trace predictability near 0.13 cps (Figure II-52)
- There is almost no coherence between east-west and north-south components even at very close distances (B-ring, 10 km)
- Coherence decreases sharply below 0.05 cps

Figure II-54 shows the coherence between A0 vertical and various combinations of horizontal sensors. The vertical component is highly predictable from nearby horizontal components in the 0.05- to 0.14-cps range. This predictability is primarily the result of coherence between the vertical and east-west components. Coherence between the vertical and north-south components is considerably less.

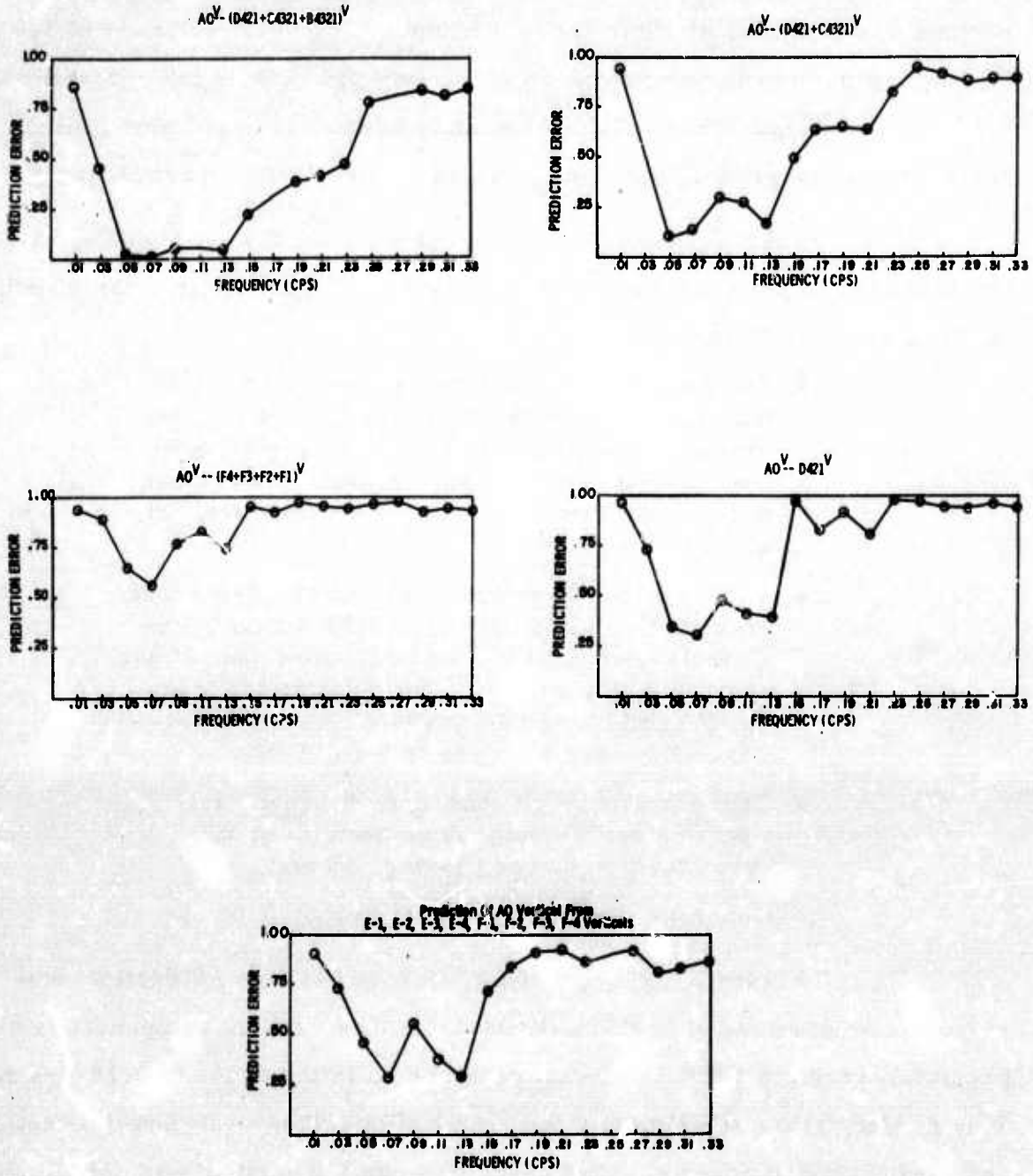


Figure II-52. Multiple Coherences Between A0 Vertical and Combinations of Vertical Components, 28 December 1966

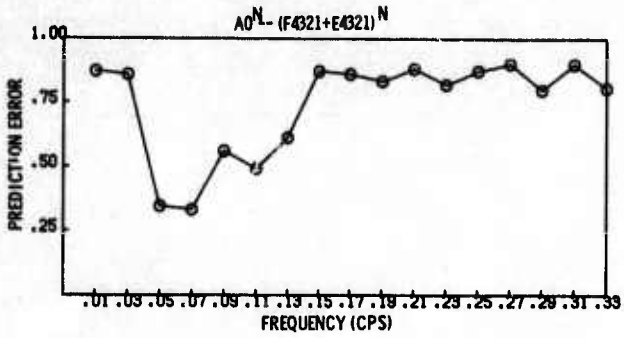
$A0^N$ - $(F4321+E4321)^N$
PREDICTION ERROR
1.00
.75
.50
.25
.01 .03 .05 .07 .09 .11 .13 .15 .17 .19 .21 .23 .25 .27 .29 .31 .33
FREQUENCY (CPS)

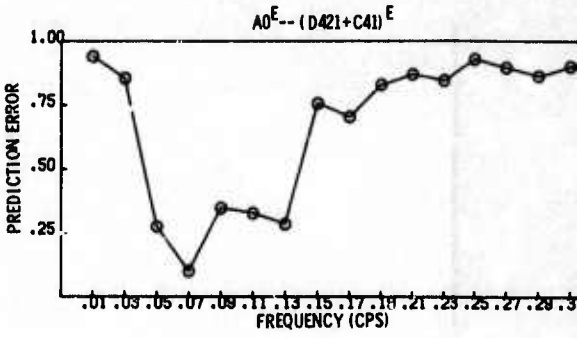
$A0^E$ -- $(D421+C41)^E$
PREDICTION ERROR
1.00
.75
.50
.25
.01 .03 .05 .07 .09 .11 .13 .15 .17 .19 .21 .23 .25 .27 .29
FREQUENCY (CPS)

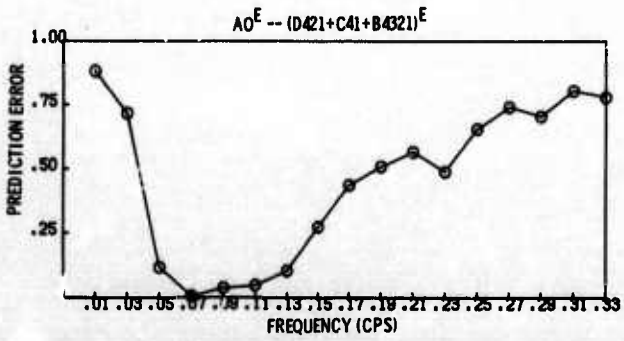
$A0^E$ -- $(D421+C41+B4321)^E$
PREDICTION ERROR
1.00
.75
.50
.25
.01 .03 .05 .07 .09 .11 .13 .15 .17 .19 .21 .23 .25 .27 .29 .31 .33
FREQUENCY (CPS)

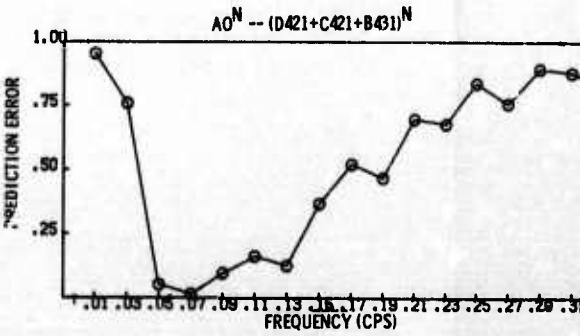
$A0^N$ -- $(D421+C421+B431)^N$
PREDICTION ERROR
1.00
.75
.50
.25
.01 .03 .05 .07 .09 .11 .13 .15 .17 .19 .21 .23 .25 .27 .29
FREQUENCY (CPS)

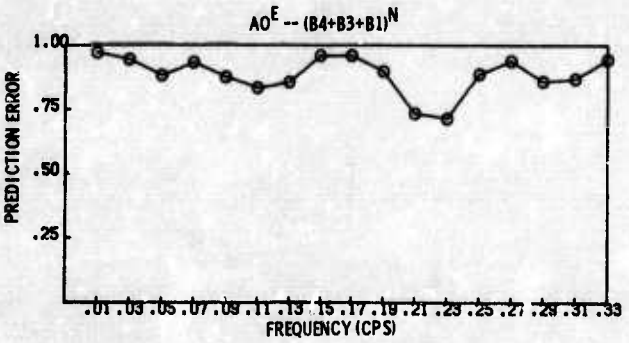
$A0^E$ -- $(B4+B3+B1)^N$
PREDICTION ERROR
1.00
.75
.50
.25
.01 .03 .05 .07 .09 .11 .13 .15 .17 .19 .21 .23 .25 .27 .29 .31 .33
FREQUENCY (CPS)

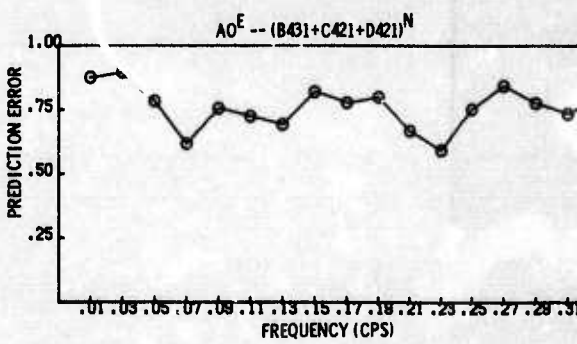
$A0^E$ -- $(B431+C421+D421)^N$
PREDICTION ERROR
1.00
.75
.50
.25
.01 .03 .05 .07 .09 .11 .13 .15 .17 .19 .21 .23 .25 .27 .29
FREQUENCY (CPS)

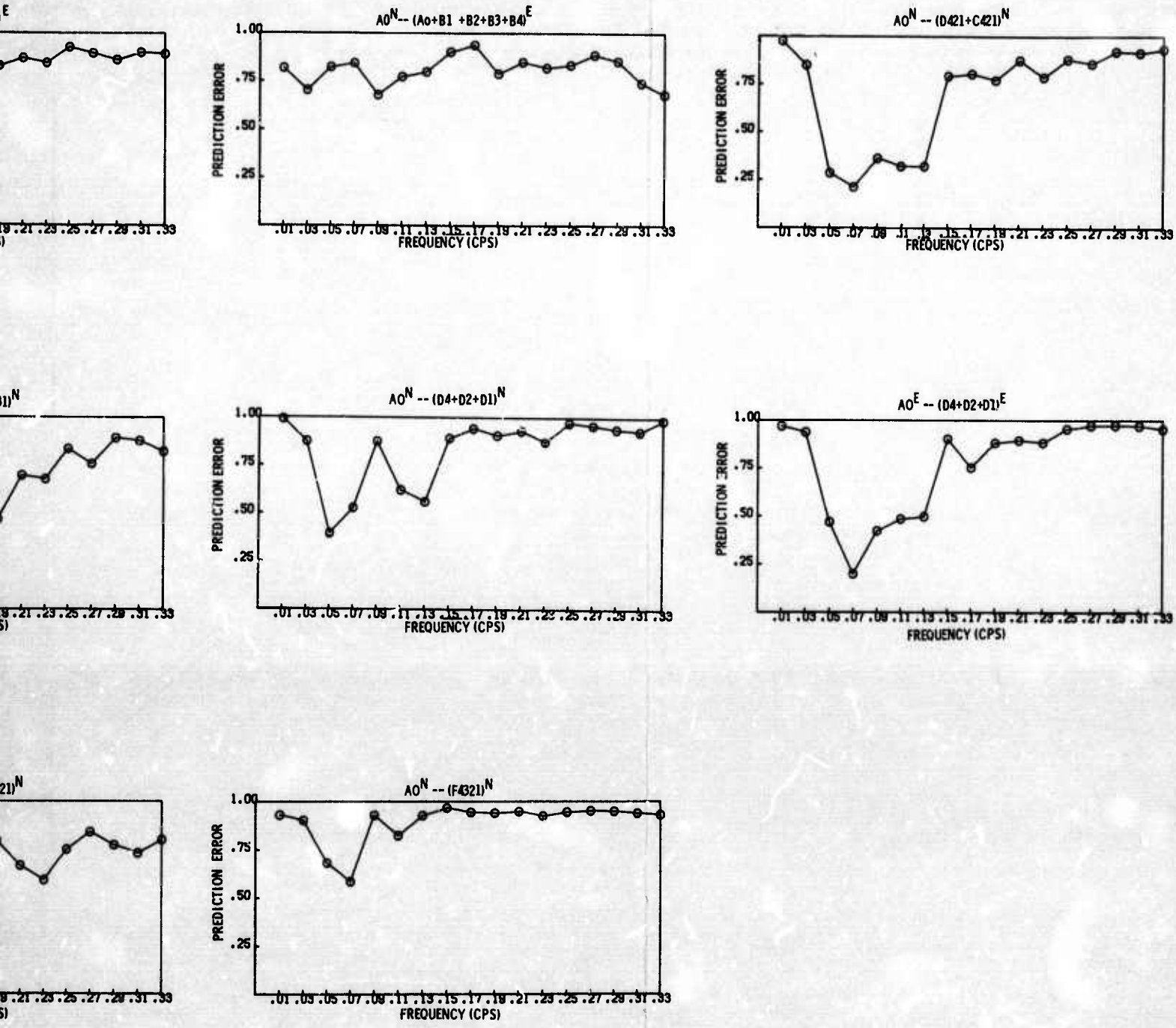


Figure II-53. Multiple Coherences Between A0 North-South and East-West and Combinations of Horizontal Sensors, 28 December 1966

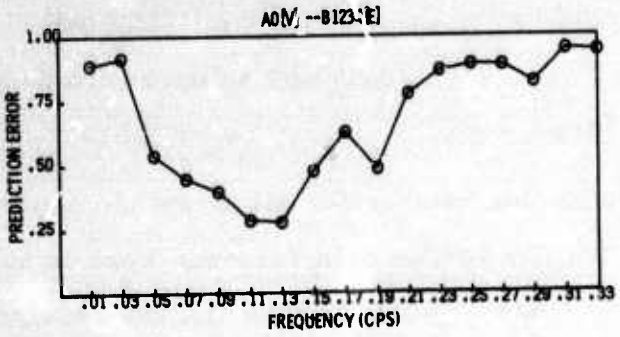


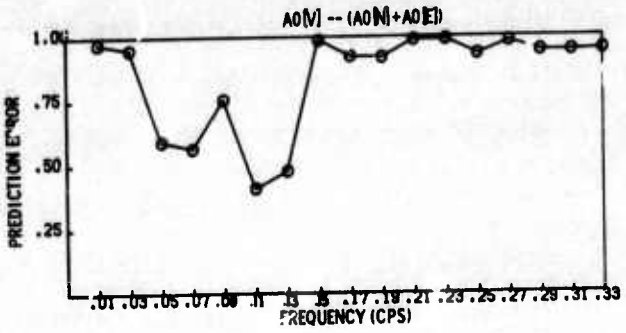


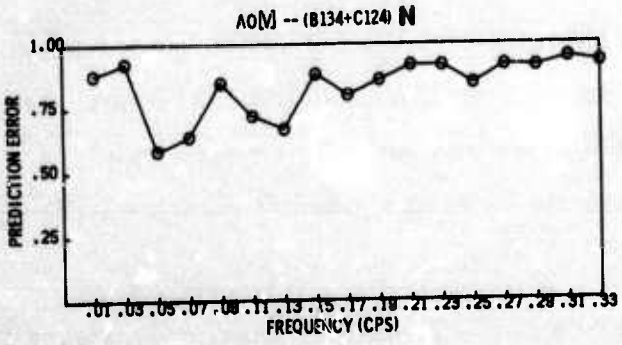


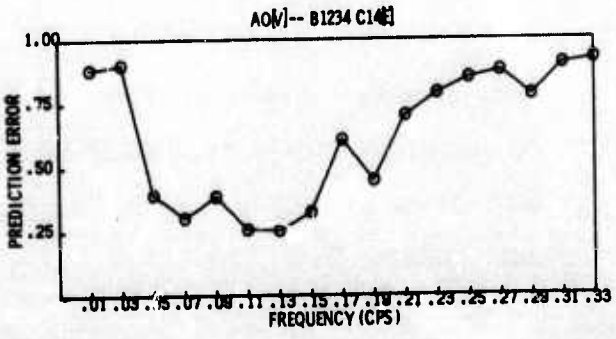


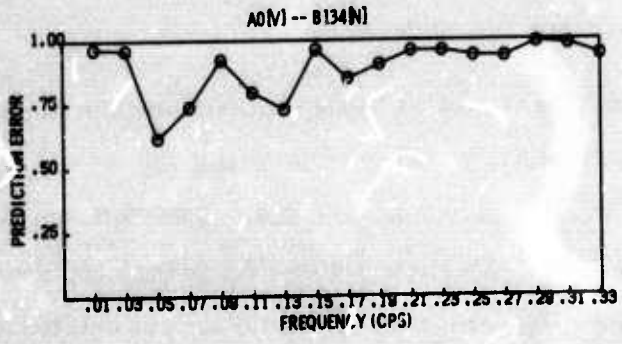


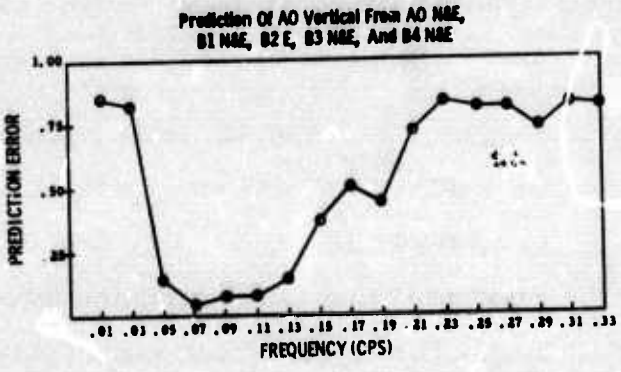


Figure II-54. Multiple Coherences Between A0 Vertical and Combinations of Horizontal Sensors, 28 December 1966

Wavenumber spectra for all three components and azimuthal power distribution plots for the north-south and east-west components at 0.08 cps for the 28 December noise sample are shown in Figure II-55. All three spectra are quite similar in that they are dominated by a source from N62°W with a velocity of about 3.5 km/sec.

Figure II-56 shows wavenumber spectra for all three components and azimuthal power distribution plots for the north-south and east-west components at 0.12 cps for the 28 December noise sample. Again, all the spectra are similar and are dominated by a peak from N60-65°W with a velocity of 3 km/sec on the vertical-component spectrum and slightly higher on the horizontal-component spectra.

Figure II-57 shows wavenumber spectra for all three components and azimuthal power distribution plots for the north-south and east-west components at 0.14 cps for the 28 December noise sample. The peak from N60-65°W is still dominant, but there is also a strong peak from the northeast quadrant.

Shown in Figure II-58 is the surface weather map on 28 December 1966 at 0000 hr. There is no obvious generator for the seismic energy from N60-65°W. It is possible that the front shown off the Pacific coast was crossing the coast in the region north of Puget Sound. This would be the correct position to generate the seismic energy observed.

For the 28 December noise sample, a time-domain multichannel filter system (MCF) was designed for a total of 10 elements using the vertical components of A0, C1, C2, C4, D1, D2, D4, E1, E2, and E4. The data were resampled to a 2-sec sampling interval, and the filters were 25 points (50 sec) long. The signal model was infinite velocity, and measured noise correlations were used. The data had been prewhitened by a short deconvolution filter. The $N_i/N_o$ ratio for the MCF and the summation are shown in Figure II-59. Also shown is the multiple coherence between A0 vertical and the outlying vertical traces used in the MCF.

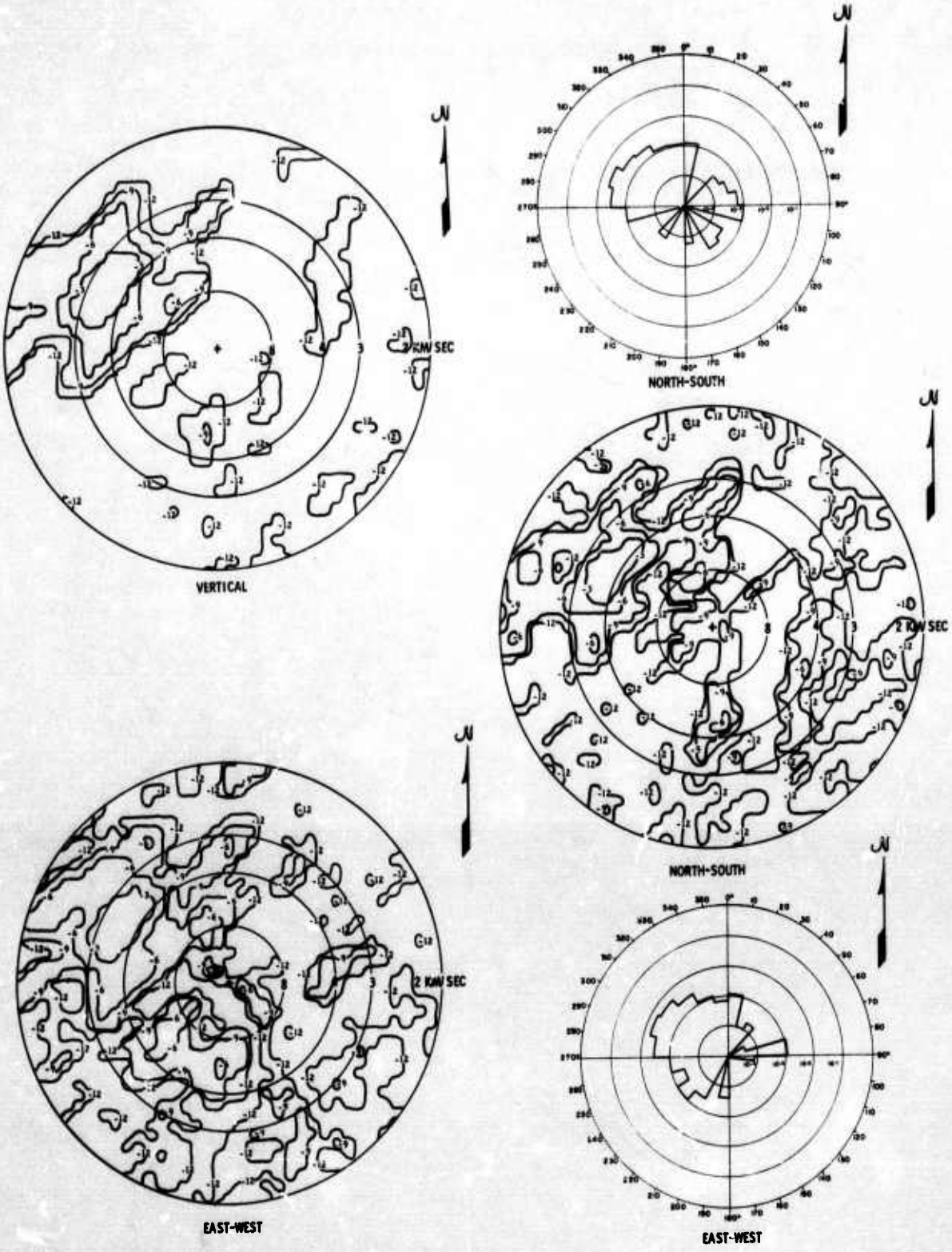


Figure II-55. Wavenumber Spectra and Azimuthal Power Distribution at 0.08 cps, 28 December 1966

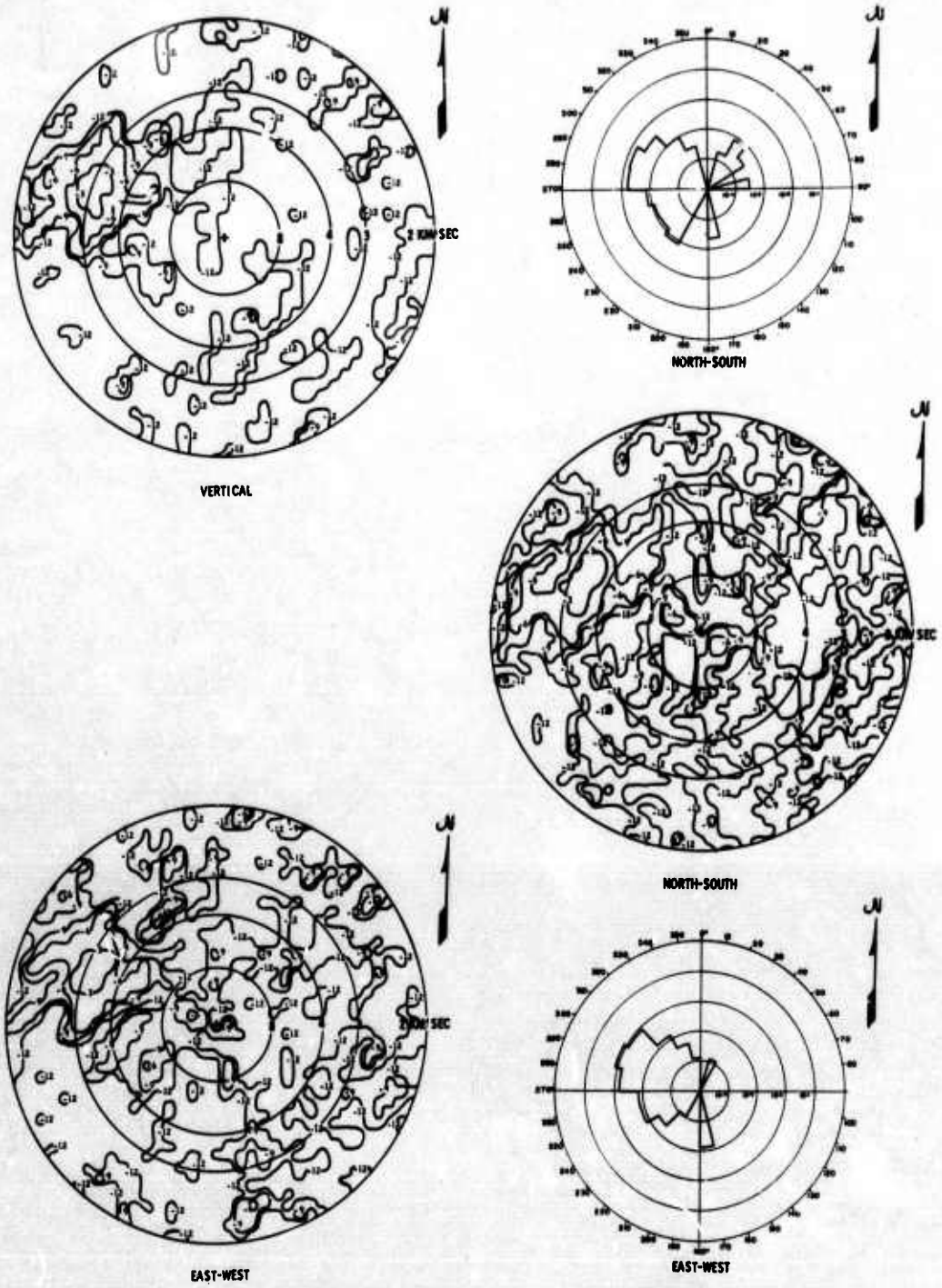


Figure II-56. Wavenumber Spectra and Azimuthal Power Distribution at 0.12 cps, 28 December 1966

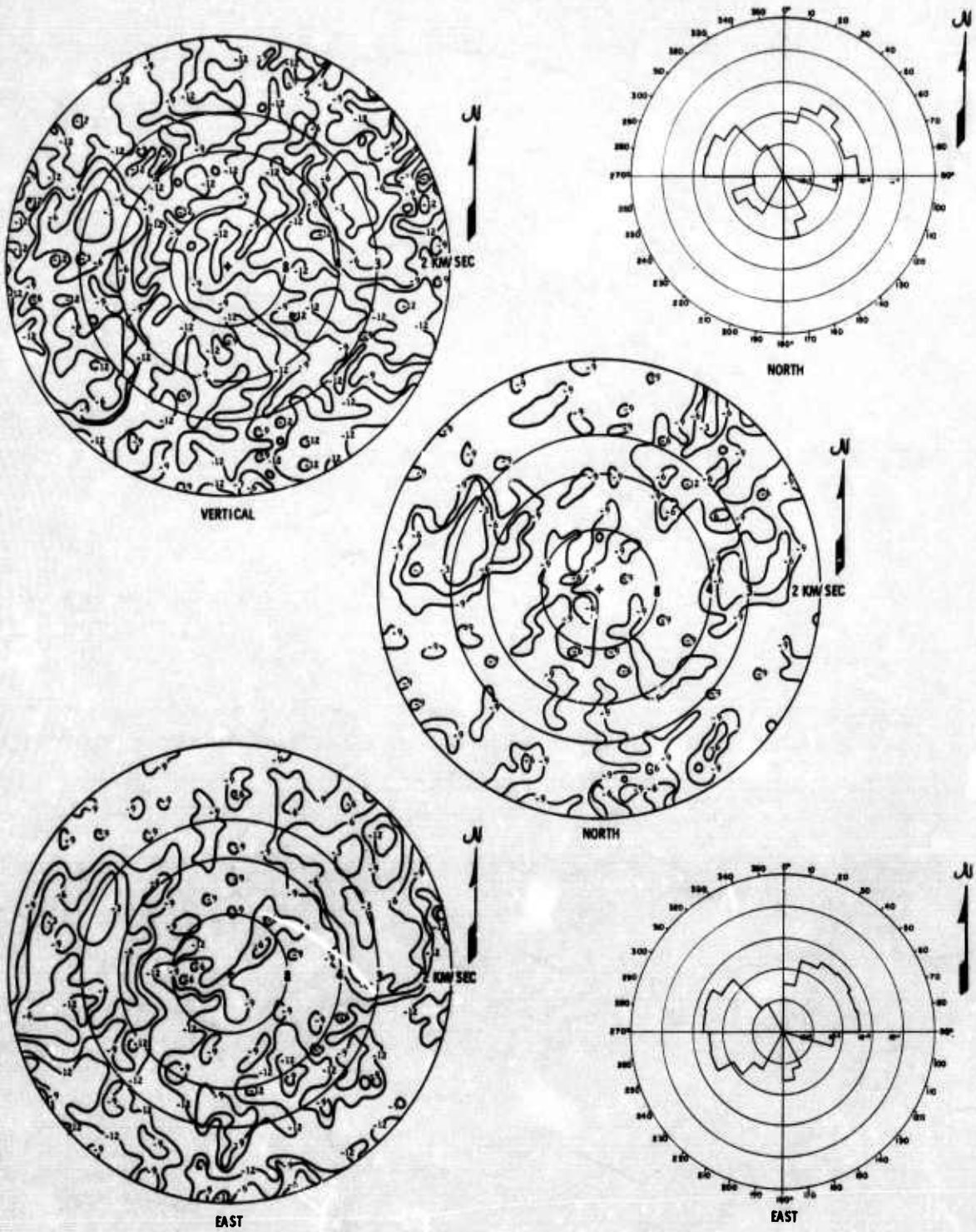


Figure II-57. Wavenumber Spectra and Azimuthal Power Distribution at 0.14 cps, 28 December 1966

Figure II-58. Surface Weather Map for 28 December 1966 at 0000 Hr

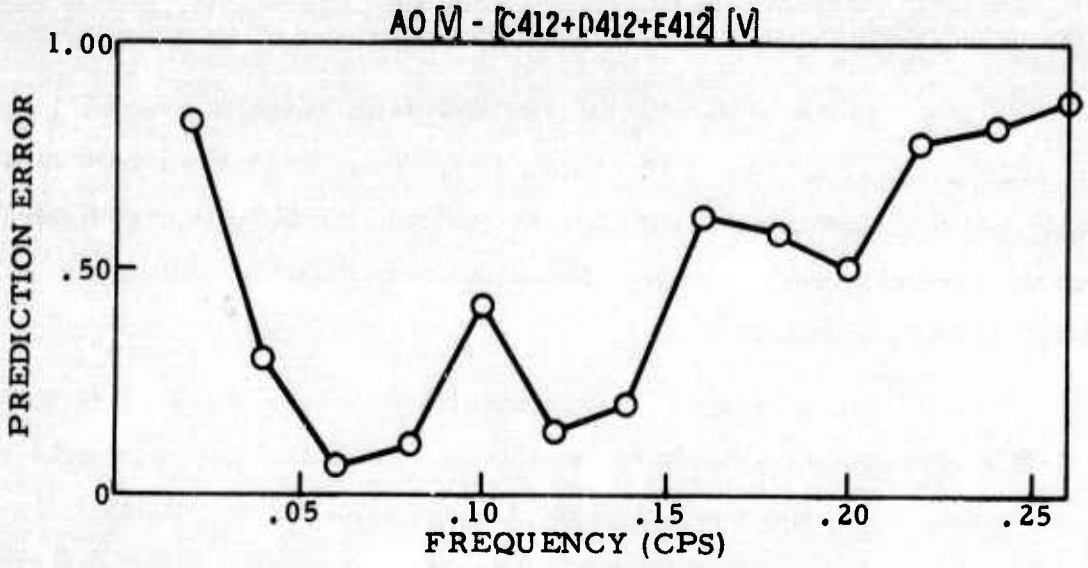


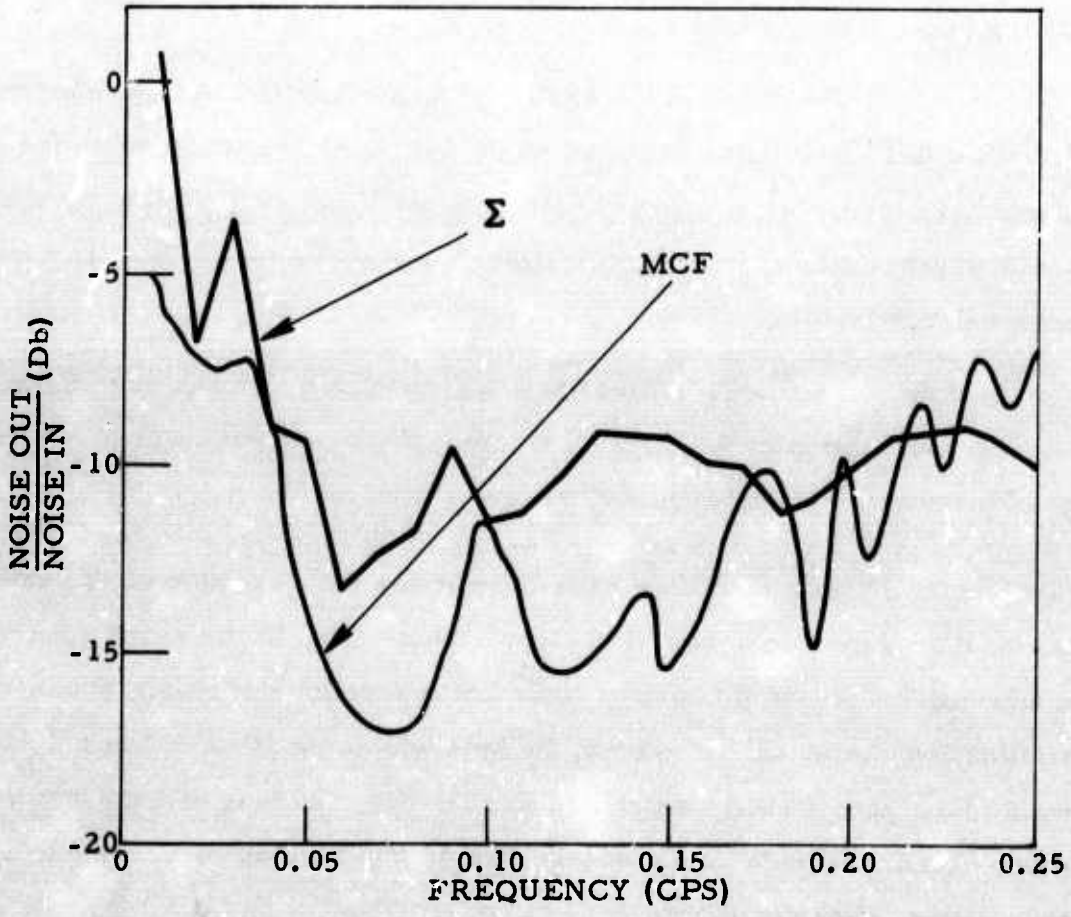


Figure II-59. MCF and Σ Noise Rejection of 28 December 1966 Sample

Figure II-60(a) shows the K-plane response of the MCF at 0.08 cps and 0.12 cps.

In the region of the 0.07-cps power-density peak (Figure II-52), the MCF gives about 15- to 18-db noise rejection, while the summation gives about 12- to 13-db noise rejection. In general, the MCF is significantly superior below about 0.16 cps. The noise rejection obtained by the MCF tends to follow the coherence.

Comparing the wavenumber response of the MCF (Figure II-59) with the wavenumber spectra of the noise (Figures II-56, II-57, and II-58), it is evident that the processor strongly attenuates the low-velocity 3- to 3.5 km/sec power peaks but attenuates most high-velocity ($V > 8.0$ km/sec) energy very little. This again indicates that the great majority of noise is directional surface-mode noise.

The noise out of the MCF processor in the frequency range $0.5 < f < 0.15$ is still as much as 12 db above the system's noise (noise level above 0.25 cps). This noise, which is down about 15 db below the directional surface-mode noise, is probably either nondirectional surface-mode noise or high-velocity noise.

Figure II-60(b) shows the wavenumber response of the 10-channel summation at 0.08 and 0.12 cps. This summation is a reasonably good processor in the frequency range of interest.

Figure II-61 shows the summation response of the entire 21-element long-period array at 0.1 cps. Depending on the exact source location, coherent surface-mode energy could come through the side lobes of the summation response. However, in general, summation of the entire array would be a good P-wave extractor even in the presence of coherent surface-mode noise. Surface-mode energy should be rejected by about 9 to 18 db for frequencies above 0.05 cps.

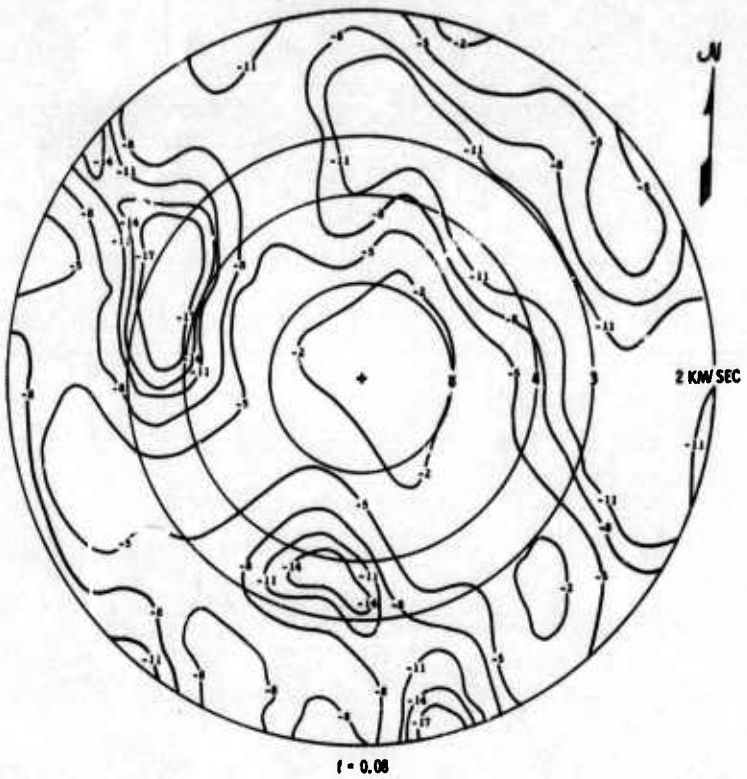


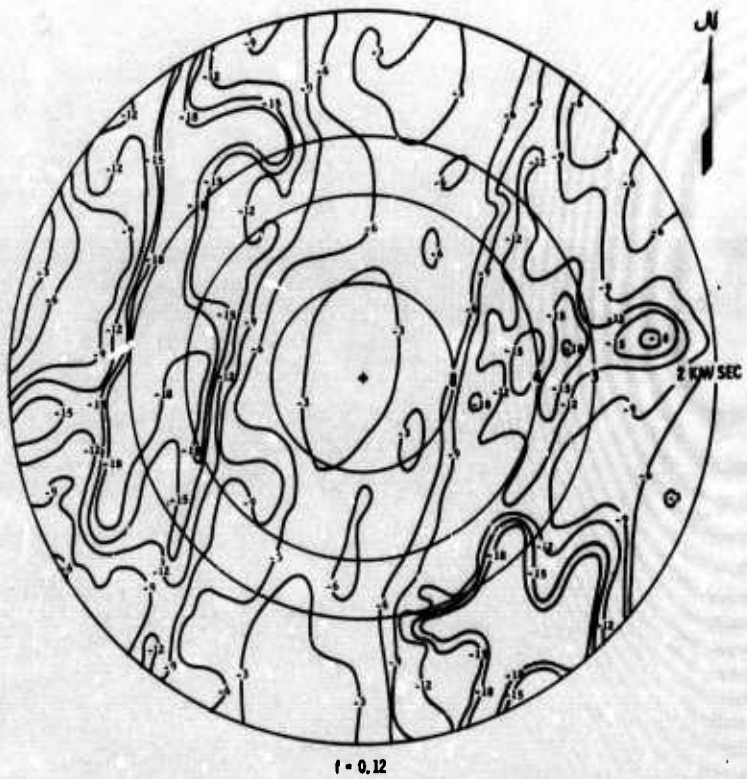


Figure II-60(a). Wavenumber Response of MCF at 0.08 and 0.12 cps

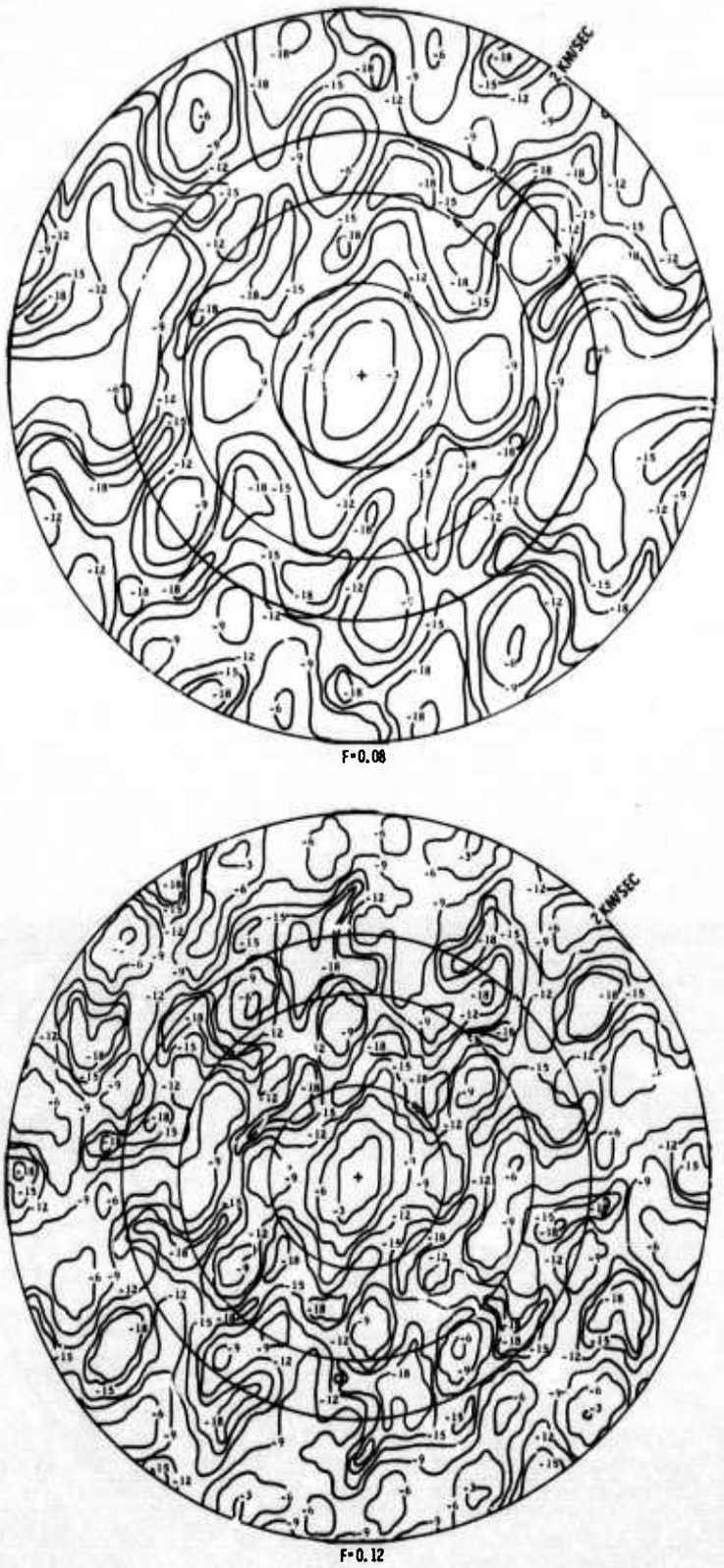


Figure II-60(b). Wavenumber Response of 10 Channel Σ at 0.08 and 0.12 cps

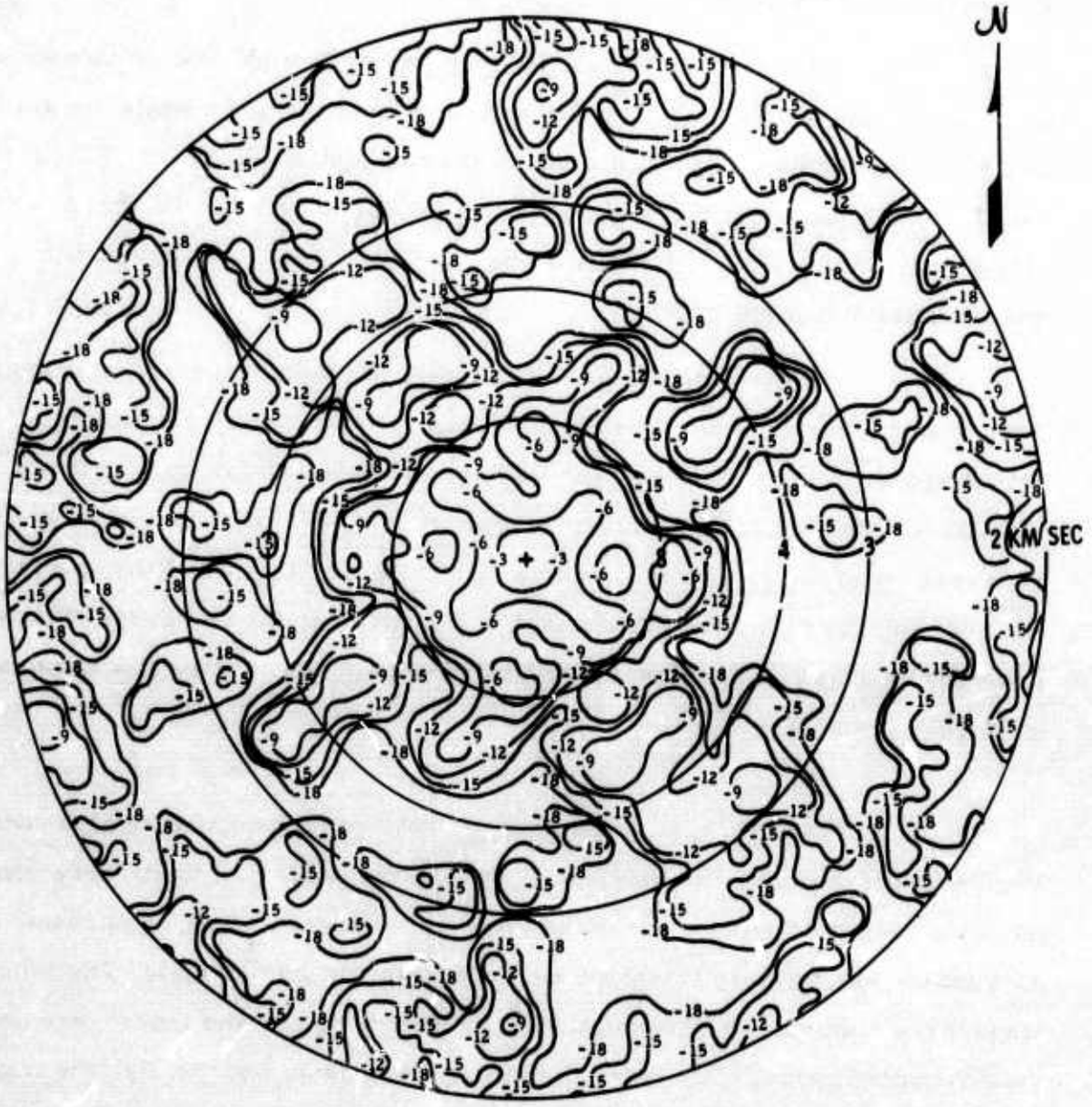


Figure II-61. Summation Response of Long-Period Array at 0.1 cps

An investigation of the relative merits of various schemes of signal processing for long-period data is underway under the extension of Contract AF 33(657)-16678.

The fact that the north-south and east-west components and the north-south and vertical components showed little coherence while the vertical and east-west components were much more correlated (Figures II-53, II-54, and II-55) suggests that the dominant point-like source from N60-65°W (Figures II-56, II-57, and II-58) may have been generating Love-mode as well as Rayleigh-mode energy.

To further test this hypothesis, all well-recorded horizontal components were "rotated," using the computer to develop components orientated N62°W and N28°E. The wavenumber spectra for each of these rotated components at 0.08 cps are shown in Figure II-62. As can be seen, both spectra are very similar and are generally a reflection of the spectral window, indicating a point-like source. The peak for the transverse component is at a noticeably higher velocity, as would be expected if a component of Love-wave energy were present.

The coherences between the rotated elements were also computed. Figure II-63(a) shows the coherence between the inline and transverse components. Figure II-63(b) shows the coherence between inline components and A0 vertical and between transverse components and A0 vertical. The inline and transverse elements are essentially independent, as are the transverse and vertical components. However, the inline components separately, the transverse components separately, and the vertical-inline combination are highly coherent. The vertical component is highly predictable from nearby inline horizontal components but essentially uncorrelated with nearby transverse components.

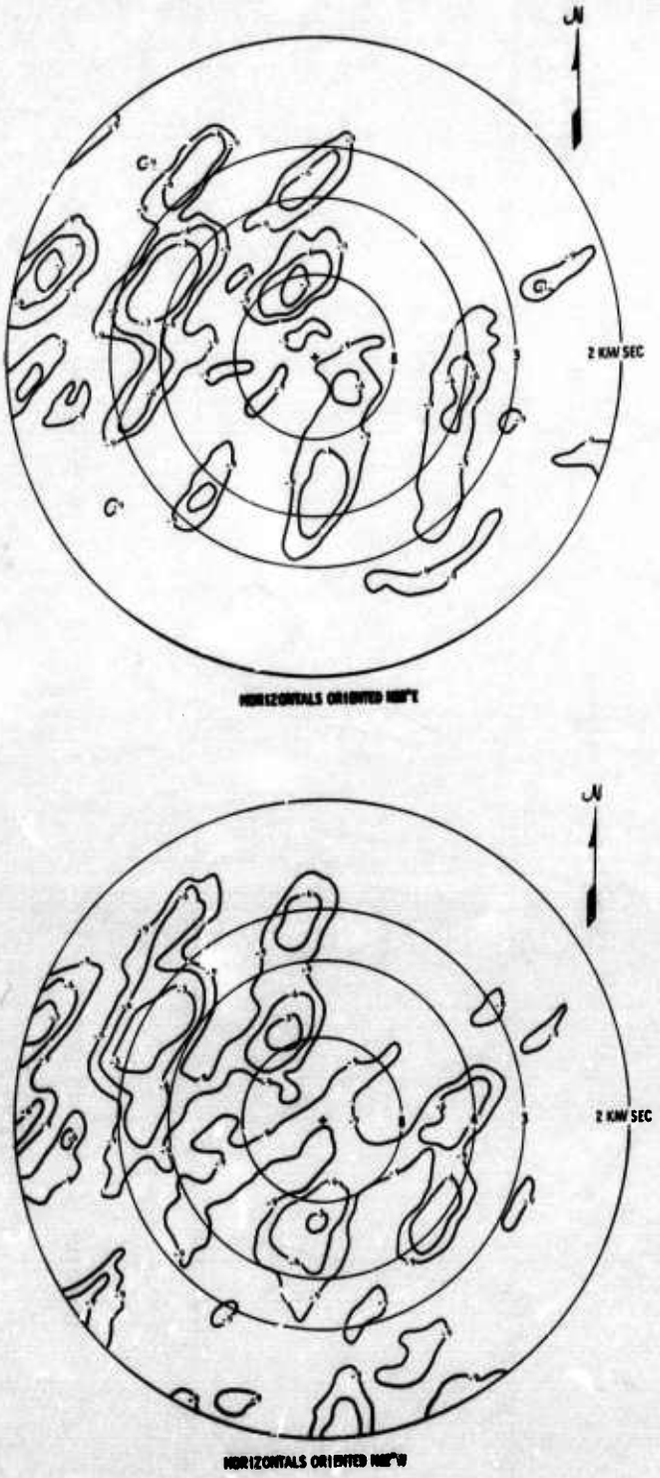


Figure II-62. Wavenumber Spectra of Rotated Horizontal Components at 0.08 cps

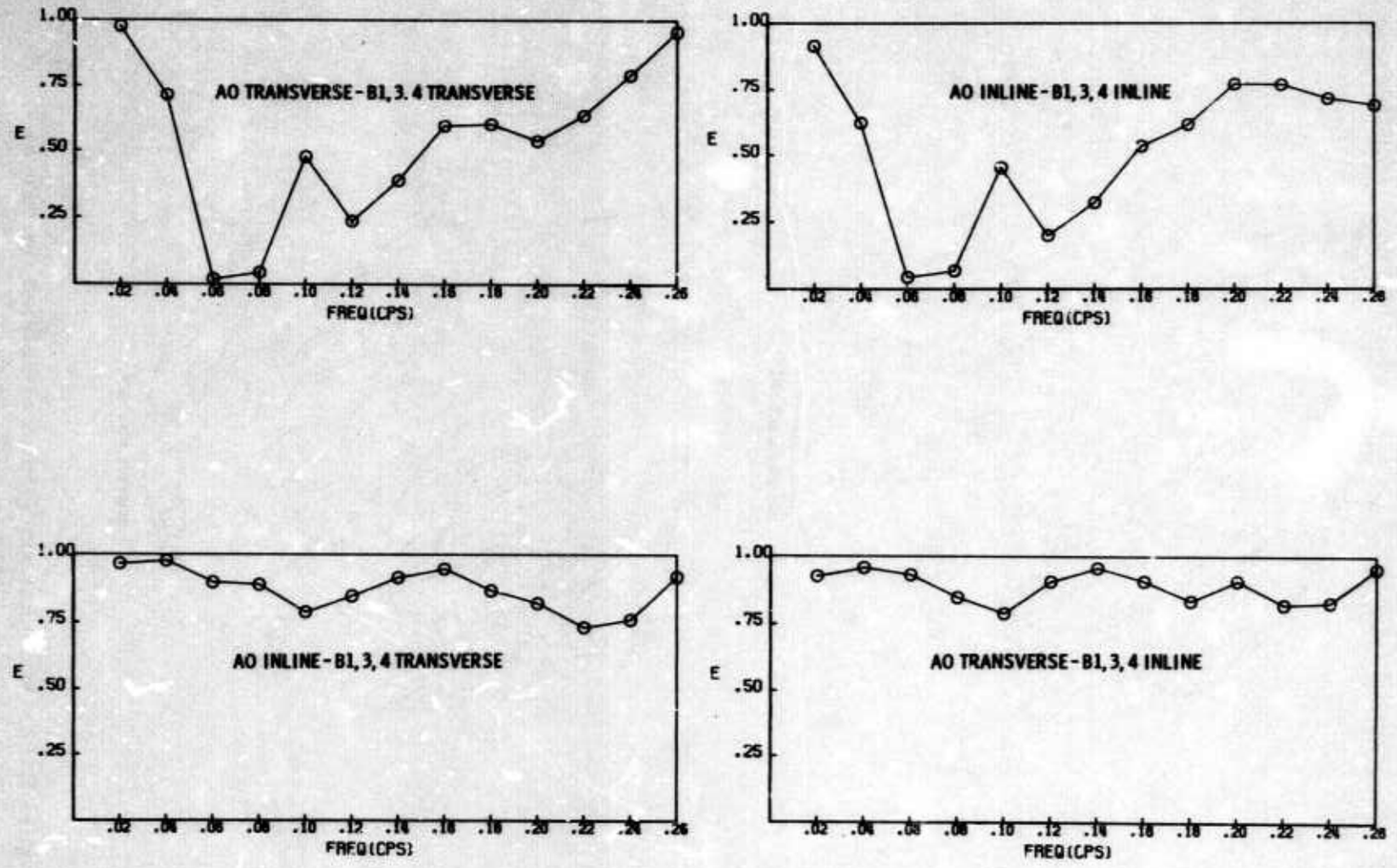


Figure II-63(a). Multiple Coherences for Rotated Elements Between Inline and Transverse Components

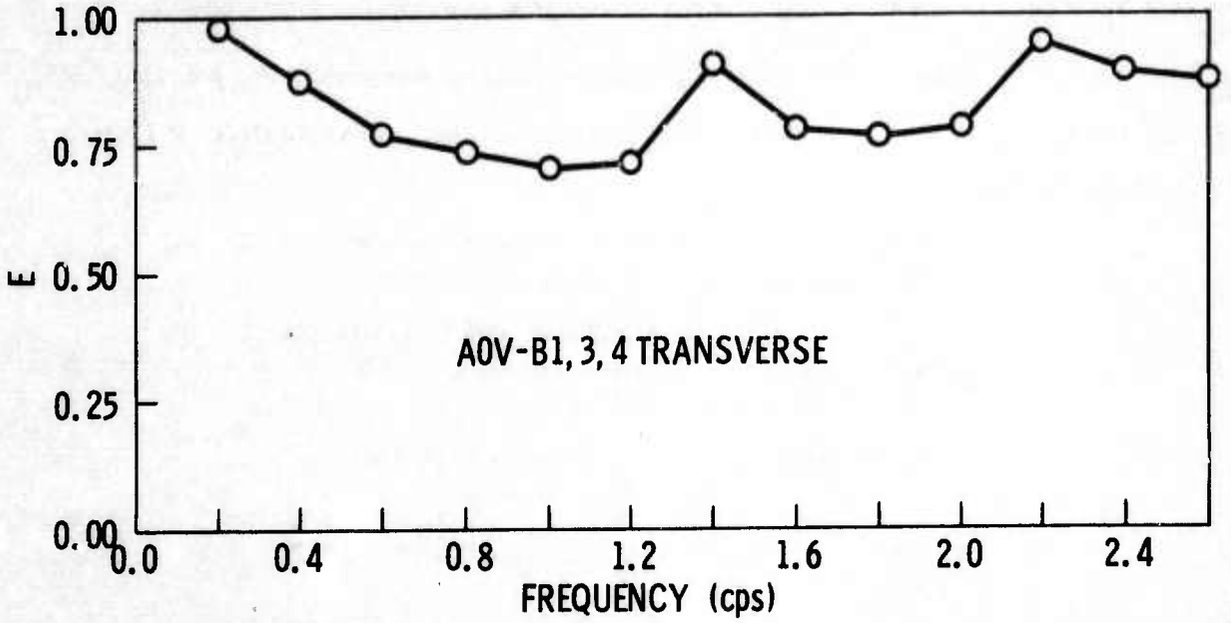


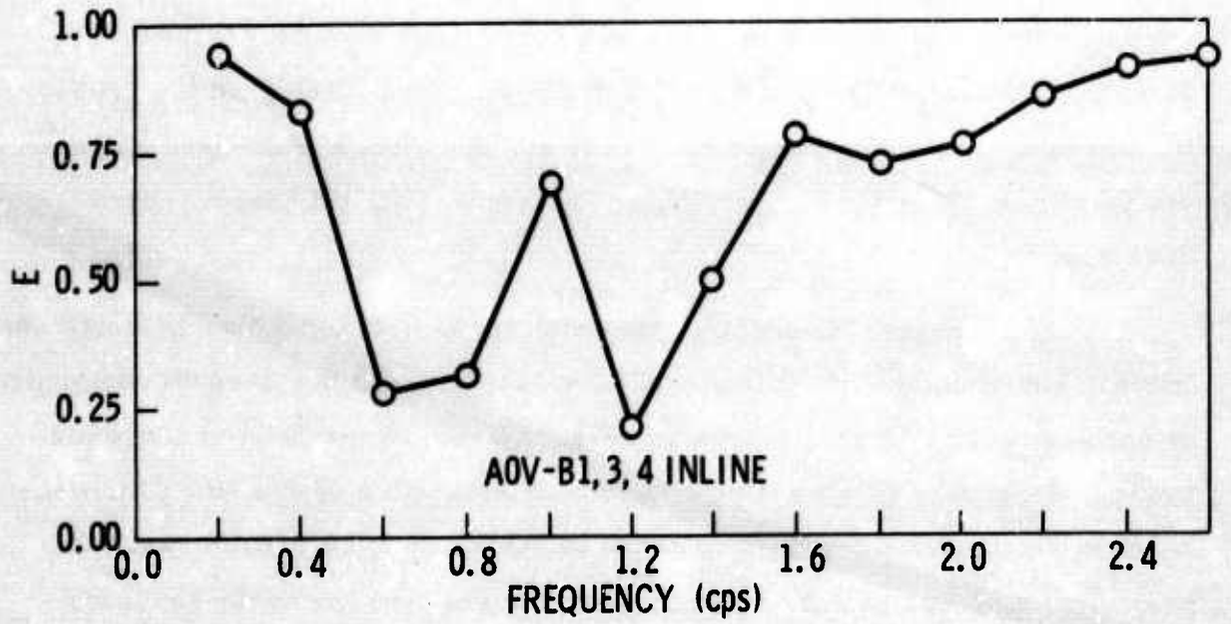


Figure II-63(b). Multiple Coherences for Rotated Elements Between Inline and A0 Vertical Components and Between Transverse and A0 Vertical Components

This evidence strongly indicates that the point-like source to the northwest is a source of both Rayleigh- and Love-mode energy.

Figure II-64 shows power spectra from the A0, F1, F2, F3, and F4 locations for the 7 February noise sample. Examination of these spectra indicates

- Peaks occur at 0.05 cps and 0.11 cps, and a broader peak occurs near 0.15 cps
- Like components (vertical and horizontal) generally have similar spectra at all locations above 0.05 cps
- Horizontal components are about 5-db noisier near the 0.15-cps peak
- There is essentially no seismic energy above 0.28 cps

Figure II-65 shows the coherences between A0 vertical and various combinations of other vertical traces. The vertical component is strongly coherent (75 percent) at a distance of 30 km (D ring) in the 0.05- to 0.14-cps range. The peaks near 0.06 and 0.11 cps are 50-percent predictable from 100-km away (F ring). Coherence falls off sharply below 0.05 cps.

Figure II-66 shows the coherences between A0 north-south and various combinations of north-south components. The north-south component is not so predictable as the vertical (Figure II-65), especially at large distances. However, using sensors as closely spaced as 30 km, the A0 north-south is strongly coherent (75 percent) in the range 0.06 to 0.14 cps. The peak near 0.10 cps is very strongly coherent for both the north-south and vertical components.

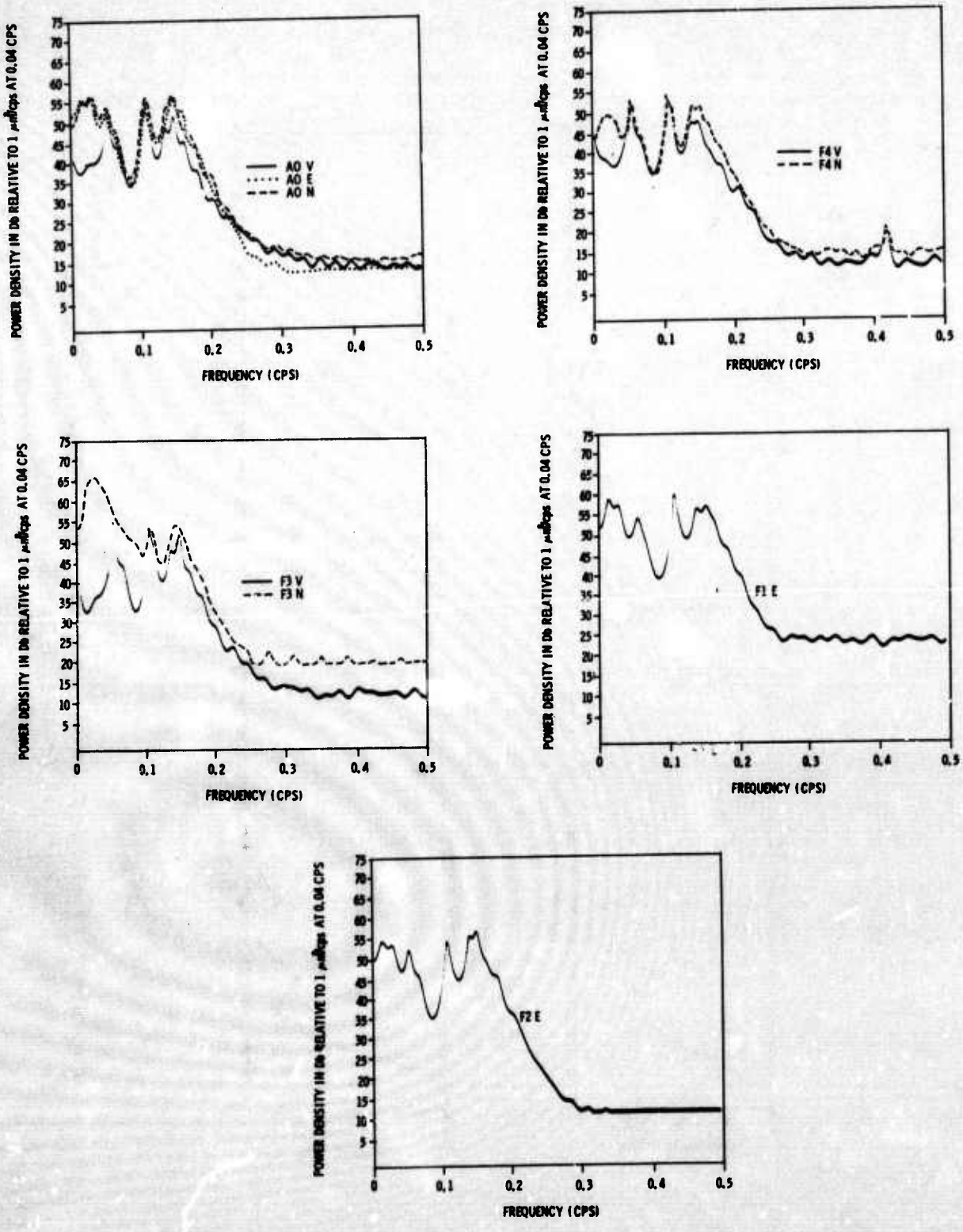


Figure II-64. Power Spectra of 7 February 1967 Noise

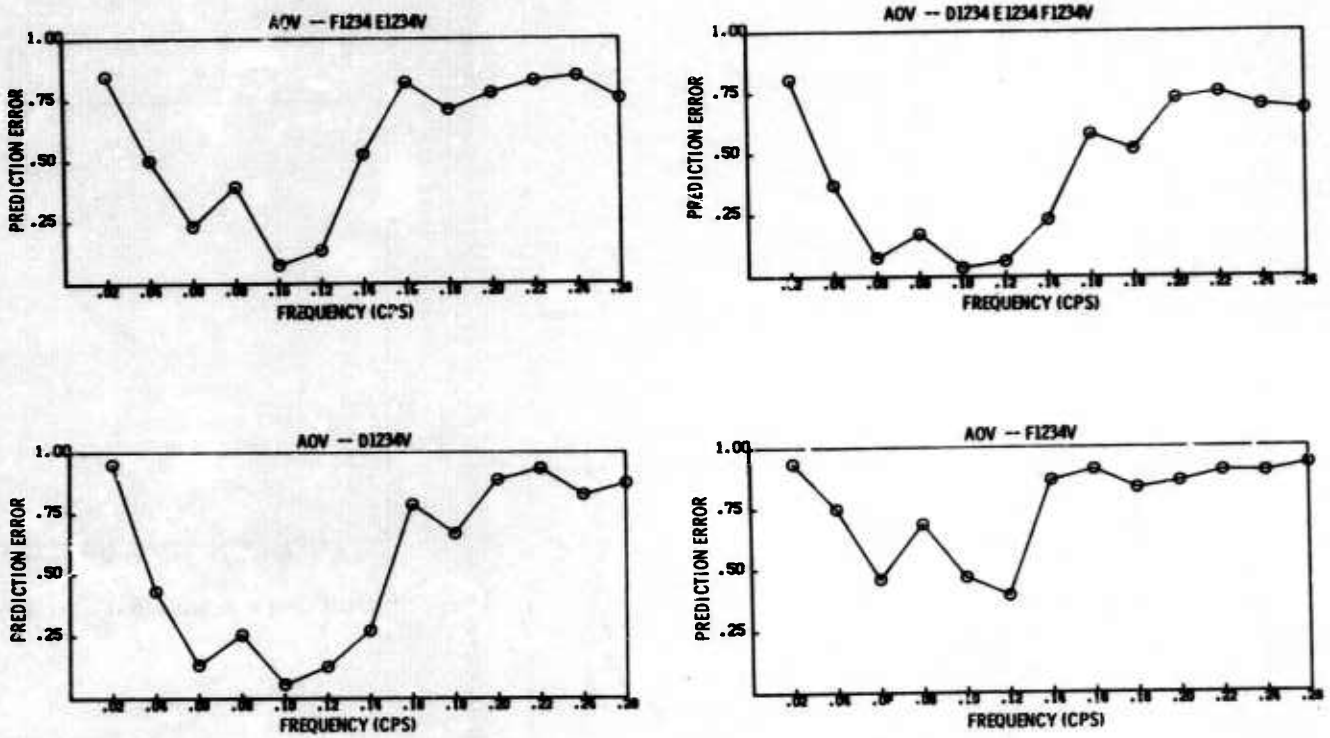


Figure II-65. Multiple Coherences Between A0 Vertical and Combinations of Vertical Traces, 7 February 1967

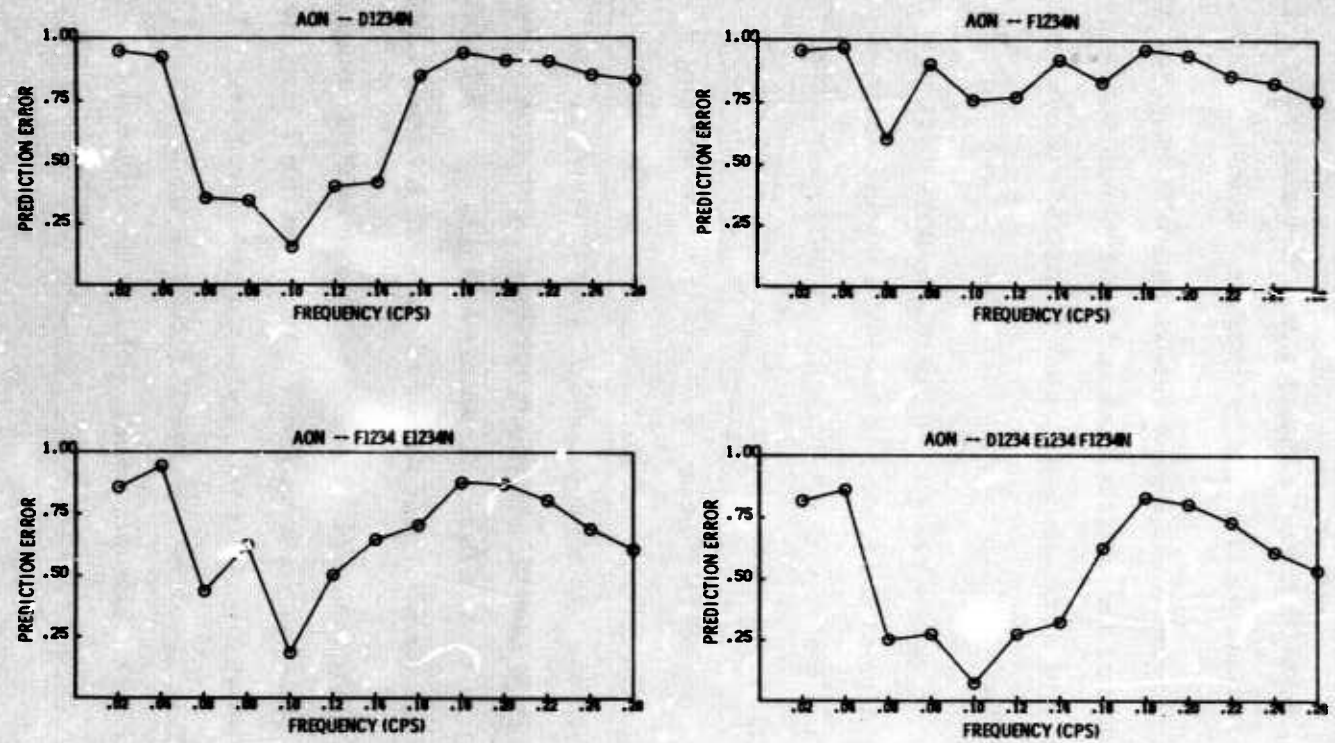


Figure II-66. Multiple Coherences Between A0 North-South and Combinations of North-South Components, 7 February 1967

Coherences between A0 vertical and various combinations of horizontal sensors are shown in Figure II-67. The A0 vertical trace is very predictable from nearby horizontals between 0.06 and 0.14 cps. The peak near 0.10 cps gives extremely high point coherence (A0 vertical to A0 north-south and east-west) which tends to indicate a point-like source.

Figure II-68 shows the wavenumber spectra and the azimuthal power distributions for the vertical and north-south components at 0.05 cps. These spectra are dominated by a peak from N45-50°W with velocity of about 3.5 km/sec.

Figure II-69 shows the wavenumber spectra and azimuthal power distribution at 0.11 cps for the vertical and north-south components. The spectra are quite simple, indicating a very point-like source from N60°W with a velocity of 3.1 to 3.3 km/sec.

Shown in Figure II-70 are the wavenumber spectra and azimuthal power distribution for the vertical and north-south components at 0.15 cps. The northwest peak has disappeared at this frequency, and the strongest seismic energy is coming from the northeast with a velocity of about 3 km/sec. Vertical spectra show a source centered at N45°E, while the north-south spectra indicate the power is smeared out over a broad azimuth.

Figure II-71 shows the surface weather map on 7 February 1967 at 1800 hr. There is a storm front between Baffin Island and Greenland and another just off the coast of Pennsylvania and New York. To the west, there is a frontal passage along the coast of British Columbia. The front along the Yukon/British Columbia coast could well explain the seismic energy from the northwest (Figure II-67).

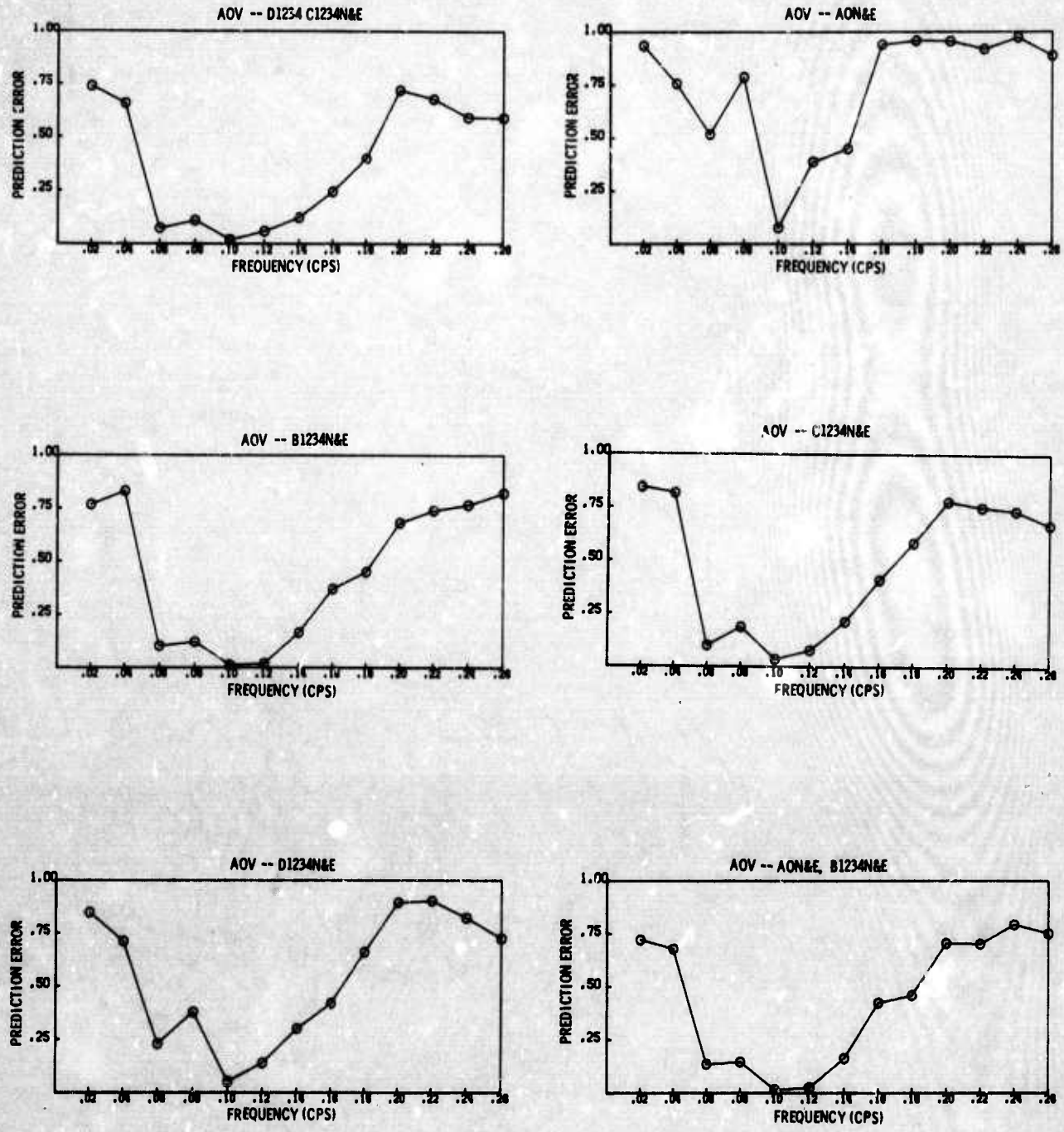


Figure II-67. Multiple Coherences Between A0 Vertical and Combinations of Horizontal Sensors, 7 February 1967

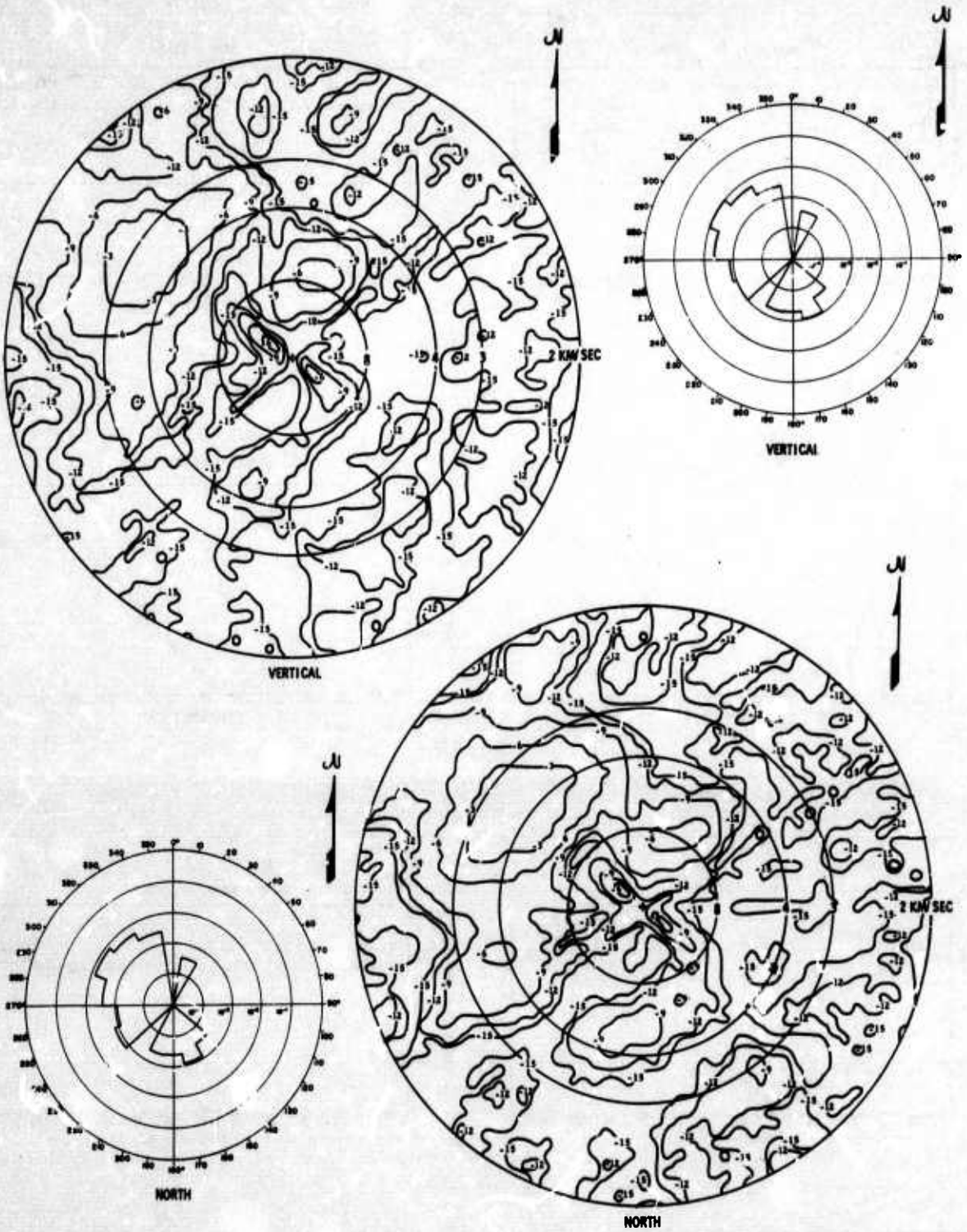


Figure II-68. Wavenumber Spectra and Azimuthal Power Distribution at 0.05 cps, 7 February 1967

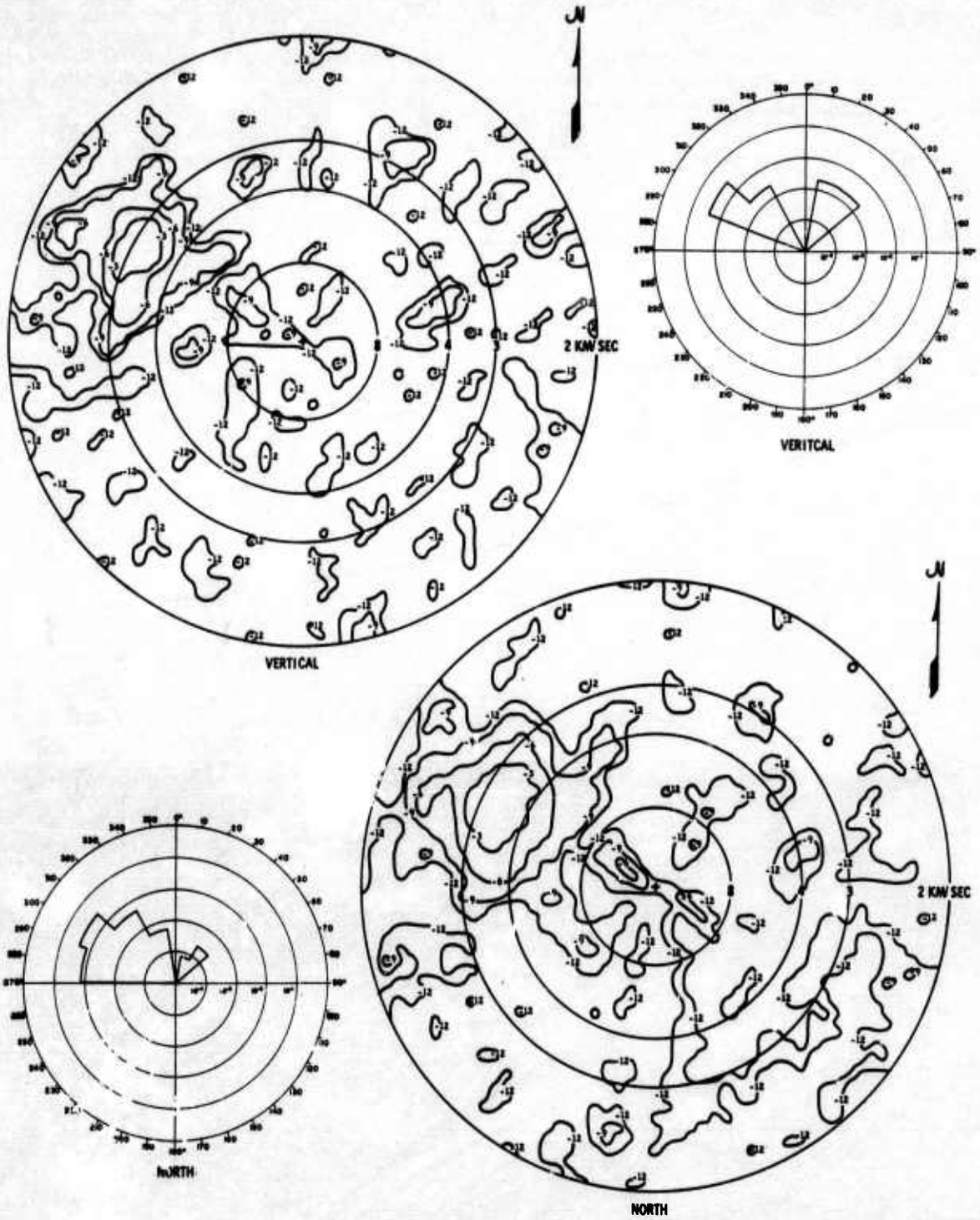


Figure II-69. Wavenumber Spectra and Azimuthal Power Distribution at 0.11 cps, 7 February 1967

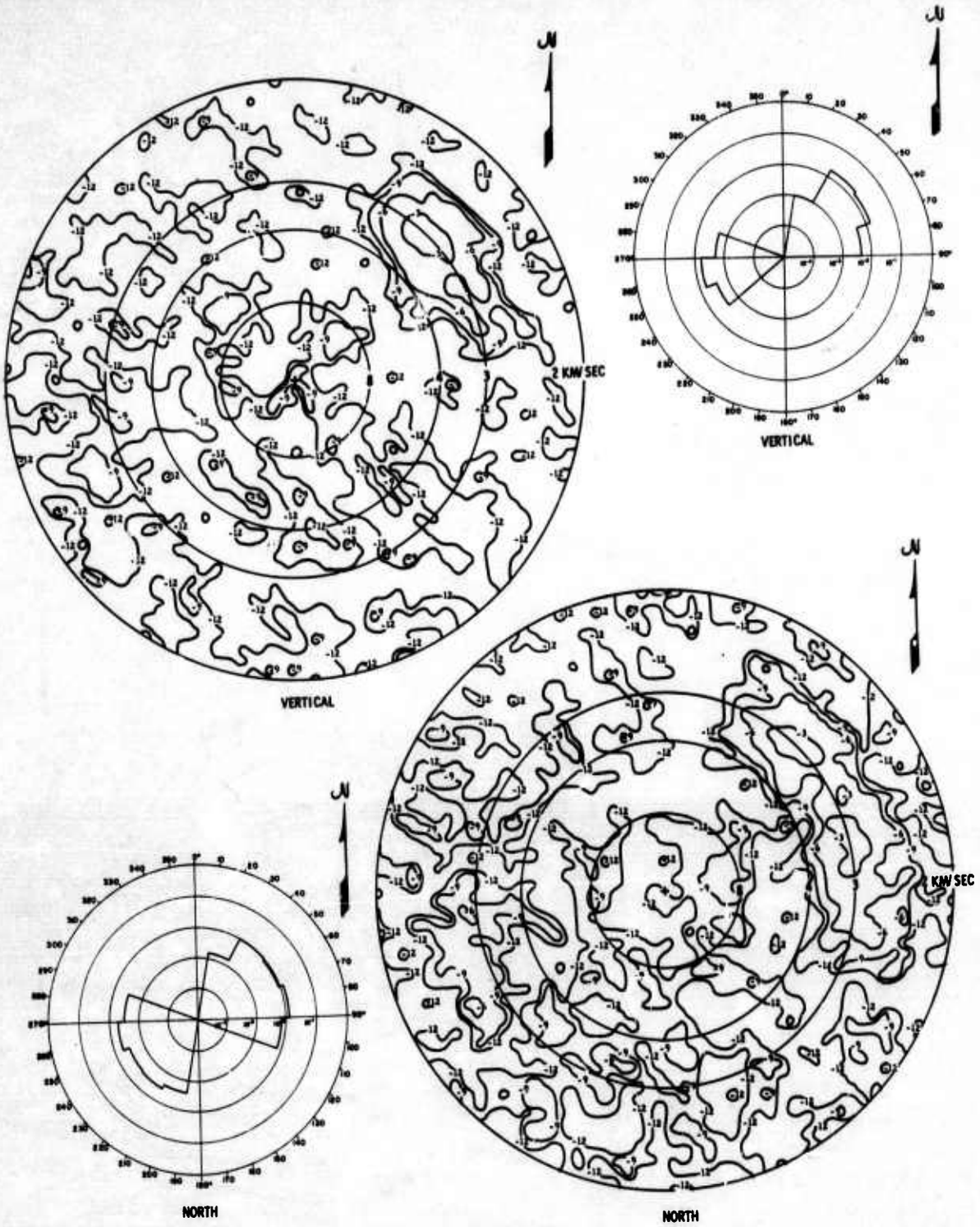


Figure II-70. Wavenumber Spectra and Azimuthal Power Distribution at 0.15 cps, 7 February 1967


Figure II-71. Surface Weather Map for 7 February 1967 at 1800 Hr

# SECTION III
# CONCLUSIONS

A study of the preceding nine long-period noise samples leads naturally to several generalizations about long-period noise. It should be kept in the mind that these noise samples were recorded during the winter months, and it is likely that important characteristics of the long-period noise are functions of the season. Because of the long wavelengths involved, the long-period noise is probably not so changable as the short-period noise field. However, extrapolation to other sites would be speculative. With these reservations, the following generalizations are presented as the author's estimate of the more important characteristics of the long-period noise.

The noise below about 0.05 cps varies highly with location and does not appear to behave as seismic noise. All noise samples show considerable variability in spectra with location and low coherence below 0.05 cps. Haubrich and MacKenzie[3] suggest that noise below 0.05 cps may be the result of wind action and changes in air pressure.

Noise in the frequency band below 0.05 cps is of considerable interest, since most signals are in this frequency range. This low-frequency noise will be studied in more detail under the extension of the present contract. A proper study will require statistics from several noise tapes.

In general, the power spectra are characterized by a peak near 0.06 to 0.08 cps, a relative null near 0.09 to 0.1 cps, and by a peak (or peaks) in the range 0.12 to 0.22 cps. The character and magnitude of the peaks are quite variable, especially above 0.1 cps. Figure III-1 shows 3-component power spectra for seven different days. Differences in shape and 20-db differences in the power levels are evident.

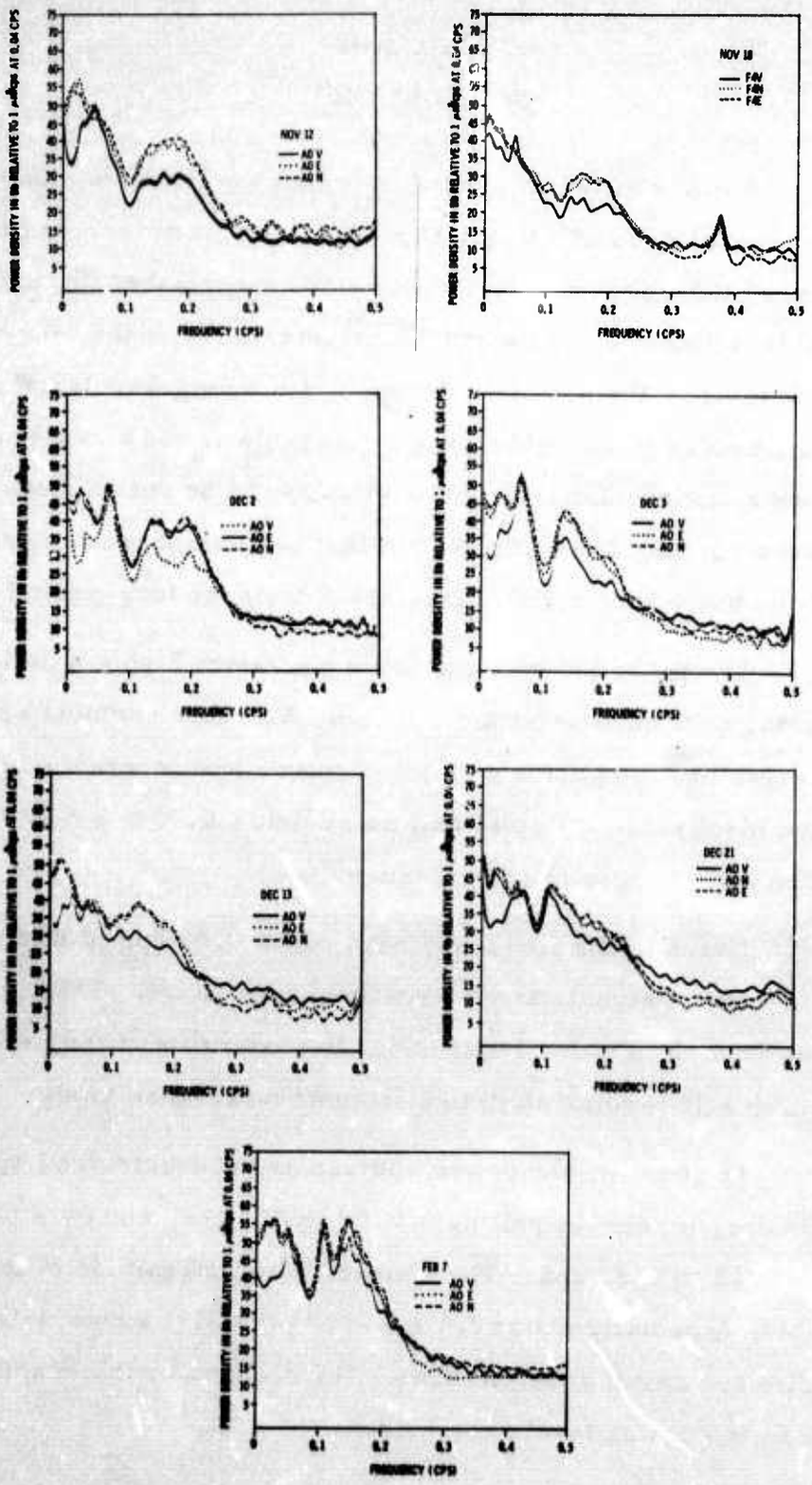


Figure III-1. Frequency Power Spectra for Seven Noise Samples

Days which show higher power density also exhibit greater predictability. This is illustrated by Figure III-2, which shows the A0 vertical predicted from the E- and F-ring vertical components, and Figure III-3, which shows the A0 vertical predicted from the D-ring horizontal components. It appears that the high-noise days are the result of increased coherent energy. The increased vertical-horizontal prediction suggests that this coherent noise is propagating in the Rayleigh mode.

In the region near 0.06 to 0.08 cps (about a 15-sec period), a highly coherent energy peak generally occurs. Both vertical and horizontal components have about equal power density. This energy appears to be mostly generated by wave activity along or fairly near the coast of North America. There is a general correspondence between weather activity and peaks in the wavenumber spectra in almost every case. Seashore wave spectra characteristically have a peak in this same frequency range.[3]

The vertical component at the 0.06- to 0.08-cps peak always has approximately the correct velocity for the fundamental Rayleigh mode.[4] The Rayleigh-mode particle motion is confirmed by the very high predictability of a vertical trace from nearby horizontal components. There is no solid indication of high-velocity noise in any of the wavenumber spectra.

The approximately 18-db noise rejection in the 0.06- to 0.08-cps range obtained using the multichannel filter designed for the 28 December noise sample (Figure II-61) gives an indication of the portion of noise which is surface-mode energy. The wavenumber response of the MCF system (Figure II-62) indicates that essentially all the 18-db noise rejection is the result of attentuation of surface-mode energy. The 18-db reduction (compared to a single sensor) indicates that 63/64 of the noise power is surface-mode energy.

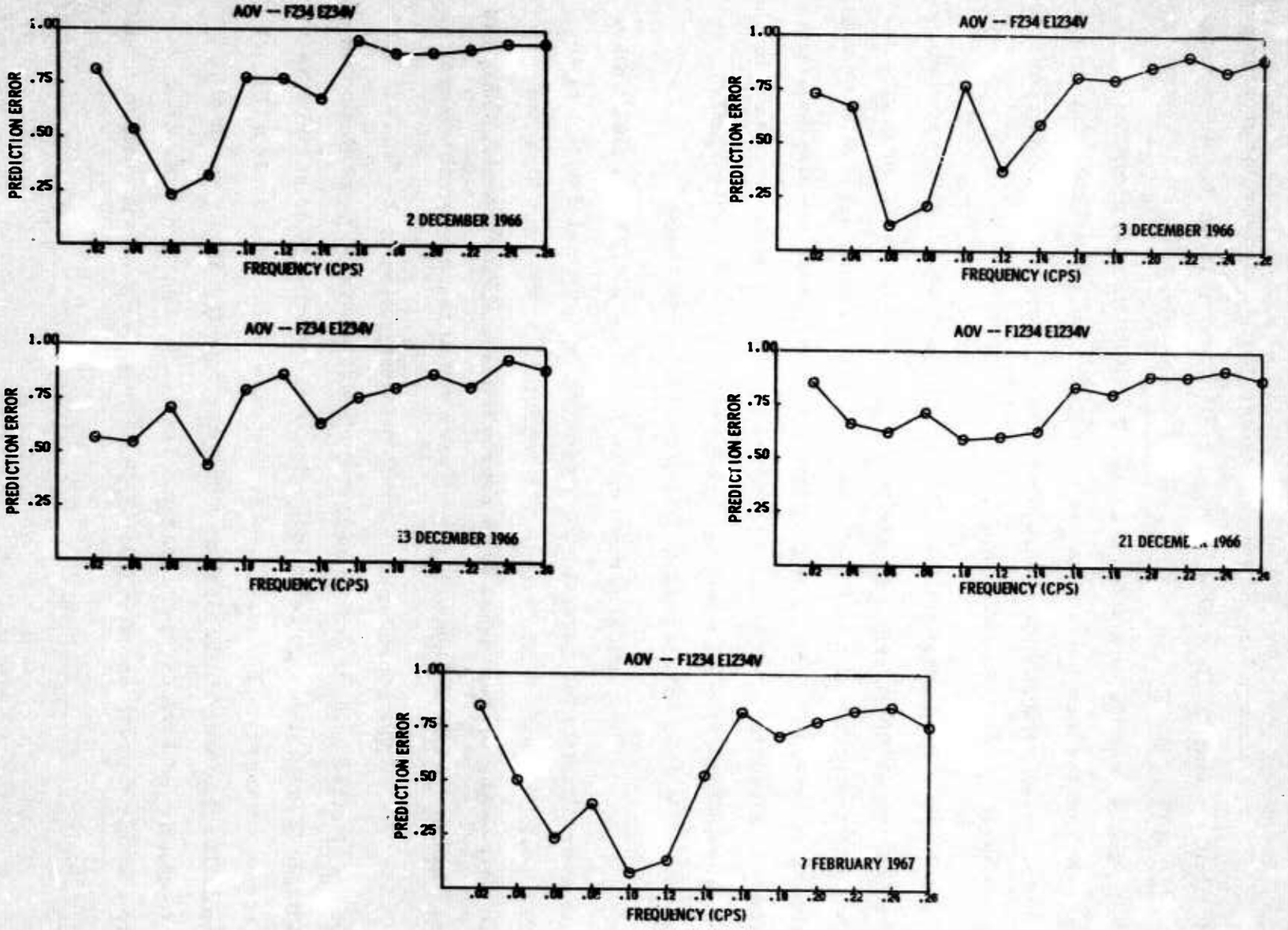


Figure III-2. Vertical Coherences of Five Noise Samples

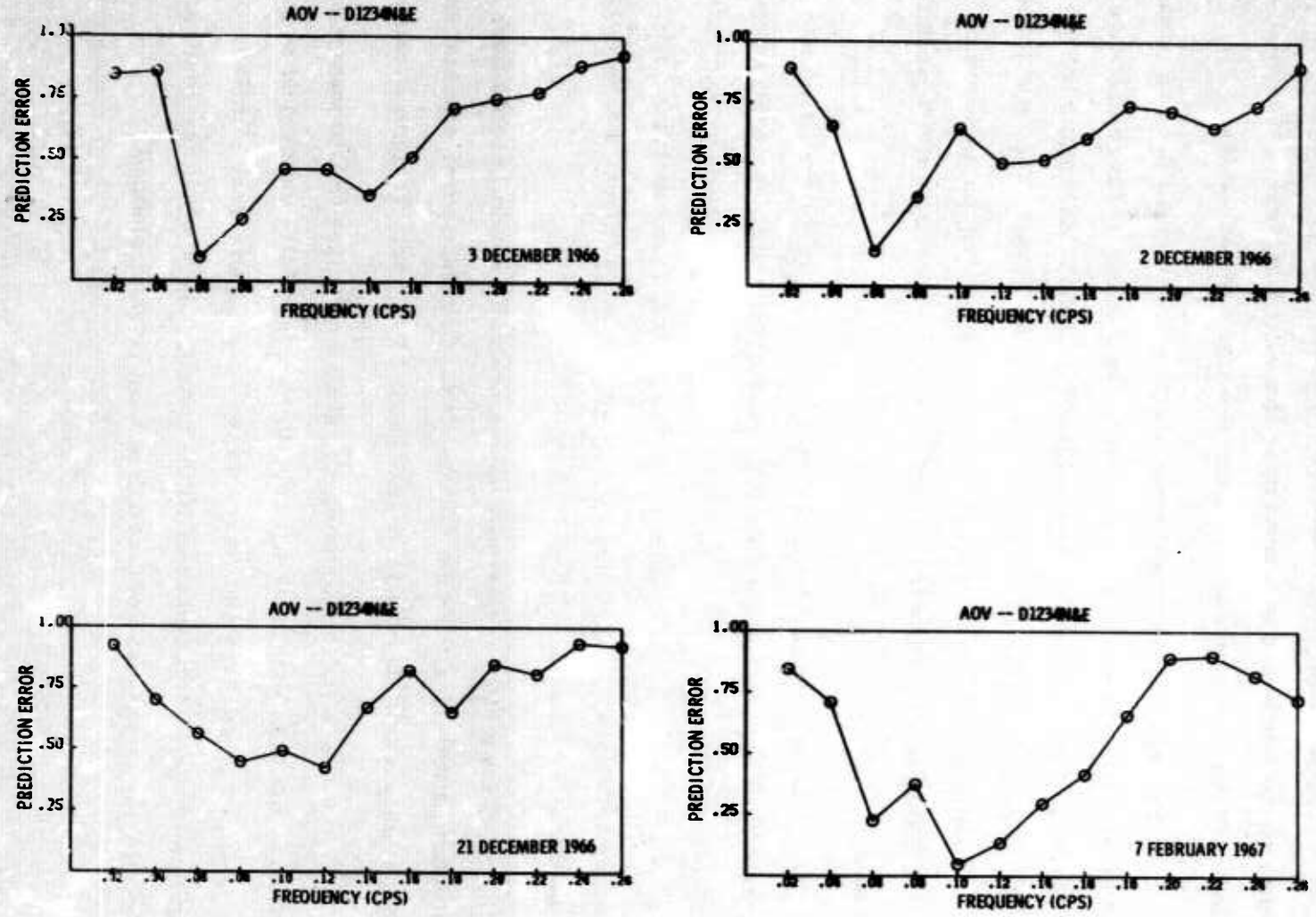


Figure III-3. Vertical-Horizontal Coherences of Four Noise Samples

The horizontal components generally have power density about equal to that of the vertical component near the 0.07-cps peak. Wavenumber spectra indicate that the sources of all components are the same.

The horizontal components are highly coherent but are usually less predictable than the vertical components, especially at large distances (50- to 100 km). The coherences and rotated component wavenumber spectra from the 28 December noise sample (Figures II-54, II-55, II-56, and II-65) suggest that some of horizontal energy may be propagating as Love-wave energy. This may account for the generally lower coherence of the horizontal components.

The nature of the hypothesized generating mechanism (storms) suggests that the noise field is highly time-variable; and the data observed are quite variable. Power density in the 0.06- to 0.08-cps peaks varies by about 15 db (Figure III-1), and wavenumber spectra indicate considerable differences in the source locations. In general, the noise sources were from the northeast and the west.

These storm-related sources probably would become considerably less dominant during the summer months. Several spring and summer long-period noise samples will be investigated as the data become available.

For the two noise samples taken 6 hr apart (2 December and 3 December), the 0.07-cps peak appears to be essentially unchanged over the period. The power spectra and wavenumber spectra are very similar. An investigation of the effectiveness of time-domain filters when designed on one noise sample and applied to another taken 6 hr later is planned.

The power-density spectra generally have a relative null near 0.09 to 0.1 cps and a peak in the range 0.12 to 0.2 cps. Near 0.2 cps, the sensing system's attenuation severely "cuts off" the seismic energy (Figure I-2). Power spectra in the 0.1- to 0.2-cps range are quite variable. Changes in the power density at 20 db and considerable changes in the locations and character of the peaks are evident in Figure III-1. Generally, the horizontal components are considerably noisier and less coherent in this frequency range. However, the 7 February noise sample is an exception to this pattern. Coherences are more variable in the 0.1- to 0.2-cps range, but there is generally considerable coherence at distances from 30 to 50 km (D and E rings).

The vertical components in the 0.12- to 0.16-cps range are generally dominated by fundamental Rayleigh-mode energy from the same sources as the 0.07-cps energy; however, sometimes there are additional or more-diffused peaks in the wavenumber spectra near 0.15 cps, compared to those near 0.07 cps. A considerably larger, uncorrelated component exists at these frequencies. Generally, coherence near 0.15 is considerably lower than at 0.07 cps.

There are some possible indications of the development of a higher-order mode. For example, the 12 November noise sample wavenumber spectra at 0.16 cps (Figure II-8) show a peak from the northeast with a velocity near 4 km/sec and another smaller peak with the approximate velocity of the fundamental Rayleigh mode (3 km/sec).

The low-frequency (near 0.2-cps) end of the short-period noise typically shows directional peaks in the wavenumber spectra with velocities near 3.5 km/sec, which must be interpreted as a higher-order mode.[5]

Above 0.15 cps, the coherence is generally down considerably even though, in many cases, the power density remains rather high (e.g., 2 December). It appears likely that noise character changes near 0.16 cps, which may be the result of higher-order modes becoming dominant or of different sources becoming dominant. The 0.15- to 0.2-cps range is a difficult frequency range in which to work, for it is the range of poor response of both the short- and long-period instruments.

The horizontal components' wavenumber spectra usually indicate the same storm sources as indicated on the vertical components. The peaks are often more spread in azimuth than on the vertical component spectra. Velocities are roughly those expected for the fundamental Rayleigh mode (3 km/sec). Love-wave energy have roughly the same velocity in this frequency range[4] and are undistinguishable from the fundamental Rayleigh mode in wavenumber spectra. No attempt has been made to demonstrate the presence of Love-mode energy in this frequency range; however, based on the results at 0.07 cps for the 28 December noise sample, some Love-mode energy could be expected at these frequencies.

There is also some indication of a higher-order mode in the horizontal wavenumber spectra. The east-west component wavenumber spectra for the 13 December noise sample at 0.14 cps (Figure II-42) show energy from the northeast which is split into two distinct peaks. One has a velocity of about 3 km/sec, the other about 3.9 km/sec. The higher-velocity peak may represent a higher-order mode.

Because of the higher percentage (generally 5 to 25 percent near 0.13 cps) of random noise than at 0.06 cps, it is more difficult to determine whether or not any high-velocity noise is present. There is no indication of

any high-velocity peaks in the wavenumber spectra. Also, the MCF system designed for the 28 December noise sample was quite effective near 0.13 cps (Figure II-61), while the wavenumber response (Figure II-62) does not show much high-velocity attenuation near 0.13 cps. These facts suggest that the P-wave noise level is insignificant in the 0.1- to 0.15-cps range.

The short-term time stability of the noise in the 0.1- to 0.2-cps range can be estimated by examination of the 2 December and 3 December noise samples which were recorded about 6 hr apart.

The wavenumber spectra at 0.14 cps (Figure II-22 and II-32) indicate that the major sources of coherent energy are essentially unchanged over the 6 hr period. The power-density spectra (Figures II-16 and II-25) are quite similar up to about 0.15 cps, above which the 3 December noise sample has considerably lower power density.

The multiple coherences (Figures II-17, II-18, II-19, II-26, II-27, and II-28) indicate that all components of the 2 December noise sample are noticeably more coherent near 0.13 cps than those of the 3 December noise sample. The partially coherent peak in the 0.18- to 0.24-cps range which is present in the 2 December noise is altogether absent from the 3 December noise.

It appears that the noise field in the 0.1- to 0.15-cps range is fairly stable over the 6 hr period while the noise above 0.15 cps has completely changed.

## SECTION IV

## REFERENCES


1. Texas Instruments Incorporated, 1967: Noise Coherence Among Subarrays, Large-Array Signal and Noise Analysis, Spec. Scientific Rpt. No. 13, Contract AF 33(657)-16678, to be published.

2. Texas Instruments Incorporated, 1965: Theoretical Capability of Systems of Horizontal Seismometers for Predicting a Vertical Component in Ambient Trapped-Mode Noise, Array Research Spec. Rpt. No. 7, Contract AF 33(657)-12747, 9 Nov.

3. Haubrich, R. A. and G. S. MacKenzie, 1965: Earth Noise 5 to 500 Millicycles Per Second, J. of Geophys. Res., v. 70, n.6, 15 Mar.

4. Texas Instruments Incorporated, 1967: Continuation of Basic Research in Crustal Studies, Final Rpt., Contract AF 49(638)-1588, 15 July.

5. Texas Instruments Incorporated, 1967: Analysis of Subarray Wavenumber Spectra, Large-Array Signal and Noise Analysis, Spec. Scientific Rpt. No. 6, Contract AF 33(657)-16678, to be published.

UNCLASSIFIED
Security Classification

**DOCUMENT CONTROL DATA - R&D**
*(Security classification of title, body of abstract and indexing annotation must be entered when the overall report is classified)*

1. ORIGINATING ACTIVITY *(Corporate author)*
Texas Instruments Incorporated
Science Services Division
P.O. Box 5621, Dallas, Texas 75222

2a. REPORT SECURITY CLASSIFICATION
Unclassified

2b. GROUP
—

3. REPORT TITLE
LARGE-ARRAY SIGNAL AND NOISE ANALYSIS — SPECIAL SCIENTIFIC REPORT NO. 12 — ANALYSIS OF LONG-PERIOD NOISE

4. DESCRIPTIVE NOTES *(Type of report and inclusive dates)*
Special Scientific

5. AUTHOR(S) *(Last name, first name, initial)*
Binder, Frank H.

| 6. REPORT DATE | 7a. TOTAL NO. OF PAGES | 7b. NO. OF REFS |
|---|---|---|
| 18 October 1967 | 115 | 5 |

| 8a. CONTRACT OR GRANT NO. | 9a. ORIGINATOR'S REPORT NUMBER(S) |
|---|---|
| Contract No. AF 33(657)-16678 | — |
| b. PROJECT NO. Project No. VT/6707 | 9b. OTHER REPORT NO(S) *(Any other numbers that may be assigned this report)* — |
| c. | |
| d. | |

10. AVAILABILITY/LIMITATION NOTICES
This document is subject to special export controls and each transmittal to foreign governments or foreign nationals may be made only with prior approval of Chief, AFTAC.

| 11. SUPPLEMENTARY NOTES | 12. SPONSORING MILITARY ACTIVITY |
|---|---|
| ARPA Order No. 599 | Air Force Technical Applications Center<br>VELA Seismological Center<br>Headquarters, USAF, Washington, D.C. |

13. ABSTRACT

This report presents the results of the analysis of nine long-period noise samples recorded at the Montana LASA between 12 November 1966 and 7 February 1967. This analysis was undertaken to describe the salient characteristics of the long-period noise. Particular attention was given to spectral analysis, coherence among channels, spatial organization, identification of modal content, and identification of noise sources. Results of the analysis of the long-period noise indicate that the noise generally appears to be related to storms and is probably the result of wave activity in the North Atlantic and North Pacific. The noise is quite time-variable and is highly coherent. The coherent-noise peaks above 0.05 cps appear to be predominantly (at least 90 percent) surface-mode energy. There is some evidence that a portion of the horizontal energy is Love-wave energy. The noise below 0.05 cps does not appear to behave as propagating plane waves. Power spectra of similar components are generally space-stationary. The horizontal components are considerably noisier than the vertical in the range $f < 0.05$ cps and $0.1 < f < 0.2$ cps.

DD FORM 1 JAN 64 1473

UNCLASSIFIED
Security Classification

| 14. KEY WORDS | LINK A | | LINK B | | LINK C | |
|---|---|---|---|---|---|---|
| | ROLE | WT | ROLE | WT | ROLE | WT |
| Large-Array Signal and Noise Analysis | | | | | | |
| Long-Period Noise | | | | | | |
| Spectral Analysis | | | | | | |
| Channel Coherence | | | | | | |
| Spatial Organization | | | | | | |
| Modal Content | | | | | | |
| Noise Sources | | | | | | |

## INSTRUCTIONS

1. ORIGINATING ACTIVITY: Enter the name and address of the contractor, subcontractor, grantee, Department of Defense activity or other organization *(corporate author)* issuing the report.

2a. REPORT SECURITY CLASSIFICATION: Enter the overall security classification of the report. Indicate whether "Restricted Data" is included. Marking is to be in accordance with appropriate security regulations.

2b. GROUP: Automatic downgrading is specified in DoD Directive 5200.10 and Armed Forces Industrial Manual. Enter the group number. Also, when applicable, show that optional markings have been used for Group 3 and Group 4 as authorized.

3. REPORT TITLE: Enter the complete report title in all capital letters. Titles in all cases should be unclassified. If a meaningful title cannot be selected without classification, show title classification in all capitals in parenthesis immediately following the title.

4. DESCRIPTIVE NOTES: If appropriate, enter the type of report, e.g., interim, progress, summary, annual, or final. Give the inclusive dates when a specific reporting period is covered.

5. AUTHOR(S): Enter the name(s) of author(s) as shown on or in the report. Enter last name, first name, middle initial. If military, show rank and branch of service. The name of the principal author is an absolute minimum requirement.

6. REPORT DATE: Enter the date of the report as day, month, year, or month, year. If more than one date appears on the report, use date of publication.

7a. TOTAL NUMBER OF PAGES: The total page count should follow normal pagination procedures, i.e., enter the number of pages containing information.

7b. NUMBER OF REFERENCES: Enter the total number of references cited in the report.

8a. CONTRACT OR GRANT NUMBER: If appropriate, enter the applicable number of the contract or grant under which the report was written.

8b, 8c, & 8d. PROJECT NUMBER: Enter the appropriate military department identification, such as project number, subproject number, system numbers, task number, etc.

9a. ORIGINATOR'S REPORT NUMBER(S): Enter the official report number by which the document will be identified and controlled by the originating activity. This number must be unique to this report.

9b. OTHER REPORT NUMBER(S): If the report has been assigned any other report numbers *(either by the originator or by the sponsor)*, also enter this number(s).

10. AVAILABILITY/LIMITATION NOTICES: Enter any limitations on further dissemination of the report, other than those imposed by security classification, using standard statements such as:

(1) "Qualified requesters may obtain copies of this report from DDC."

(2) "Foreign announcement and dissemination of this report by DDC is not authorized."

(3) "U. S. Government agencies may obtain copies of this report directly from DDC. Other qualified DDC users shall request through _____."

(4) "U. S. military agencies may obtain copies of this report directly from DDC. Other qualified users shall request through _____."

(5) "All distribution of this report is controlled. Qualified DDC users shall request through _____."

If the report has been furnished to the Office of Technical Services, Department of Commerce, for sale to the public, indicate this fact and enter the price, if known.

11. SUPPLEMENTARY NOTES: Use for additional explanatory notes.

12. SPONSORING MILITARY ACTIVITY: Enter the name of the departmental project office or laboratory sponsoring *(paying for)* the research and development. Include address.

13. ABSTRACT: Enter an abstract giving a brief and factual summary of the document indicative of the report, even though it may also appear elsewhere in the body of the technical report. If additional space is required, a continuation sheet shall be attached.

It is highly desirable that the abstract of classified reports be unclassified. Each paragraph of the abstract shall end with an indication of the military security classification of the information in the paragraph, represented as *(TS)*, *(S)*, *(C)*, or *(U)*.

There is no limitation on the length of the abstract. However, the suggested length is from 150 to 225 words.

14. KEY WORDS: Key words are technically meaningful terms or short phrases that characterize a report and may be used as index entries for cataloging the report. Key words must be selected so that no security classification is required. Identifiers, such as equipment model designation, trade name, military project code name, geographic location, may be used as key words but will be followed by an indication of technical context. The assignment of links, rules, and weights is optional.